



TECHNISCHE UNIVERSITÄT MÜNCHEN

TUM School of Life Sciences

**Functional analysis of
the bHLH transcription factor CESTA and interacting
partners of the TCP family**

HAIWEI SHUAI

Vollständiger Abdruck der von der TUM School of Life Sciences zur Erlangung des akademischen Grades eines

Doktors der Naturwissenschaften

genehmigten Dissertation.

Vorsitzende: Prof. Dr. Caroline Gutjahr

Prüfer der Dissertation: 1. Prof. Dr. Brigitte Poppenberger-Sieberer
2. Prof. Dr. Gerd Patrick Bienert

Die Dissertation wurde am 16.05.2022 bei der Technischen Universität München eingereicht und durch die TUM School of Life Sciences am 28.07.2022 angenommen.

Contents

Abstract	I
Zusammenfassung	II
Abbreviations	III
1. Introduction	1
1.1. Brassinosteroids regulate plant growth and development	1
1.2. The BR biosynthesis pathway	2
1.3. BRs perception and upstream signaling	3
1.4. BR-regulated transcription factors of the BES1/BZR1 subfamily	5
1.5. The bHLH proteins BEEs and CESTA	6
1.6. Transcription factors of the TCP family and their implication with BRs and GAs	8
1.7. BRs induce posttranslational modifications of transcription factors	9
1.8. BR activity in tomato	10
1.9. Aims of this study	12
2. Results	13
2.1. TCP15 is a CES interacting factor that takes part in BR responses	13
2.1.1. CES interacts with TCP8, TCP14 and TCP15 in yeast	13
2.1.2. A loss-of-function of TCP15 and its homologues TCP8 and TCP14 results in symptoms of BR deficiency in plants	14
2.1.3. <i>TCP15</i> over-expression promotes flowering	16
2.1.4. <i>TCP15</i> over-expression decreases BR sensitivity in the light	16
2.1.5. TCP15 and its homologues TCP8 and TCP14 are required for hypocotyl elongation in the dark	19
2.1.6. Over-expression of <i>TCP15</i> alters BRZ sensitivity in the light and dark	19
2.1.7. Over-expression of <i>CES</i> in <i>tcp8,14,15</i> has pleiotropic effects	22
2.1.8. Transcriptome analyses identify putative shared targets of CES and TCPs	25
2.1.9. <i>TCP15</i> over-expression promotes <i>CPD</i> and <i>EXPA1</i> expression	28
2.1.10. BR treatment increases the protein abundance of TCP15	29
2.1.11. TCP14 and TCP 15 directly bind to the promoter of <i>CES</i>	31
2.2. <i>SICES</i> is a functional CES orthologue	32
2.2.1. <i>SICES</i> over-expression alters GA homeostasis	32
2.2.2. <i>SICES</i> over-expression improves growth and fruit set at low ambient temperature	34
2.2.3. <i>SICES</i> over-expression impacts tomato fruit development	36
3. Discussion	38
4. Materials and methods	45
4.1 Plant material	45
4.2. Phenotyping in the seedling stage	45
4.3. Phenotyping of adult plants	46
4.4. Quantitative real-time PCRs (qPCRs)	47
4.5. Immunoblotting for detection of TCP15-YFP	47
4.6. Dual-luciferase reporter assay in Arabidopsis protoplasts	48
4.7. Yeast two-hybrid assays	49

4.8. Transcriptome analysis	49
4.9. GA measurement	50
4.10. Statistical analyses	50
References	51
Supplementary Information.....	60
Supplementary Tables.....	60
Acknowledgements	69

Abstract

Brassinosteroids (BRs) are plant hormones that are required for various aspects of plant growth and development, but also participate in stress responses. They utilize a phosphorylation-dependent signal transduction cascades, to alter the phosphorylation state of transcription factors that regulate BR responsive gene expression. One BR-controlled transcription factor is the basic helix-loop-helix (bHLH) protein CESTA (CES), which, together with its homologues BR ENHANCED EXPRESSION 1 (BEE1) and BEE3, participates in different BR-controlled processes, including vegetative growth, fruit development and cold stress tolerance.

In this thesis, molecular modes of CES activity were studied in the model plant *Arabidopsis thaliana* and, using a translational research approach, it was tested if CES activity in fruit growth and cold stress tolerance are conserved in the fruit crop *Solanum lycopersicum*. In *A. thaliana* it was investigated, if CES can interact with transcription factors of the TEOSINTE BRANCHED1/ CINCINNATA/ PROLIFERATING CELL (TCP) group, more specifically with the class I TCPs TCP8, TCP14 and TCP15, one of which had previously been isolated as putative CES-interacting partner in a yeast-two-hybrid screen. It was revealed that CES can interact with TCP8, TCP14 and TCP15 in yeast and that a loss-of-function of these TCPs in the triple mutant *tcp8,14,15* produced phenotypes indicative of impaired BR responses, including de-etiolated seedling morphologies in the dark and rounder leaves with shorter petioles in the light. An over-expression of *TCP15* resulted in phenotypes indicative of elevated BR responses, including increased hypocotyl elongation and a decreased sensitivity to the BR biosynthesis inhibitor brassinazole, phenotypes that resemble those of CES gain-of-function mutants. Transcriptome analysis uncovered joined CES and TCP targets, which were verified by qPCRs. Based on evidence that TCP14 and TCP15 can induce *CES* expression and that TCP15 protein abundance is increased by BRs, a model is proposed in which TCPs contribute to BR signaling, through transcriptional regulation of and interaction with CES and redundant factors.

In *S. lycopersicum* plants over-expressing a CES orthologue (SICES) were characterized, which showed that CES could promote fruit growth and cold stress tolerance in tomato. The possibilities and potential limitations of SICES over-expression as a breeding strategy for cultivated tomato are discussed.

Zusammenfassung

Brassinosteroide (BRs) sind Pflanzenhormone, die für verschiedenste Aspekte des Wachstums und der Entwicklung von Pflanzen benötigt werden, aber auch an ihrer Stressantwort beteiligt sind. Die BRs nutzen eine phosphorylierungsabhängige Signalübertragungskaskade, um den Phosphorylierungsstatus von Transkriptionsfaktoren zu verändern, welche die Expression von BR-regulierten Genen steuern. Ein solcher BR-regulierter Transkriptionsfaktor ist das basic helix-loop-helix (bHLH)-Protein CESTA (CES), das zusammen mit seinen Homologen BR ENHANCED EXPRESSION 1 (BEE1) und BEE3 an verschiedenen BR-kontrollierten physiologischen Prozessen, wie dem vegetativen Wachstum, der Fruchtentwicklung und der Kältestresstoleranz, beteiligt ist.

In dieser Arbeit wurden molekulare Mechanismen der CES-Aktivität in der Modellpflanze *Arabidopsis thaliana* untersucht und mit einem translationalen Forschungsansatz getestet, ob CES-Aktivität im Fruchtwachstum und der Kältestresstoleranz in der Kulturtomate *Solanum lycopersicum* konserviert ist.

In *A. thaliana* wurde untersucht, ob CES mit Proteinen aus der TEOSINTE BRANCHED1/ CINCINNATA/ PROLIFERATING CELL (TCP) Familie interagieren kann, spezifischer mit den Klasse I TCPs TCP8, TCP14 und TCP15, von welchen einer zuvor, als potentieller CES-Interaktionspartner, in einem yeast-two-hybrid screen isoliert worden war. Es konnte gezeigt werden, dass CES mit diesen TCPs in Hefe interagiert und dass ein Verlust der Funktion aller Proteine in einer *tcp8,14,15* Dreifachmutante zu Phänotypen führte, die einen Mangel an BR Signalübertragungsaktivität nahelegen. Eine TCP15 Überexpression führte hingegen zu Phänotypen die auf eine erhöhte BR Signalübertragung schließen ließen, Phänotypen die auch in CES gain-of-function Mutanten vorkommen. Basierend auf Evidenz, dass TCP14 und TCP15 CES Expression induzieren können und dass TCP15 Proteinstabilität durch BRs erhöht wird, wird eine Modell postuliert in dem TCPs zur BR Antwort beitragen, indem von CES und redundanten Faktoren sowohl die Transkription fördern, als auch mit diesen Faktoren interagieren.

In *S. lycopersicum* wurden Pflanzen die einen CES Orthologen überexprimieren charakterisiert, was zeigte, dass CES auch in Tomate die Fruchtentwicklung und Kältestressresistenz fördern kann. Chancen und mögliche Einschränkungen einer Erhöhung der CES-Aktivität als Züchtungsstrategie bei Tomate werden diskutiert.

Abbreviations

3-AT	3-Amino-1,2,4,-triazole
ABA	abscisic acid
bHLH	basic helix-loop-helix
bikin	4-[(5-bromo-2-pyridinyl)amino]-4-oxobutanoic acid
BL	Brassinolide
BRRE	BR-response element
BRZ	Brassinazole
CBB	Coomassie brilliant blue
DAG	Days after germination
DEGs	Differentially expressed genes
DMSO	Dimethylsulfoxide
DTT	1,4-dithiothreitol
GA	Gibberellic acid
GAPC2	Glyceraldehyde 3-phosphate dehydrogenase C2
GFP	Green fluorescent protein
GO	Gene ontology
HRP	Horseradish peroxidase
LUC	Luciferase
MS	Murashige and Skoog
NaCl	Sodium chloride
PCR	Polymerase chain reaction
PEG	Polyethylene glycol
PMSF	Phenylmethylsulfonyl fluoride
qPCR	Quantitative real-time PCR
SD	Selection drop-out medium
SDS	Sodium dodecyl sulfate
Tris-HCl	Tris(hydroxymethyl)aminomethane hydrochloride
wt	Wild-type
YFP	Yellow fluorescent protein

1. Introduction

1.1. Brassinosteroids regulate plant growth and development

As sessile organism, plants have to adapt to changes in their environments by adjusting their own growth and development and plant hormones significantly contribute to this ability. Brassinosteroids (BRs) are a class of hormones that are considered to play critical roles in adaptive growth, but also control developmental programs including seed germination, seedling development in the light and dark, vegetative growth processes, flowering time control and floral organ development (Clouse. 2011). In addition, BRs take part in stress responses, with a promotive role in tolerance against abiotic stress types such as cold, heat and drought stress and a repressive role in biotic stress resistance (Nolan et al., 2020; Ramirez and Poppenberger. 2020). This is achieved through a sophisticated interplay with other classes of hormones and in particular the cross-talk with auxins and gibberellins (GAs) during elongation growth, with ethylene during fruit development and with ABA during stress responses has been well-studied (Unterholzner et al., 2015; Ackerman-Lavert and Savaldi-Goldstein. 2020; Hu et al., 2020; Li et al., 2021).

In support of BRs playing essential roles in plant development, mutants impaired in BRs biosynthesis or signaling display extreme dwarf phenotypes, with dark green, round, cabbage-like leaves (Clouse. 2011). When BRs biosynthesis or signaling is hyperactive, plants show increased elongation of certain organs such as the hypocotyl and the leaves, which results in growth-distortion and sometimes in outwardly curving, epinastic leaves in *Arabidopsis thaliana* (Tsuge et al., 1996; Wang et al., 2001). However, and importantly, BR effects are concentration- and organ-dependent. While promoting hypocotyl elongation, BR application to roots, represses root growth already at relatively low concentrations. Moreover, BR hyper-response mutants of *A. thaliana* and *Oryza sativa* (rice) can show aspects of impaired elongation, such as reduced growth of the shoot and delayed flowering (Mora-García et al., 2004; Tong et al., 2014; Albertos et al., 2022). Thus, since altered BR levels and signaling capacities have drastic effects, maintaining a homeostasis of biologically active BRs is crucial to proper plant growth and development.

1.2. The BR biosynthesis pathway

BRs are polyhydroxylated steroids that can be classified into C₂₇, C₂₈ and C₂₉ BRs according to the alkyl substitutions on the C-24 position (Fujioka and Sakurai. 1997b; Jang et al., 2000). More than 70 BRs have been identified and among them, Brassinolide (BL) is the biologically most active form in many species, including the model plant *A. thaliana* (Fujioka and Yokota. 2003; Bajguz et al., 2020). Studies have shown that the biosynthesis of BL utilizes two parallel pathways, the early and the late C-6 oxidation route (Fujioka and Sakurai. 1997b; Fujioka and Sakurai. 1997a), which are interconnected (Fujioka and Yokota. 2003). The precursor for BR biosynthesis is the bulk sterol campesterol (CR), which undergoes multiple oxidation and hydroxylation events, to yield the polyhydroxylated steroid castasterone (CS). CS is the first product of BR biosynthesis that exhibits biological activity and is oxidized to BL, using the BR-6-OXIDASES 1 and 2 (Fujioka and Yokota. 2003; Choe. 2006; Ohnishi. 2018).

Many genes encoding key enzymes for BRs biosynthesis have been discovered, including *CONSTITUTIVE PHOTOMORPHOGENIC DWARF (CPD)/CYP90A1*, *DWARF4 (DWF4)/CYP90B1*, *ROTUNDIFOLIA 3 (ROT3)/CYP90C1*, *DE-ETIOLATED 2 (DET2)*, *BR6ox1* and *BR6ox2* (Bishop. 2007; Clouse. 2011; Zhao and Li. 2012; Rozhon et al., 2019). DET2 acts quite upstream in BR biosynthesis and is highly similar to the mammalian steroid 5 α -reductase. Since *det2* mutant phenotypes could be restored through complementation with the human 5 α -reductase (Li et al., 1996; Kushiro et al., 2001), there is evidence that DET2 is required for 5 α -reduction of sterols (Fujioka and Yokota. 2003). *CPD*, also known as *CYP90A1*, encodes a member of the cytochrome P450 family and it was the first P450 identified, that's involved in the BRs biosynthesis pathway. It is a 23 α -hydroxylase, which can catalyze C-3 oxidation of various early BRs intermediates (Szekeres et al., 1996; BancosÍ et al., 2002; Ohnishi et al., 2012). *DWF4* encodes another cytochrome P450 monooxygenase (CYP90B1). The phenotype of a *dwf4* mutant could be rescued by application of 22 α -hydroxylated BRs, and *in vitro* assays confirmed that *DWF4* encodes a 22 α -hydroxylase whose reaction is a rate-limiting step in the BR biosynthetic pathway (Choe et al., 1998; Fujita et al., 2006). ROT3 is considered to be a 23 α -hydroxylase and since its recombinant protein could catalyze C-23 hydroxylation of various 22 α -hydroxylated BRs *in vitro*. Consistent with the biochemical results, the BR-deficient phenotypes of a *ROT3* higher order mutant with its closest homologue *CYP90D1*,

cyp90c1/cyp90d1, could be rescued with external 22 α -hydroxylated BRs (Ohnishi et al., 2006). *BR6ox1* and *BR6ox2* encode 6 α -oxidases that act late in BR biosynthesis, with *BR6ox1* converting 6-deoxo-CS to CS, and *BR6ox2* converting CS to BL (Bishop et al., 1999; Shimada et al., 2001; Kim et al., 2005).

1.3. BRs perception and upstream signaling

Most key enzymes of BR biosynthesis were identified using forward genetic screens and *A. thaliana* as a model and this approach was also instrumental for identifying BR signaling components. *brassinosteroid-insensitive 1 (bri1)*, an EMS mutant, was identified because of its BR-insensitivity and its characteristic phenotypes, which include a de-etiolated seedling phenotype in the dark and a dwarf stature, dark-green, round leaves and strongly reduced fertility in the light (Clouse et al., 1996; Li and Chory. 1997). A positional cloning approach revealed that the phenotype is caused by mutation of a locus, positioned on chromosome 4, that encodes a leucine-rich repeat (LRR) receptor kinase. *BRI1* was found to be expressed in all tissues and organs, including leaves, stems, flowers and siliques (Li and Chory. 1997) and to be part of a small family of receptor-like kinases; its homologues are the *BRI1-LIKE* proteins *BRI1-LIKE 1 (BRL1)* and *BRL3* (Caño-Delgado et al., 2004).

BR binding studies that were conducted later, showed that *BRI1* can bind BR with its extracellular domain and transduce the hormonal signal across the plasma membrane via auto-phosphorylation of its intracellular kinase domain (Wang et al., 2001). An analysis of the amino acid sequence of *BRI1*, showed that the *BRI1* extracellular domain contains 24 leucine-rich repeats (LRRs) with an island domain (ID) between the 20 and 21 LRRs (Li and Chory. 1997). The cytoplasmic domain consists of three parts: a serine/threonine kinase domain, a juxta-membrane region and the C-terminal extension (Li and Chory. 1997). When *BRI1* binds bioactive BRs, its structure changes and a pronounced non-polar surface groove is created to facilitate BR binding (Hothorn et al., 2011; She et al., 2011).

BRI1-ASSOCIATED RECEPTOR KINASE (BAK1) is a co-receptor of *BRI1*, which associates with *BRI1* following BL-binding (Sun et al., 2013). Over-expression of *BAK1* can partially rescued the phenotypes of *bri1-5*, while over-expression of an inactive *BAK1* form resulted in dominant-negative phenotypes (Li et al., 2002). *BAK1* and *BRI1* can phosphorylate and trans-phosphorylate each other in sequential reactions (Li et al., 2002). *BAK1* directly interacts with *BRI1* upon BL-binding, which

results in BAK1 phosphorylation by BRI1 and an activation of BAK1. Activated BAK1 does then, in turn, trans-phosphorylate BRI1 and BRI1 obtains its full activity (Wang et al., 2008).

In addition to BAK1, also other proteins interact with BRI1. A well-characterized example is BRI1 KINASE INHIBITOR 1 (BKI1), which represses BRI1 function. This is achieved by dual modes. On the one hand BKI1 directly interacts with BRI1 and prevents it to convert into its active form. On the other hand BKI1 can reduce the interaction between BRI1 and BAK1. When BRI1 is activated through BL-binding, it phosphorylates BKI1 to inhibit their interaction, enabling BAK1 interaction and full activity (Wang and Chory. 2006).

BR signaling then commences via further phosphorylation and de-phosphorylation events and important phosphatases that take part are BRI1 SUPPRESSOR 1 (BSU1) and its homologues, which act as positive regulators of the pathway (Mora-García et al., 2004; Kim et al., 2009). BSU1 encodes a serine/threonine protein phosphatase and its over-expression can rescue the dwarf phenotype of *bri1*. This is proposed to be enabled by BSU1 activity in de-phosphorylation and inhibition of BRASSINOSTEROID-INSENSITIVE 2 (BIN2), a GSK3-shaggy-like kinase, which phosphorylates transcription factors, to repress their activity in the control of BR responsive genes.

The by far best-characterized negative regulators of BR signaling are BIN2 and its homologues BIN2-LIKE 1 (BIL1) and BIL2. BIN2 has various substrates in BR signaling, including the BR transcription factors BRASSINAZOLE-RESISTANT 1 (BZR1) and BRI1-EMS-SUPPRESSOR 1 (BES1). BIN2 targets a classical GSK3 consensus motif, namely tandemly repeated S/TxxxS/T sequences (Cohen and Frame. 2001), which are present in BZR1 and BES1 (He et al., 2005; Yin et al., 2005; Rozhon et al., 2010). When BR is low, BIN2-mediated phosphorylation inactivates BZR1 and BES1 by multiple mechanisms, including inhibiting their DNA-binding activity, stimulating their protein degradation and preventing their nuclear localization (He et al., 2002; Yin et al., 2002; Vert and Chory. 2006). In addition, many other transcription factors have been identified as BIN2 substrates, including MYELOBLASTOSIS FAMILY TRANSCRIPTION FACTOR-LIKE 2 (MYBL2), ATBS1-INTERACTING FACTOR 2 (AIF2), and HOMEODOMAIN-LEUCINE ZIPPER PROTEIN 1 (HAT1), and thereby BIN2 participates in the regulation of many aspects of plant growth (Ye et al., 2012; Zhang et al., 2014; Kim et al., 2017).

1.4. BR-regulated transcription factors of the BES1/BZR1 subfamily

The best-studied BR-regulated transcription factors are BZR1 and BES1, two homologous proteins that are part of a small subfamily of 6 homologous BES1 HOMOLOGUES (BEHs), which were both identified in mutant screens. *bzr1-ID*, was isolated in a screen for mutants insensitive against brassinazole (BRZ), an inhibitor of BR biosynthesis, which targets DWF4 (Asami et al., 2001). It is a gain-of-function mutant, which suppressed the ‘de-etiolation in the dark’ and ‘dwarf in the light’ phenotype of the weak *bri1-5* mutant (Wang et al., 2002). Sequencing of the mutated locus showed that in *bzr1-ID*, a single-point-mutation in the BZR1-encoding gene yielded a substitution of proline with leucine at amino acid 234. This increased the stability of BZR1 and produced aspects of growth phenotypes indicative of constitutive BR responses (Wang et al., 2002). Similarly, in *bes1-D* an amino acid change from proline to leucine in amino acid 233, increased BES1 protein stability and yielded similar phenotypes (Yin et al., 2002). BES1 and BZR1 are part of a small subfamily of proteins and, in line with a role as positive regulators of BR responses, an RNAi lines in which BES1 and homologues were targeted for silencing, produced dwarf phenotypes (Yin et al., 2002). A line generated with Crispr/Cas9 genome editing, where all 6 BEHs were mutated at the same time, showed as extreme dwarf phenotype, resembling strong BRI1 alleles, evidence for an essential function of the BEH proteins in BR signaling (Chen et al., 2019).

BES1 and BZR1 confer their activity by binding a regulatory motif called BR-response-element (BRRE; 5'-CGTGT/CG-3'), which is present in target promoters such as those of BR biosynthetic genes like *CPD* and *DWF4*, genes that are feedback repressed by BR (He et al., 2005). This activity is partly enabled by dimerization, either homo- or hetero-dimer formation, and in particular an interaction with basic helix-loop-helix (bHLH) proteins has been shown to be relevant. BES1 can interact with the bHLH transcription factor BES1-INTERACTING MYC-LIKE 1 (BIM1), to jointly bind to E-box motifs (5'-CANNTG-3') and promote expression of BR-induced genes such as *SAUR-AC1* (Yin et al., 2005).

Moreover, an interplay with the bHLH PHYTOCHROME-INTERACTING FACTOR 4 (PIF4), an essential component of light and high ambient temperature responses of plants, has also been reported. BZR1 can directly interact with PIF4 to control a subset of overlapped downstream target genes,

thereby promoting plant growth in response to BR in darkness, or at elevated ambient temperature (Oh et al., 2012; Yang et al., 2021). Light and warmth also impacted interactions of PIF4 with BES1, since light destabilized PIF4 and this, via promoting PIF4-BES1 interaction, repressed expression of the BR biosynthetic genes *DWF4* and *CPD*. When the accumulation of PIF4 was increased by elevated temperature, an improved interaction of PIF4 with BES1 enabled BES1 to activate BR biosynthetic genes via PIF4, which is a positive regulator of BR biosynthesis (Martínez et al., 2018). BES1/BZR1 activity is not only controlled by BRs, but also by GAs, through the transcriptional repressors DELLAs, which can interact with BES1 and BZR1 to inhibit their activity in a GA-repressed manner (Bai et al., 2012b; Gallego-Bartolomé et al., 2012). In line with an implication in GA responses, BES1/BZR1 can control certain GA-regulated gene classes, and this has been well-studied for GA biosynthetic genes. In *A. thaliana*, BES1 can directly bind to the promoters of *GA20ox1*, *GA3ox1* and *GA3ox4* to induce their expression in response to BR (Unterholzner et al., 2015). In rice, *GA3ox2* expression was enhanced by BZR1 (Tong et al., 2014). Since *GA20oxs* and *GA3oxs* are key genes that catalyze the formation of bioactive GA, BR can stimulate GA biosynthesis (Tong et al., 2014; Unterholzner et al., 2015) and that this activity is under DELLA control.

1.5. The bHLH proteins BEEs and CESTA

In addition to the BIMs and PIF4, also other typical bHLH proteins have been shown to be involved in BR signaling. One subfamily is the BR-induced genes *BR EARLY EXPRESSION 1-3* (*BEE1-3*), which act downstream of BRI1 and are rapidly induced by BL treatment. While single or double BEE mutants did not show notable phenotypes, a triple *bee1,2,3* mutant showed reduced BR responses, and subtle growth defects indicative of reduced BR signaling capacity in hypocotyls and flowers (Friedrichsen et al., 2002).

Close homologues of the BEEs are HOMOLOG OF BEE2 INTERACTING WITH IBH 1 (*HBI1*) and CESTA (*CES*), which, like PIF4, act as positive regulators of BR biosynthesis (Poppenberger et al., 2011; Fan et al., 2014). *HBI1* is the closest homologue of BEE2 and it has been shown that it can directly activate the expression of the BR biosynthetic genes *CPD*, *DWF4* and *BR6ox1* (Fan et al., 2014). Consistent with its positive role in BR biosynthesis, overexpression of *HBI1* yielded increased hypocotyl and petiole elongation, while inactivation of *HBI1* and its homologs caused a dwarf

phenotype (Bai et al., 2012a; Fan et al., 2014).

CES is the closest homologue of BEE1 and BEE3, with 34% and 36% amino acid sequence similarity respectively (Friedrichsen et al., 2002). It is expressed in all organs and developmental stages of Arabidopsis plants and is enriched in vascular and female reproductive tissues, in particular the reproductive tract (Crawford and Yanofsky. 2011; Poppenberger et al., 2011). CES was initially identified in a screen of an activation-tagged population of *A. thaliana* mutants by the gain-of-function phenotypes of *ces-D*. *ces-D* is a dominant mutant, that has longer hypocotyls and petioles, flowers late and has a specific leaf morphology, characterized by outwardly curving, epinastic growth (Poppenberger et al., 2011), phenotypic features that are also seen in mutants that over-express *DWF4*, *BR11* or *BSUI* (Wang et al., 2001; Mora-García et al., 2004).

Since *ces-D* showed phenotypes indicative of increased BR biosynthesis and/or responses, BR concentrations were measured in the mutant, and it was found that 6-deoxocastasterone and CS, were significantly increased as compared to wild-type. Moreover, the expression of the BR biosynthetic genes *CPD*, *DWARF4*, and *ROT3* was elevated in *ces-D* and it was shown that this is achieved through the ability of CES to bind G-box motifs (5'-CACGTG -3') in their promoters (Poppenberger et al., 2011). Some of the growth phenotypes of CES gain-of-function plants, such as *ces-D* and *35S:CES* over-expression lines, could be rescued by GA application, and it was shown that CES can increase the expression of both GA biosynthetic and catabolizing genes, in particular the GA-2-oxidase *GA2ox7* (Albertos et al., 2022), which catalyzes conversion of an upstream GA (Lange et al., 2005; Lange et al., 2020). In addition, a gain of CES function increases freezing tolerance, which is enabled by CES binding to G-box motifs in the promoters of the *C-REPEAT/DEHYDRATION-RESPONSIVE ELEMENT BINDING FACTORS* (*CBFs1-3*), *CENTRAL REGULATORS OF COLD-RESPONSIVE* (*COR*) genes (Eremina et al., 2016). In line with these activities, a loss of CES function in higher order mutant combinations with the BEEs, namely a triple mutant *tM* (*ces bee1 bee3*) and quadruple mutant *qM* (*ces bee1 bee2 bee3*), yielded reduced *CBFs* and *COR* gene expression as well as freezing tolerance (Eremina et al., 2016). Moreover, CES/BEE *tM* and *qM* plant were unable to induce *GA2ox7* expression in response to BR and were GA hypersensitive (Albertos et al., 2022).

In addition to impacting growth and cold stress responses, CES is also known to play a role in

reproductive tract development, since *ces bee1 bee3* triple mutants showed half-filled siliques, which was found to be caused by defective extracellular matrix production and induced cell death events (Crawford and Yanofsky. 2011). However, direct CES targets that enable its function in reproductive development have remained unknown.

1.6. Transcription factors of the TCP family and their implication with BRs and GAs

TEOSINTE BRANCHED1/CYCLOIDEA/PROLIFERATING CELL FACTORS (TCPs) are a group of plant-specific transcription factors that have also been implicated in BR signaling and contain a domain with bHLH-like features. This domain, also known as TCP domain, is mainly needed for protein-protein interaction and DNA binding capacities (Cubas et al., 1999). In *A. thaliana*, a total of 24 TCP transcription factors exists, which can be classified into two classes, the TCP I and TCP II class, whose amino acid sequences differ in the TCP domain, where TCP I factors have four amino acids less. TCP class II proteins can be further divided into two subclasses CYC/TB1 and CIN based on the difference of additional diagnostic residues (Nicolas and Cubas. 2016).

TCP I subfamily members can recognize a conserved classical binding site, namely 5'-GGNCCCAC-3'; however some shorter versions, such as 5'-(T)TGGGCC-3', 5'-GCCCR-3' and 5'-GG(A/T)CCC-3', have also been shown to be bound (Kosugi and Ohashi. 2002; Trémousaygue et al., 2003; Martín-Trillo and Cubas. 2010). TCP II factors recognize a distinct but similar site, 5'-GTGGNCCC-3', indicating that the core sequence 5'-GGNCCC-3' plays a key role in sequence recognition (Martín-Trillo and Cubas. 2010). Since TCP II factors can also bind TCP I sites, there may be competition in DNA binding among the TCPs (Costa et al., 2005).

Dimer formation plays an important role in TCP DNA binding activity (Kosugi and Ohashi. 1997), because when the dimerization capacity is lost, the DNA binding ability of the proteins is impaired (Kosugi and Ohashi. 2002). Yeast two-hybrid (Y2H) assays showed that TCP factors can interact with themselves or with other TCPs to form homo- or hetero-dimers, with a preference to hetero-dimerize with TCPs from the same clade (Danisman et al., 2013). The formation of dimers greatly increases the diversity of downstream targets recognized by TCP proteins, which may diversify their function in growth and development processes.

Functional redundancy is an important feature of TCP activity and many show over-lapping

expression patterns (Danisman et al., 2013). Most TCP single mutants usually don't show obvious phenotypic changes (Li et al., 2005; Takeda et al., 2006; Tatematsu et al., 2008). Studies thus usually used higher order mutants and with this approach it has been shown that the TCPs are involved in the regulation of cell proliferation and growth (Nicolas and Cubas. 2016), with many connections to BR and GA signaling.

TCP1, a member of clade II, was shown to act as a positive regulator of BR biosynthesis. Overexpression of *TCP1* repressed the weak BR-deficient and BR-insensitive phenotypes of the *det2* and *bri1-5* mutants, and *TCP1* expression was up-regulated by BR (Guo et al., 2010). Further studies confirmed that TCP1 can promote expression of the BR biosynthetic gene *DWF4* by directly binding to its promoter (Guo et al., 2010).

The clade I TCPs TCP14 and TCP15 have not as yet been implicated in BR signaling, but like BES1/BZR1 can interact with DELLA proteins. In seeds, the two DELLA proteins GAI and RGL2, were shown to interact with TCP14 and TCP15 to inhibit their activities, and TCP14 and TCP15 double loss-of-function mutant showed lower germination rates, due to a reduced cell division in the root apical meristems (Resentini et al., 2015). In addition, there is evidence that in the inflorescence shoot apex, the interaction between TCP factors and DELLAs affects the outgrowth of inflorescence primordia (Davière et al., 2014). In line with these TCPs being controlled by DELLAs, a *tcp14 tcp15* double mutant was less sensitive to GA treatment (Davière et al., 2014; Resentini et al., 2015).

In analogy with BES1 and CES, TCP factors have also been shown to be involved in the regulation of GA biosynthesis. In *A. thaliana*, TCP15, like BES1, can directly bind to the promoter of the GA biosynthesis gene *GA20ox1* and induce its expression during thermomorphogenetic growth (Ferrero et al., 2019). In tomato, the TCP4 ortholog *LANCEOLATE* was shown to regulate GA biosynthesis by upregulating the expression of *SIGA20ox1* (Yanai et al., 2011).

1.7. BRs induce posttranslational modifications of transcription factors

The function of BR-regulated transcription factors is controlled via posttranslational modifications, which are catalyzed by different factors and induce various effects, including an impact on protein stability, cellular localization and transcriptional activity. The best studied regulatory routes are BIN2-mediated phosphorylation events, which are repressed by BRs. An activation of BR signaling

inactivates BIN2 and homologues, which phosphorylate BES1 and BZR1, and thereby induces accumulation of these transcription factors in their non-phosphorylated, active forms (Wang et al., 2002; Yin et al., 2002; Zhao et al., 2002). Moreover, BES1 and BZR1 are SUMOylated, which is thought to impact their stability, but in opposite manners. BES1 can be SUMOylated by the E3 ligase SAP AND MIZ1 DOMAIN-CONTAINING LIGASE1 (SIZ1), which destabilizes and inhibits it (Zhang et al., 2019). In contrast, SUMOylation stabilized BZR1 in the nucleus by inhibiting its interaction with BIN2 kinase (Srivastava et al., 2020).

CES is also controlled by phosphorylation, mediated by BIN2. However, as opposed to BES1/BZR1 phosphorylated CES was more stable and transcriptionally active, indicating that CES activity, at least on certain promoters, is repressed by BRs (Khan et al., 2014). In addition to phosphorylation, CES was also regulated by SUMOylation and this was shown to control CES protein stability, but more interestingly also its subnuclear distribution. An activation of BR signaling resulted in CES accumulation in distinct subnuclear foci and this re-localization was lost when a SUMOylation site, through mutation of lysine 72, was deleted. Two phosphorylation sites close to the SUMOylation site antagonized SUMOylation, which were phosphorylated, at least *in vitro*, by calcium-dependent protein kinases (Khan et al., 2014). SUMOylation not only affected CES protein stability and subnuclear distribution, but also its transcriptional activity and is thus a means to alter the localization and activity of this protein (Miura et al., 2007; Eremina et al., 2016).

Interestingly, there is first evidence that also some TCPs are regulated by SUMOylation. SCE1 is a SUMO conjugating enzyme, and studies have shown that multiple TCP factors can interact with SCE1 through their catalytic sites, including TCP8, TCP14 and TCP15 as well as TCP1 and TCP3 (Mazur et al., 2017). Moreover, TCP proteins re-localized to the nucleus after SUMOylation and TCP3, TCP8, TCP14 and TCP15 proteins show a speckled nuclear expression pattern (Mazur et al., 2017).

1.8. BR activity in tomato

Most of the BR research published today, used *A. thaliana* as a model, to facilitate molecular genetic studies. However, also research with crops is being performed, and BR activity has in particular been studied in rice, *Pisum sativum* (pea) and *Solanum lycopersicum* (cultivated tomato). *S. lycopersicum* is a highly valued, nutritious fruit crop that serves as a model to investigate chilling tolerance and

fleshy fruit development, where BRs contribute.

Multiple components of BR biosynthesis or signaling have been studied in *S. lycopersicum* and shown to impact relevant traits. For example, over-expression of *SIDWARF* promoted seed germination and increased the carotenoid content of tomato fruits. Although the fruit yield per plant was not affected, over-expressing *SIDWARF* led to a more compacted plant architecture, with the fruit yield per square meter being significantly increased (Li et al., 2016). Over-expression of *SICYP90B3*, a homologue gene of *SIDWARF*, in tomato promoted fruit ripening and increased the content of carotenoids, the process depending on the plant hormone ethylene, since treatment with 1-MCP, an ethylene-perceiving inhibitor, repressed the increase of carotenoids in *SICYP90B3* over-expression fruits (Hu et al., 2020).

In terms of BR signaling, tomato has allowed for early studies on BR perception, where it was found that the BRs signaling receptor *SIBRI1* was essential for the root elongation response induced by systemin (Holton et al., 2007). Systemin is an 18 amino acid peptide, which is considered to be involved in the spreading of signals that trigger systemic defense responses. Further study confirmed that the *SIBRI1* homologue SYSTEMIN RECEPTOR 160 (SYR160) was the receptor of systemin (Wang et al., 2018). Over-expression of *SIBRI1* promoted seed germination and seedling development, and increased the expression of ethylene biosynthetic genes as well as the accumulation of ethylene during fruit development. Thereby fruit quality parameters, such as the accumulation of carotenoids, were improved (Nie et al., 2017).

Over-expression of an auto-phosphorylated, constitutively active *SIBRI1* version, promoted internode length and stem diameter resulting in larger plants with larger leaves. Also, the size of individual fruits increased due to faster cell division and expansion during fruit development (Wang et al., 2019a; Wang et al., 2021). In addition to affecting growth, constitutive autophosphorylation of *SIBRI1* affected abiotic stress tolerance. When over-expressing an *SIBRI1* form that was auto-phosphorylated at serine 1040, heat stress tolerance was increased (Wang et al., 2020).

Tomato has also been used to investigate the function of different BR-regulated transcription factors. Ectopic over-expression of *Arabidopsis AtBZR1-ID* in tomato promoted fruit ripening and increased the content of soluble sugars, carotenoids, and ascorbic acid in fruits (Liu et al., 2014). In the *SIBZR1*

loss-of-function mutant *Sibzr1-1*, pollen viability and germination, as well as the number of seeds per fruit were decreased when compared with wild-type plants (Yan et al., 2020). Moreover, it was shown that *SIBZRI* expression was induced by chilling stress and that, in analogy to its Arabidopsis orthologue, it could directly bind to the promoters of the *SICBFs 1-3*, to promote their expression and increase the chilling tolerance of tomato plants (Chi et al., 2020; Fang et al., 2021). Over-expression of *SIBES1* promoted fruit softening (Liu et al., 2021) while *SIBIM1a* overexpression repressed fruit growth and produced strongly dwarfed plants (Mori et al., 2021).

1.9. Aims of this study

In this thesis, the function of the bHLH transcription factor CES was studied in *A. thaliana* and *S. lycopersicum*, to increase our understanding of interacting partners and modes of activity in cold stress tolerance and fruit development.

In the first part of the work it was investigated, if CES can interact with TCP14 and its homologues TCP8 and TCP15. Y2H interaction experiments were performed and the effects of a loss-of-function of all three TCPs (in a *tcp8,14,15* triple mutant), or an over-expression of *TCP15*, on plant growth and BR responses were investigated. Moreover, it was assessed if CES gain-of-function phenotypes rely on these TCPs, by generating and analyzing a *ces-D x tcp8,14,15* quadruple mutant, and if *CES* expression is TCP-controlled. Using generated *35S:TCP15-YFP* lines, it was further tested, if TCP15 protein stability is impacted by BR application, to address if TCP15 and its homologues TCP8 and TCP14 may be components of BR signaling. A model, integrating the findings of this work into our current understanding of BR signaling is proposed.

In the second part of the thesis, using a translational research approach, it was aimed to identify a CES orthologue of tomato, and investigate, if it can be utilized to promote cold stress tolerance and fruit growth through over-expression. Based on amino acid sequence similarity and the presence of regulatory motifs, a tomato CES orthologue (*SICES*) had previously been identified, and the effects of a hyper-accumulation of *SICES* were analysed here. Independent transgenic lines over-expressing *SICES* were chemotyped and phenotyped, with a focus on altered GA metabolism for the former and altered cold tolerance and fruit characteristics for the latter. The possibilities and limitations of increasing *SICES* activity as a breeding strategy for tomato are discussed.

2. Results

2.1. TCP15 is a CES interacting factor that takes part in BR responses

2.1.1. CES interacts with TCP8, TCP14 and TCP15 in yeast

A Y2H screen, which had previously been conducted in the Poppenberger lab with CES as a bait, had pulled TCP14 and it was thus a candidate for a CES interacting factor. To verify if CES can interact with TCP14 and also test homologues for interactions, the clade I TCPs TCP8, TCP14, TCP15, as well as CES, were cloned into the Y2H vectors pGADT7 and pGBKT7, respectively, where pGADT7 contains the activation domain (AD) and pGBKT7 contains the binding domain (BD) of GAL4 (Louvét et al., 1997). Different vector combinations were transformed into competent cells of the yeast strain AH109, and transformants were selected on drop-out medium without tryptophan and leucine (SD-TL). Yeast cells that grew on SD-TL were then spotted in different dilutions, onto drop-out medium without tryptophan, histidine and leucine (SD-TLH), containing 3-amino-1,2,4-triazole (3-AT) to inhibit a potential auto-activation of CES in the binding domain vector, something that is frequently seen for transcription factors (Joung et al., 2000).

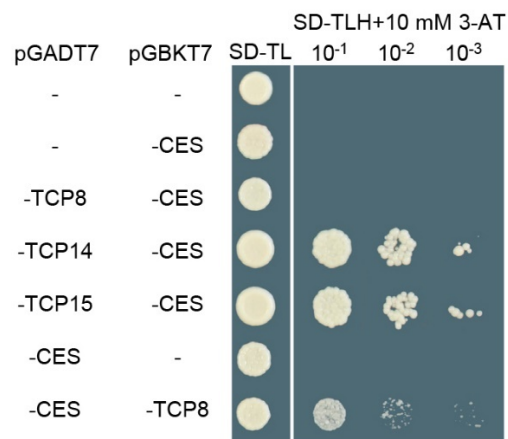


Figure 1. CES interacts with TCP8, TCP14 and TCP15 in yeast.

Yeast was transformed with the combination of constructs shown on the left and spotted onto SD-TL or SD-TLH+10 mM 3-AT in different concentrations. The plates were then incubated for 5 days at 28°C and photos were taken.

The results showed that the two negative controls (empty pGADT7 + pGBKT7-CES and pGADT7-CES + empty pGBKT7) did not grow in the absence of histidine. However, when BD-CES was

combined with AD-TCP14 or AD-TCP15, growth on -histidine drop-out medium was observed, showing that CES interacts with both TCP14 and TCP15 in yeast (Figure 1). No growth was enabled when BD-CES was combined with AD-TCP8.

To exclude the possibility that this AD-BD combination was unsuitable to enable interaction, CES was cloned into pGADT7 and TCP8 was cloned into pGBKT7 and the assay was performed again. This showed that yeast cells transformed with AD-CES+BD-TCP8 could grow on SD-TLH medium, albeit with a weaker efficiency than yeast containing BD-CES with AD-TCP14 or BD-CES with AD-TCP15. Thus, in summary, CES can interact with all three TCPs in yeast, but shows a better interaction with TCP14 and TCP15, than with TCP8, in the Y2H system.

2.1.2. A loss-of-function of TCP15 and its homologues TCP8 and TCP14 results in symptoms of BR deficiency in plants

Since CES could interact with TCP14 and TCP15 in yeast, the question was asked, if this interaction may be relevant and impact CES activity *in planta*. To address this, a published *TCP15* over-expression line (*35S:TCP15*) (Viola et al., 2016) and a *tcp8,14,15* triple mutant (Kim et al., 2014) were phenotyped in short-day growth conditions in soil, and compared to *ces-D* and the *ces bee1,2,3* quadruple mutant (*ces bee qM*). TCP15 was chosen, since, as opposed to TCP14, an over-expression line was available, allowing for gain-of-function studies.

The results showed that in line with previous observations (Poppenberger et al., 2011; Albertos et al., 2022), *ces-D* developed leaves with an outwardly curving, epinastic shape and longer petioles (Figure 2A, E), a smaller rosette and an increased leaf number, produced from secondary rosettes (Figure 2B, D). Also, in line with previous work, the *ces bee qM* did not show significant changes in terms of rosette size and number of secondary rosettes, but had flatter leaves than wild-type (Figure 2A). The *tcp8,14,15* triple mutant plants had a significantly reduced number of secondary rosette leaves, with the leaves showing a more roundish shape, with flatter blades and hardly any serration (Figure 2A, D, E), which corresponded with a decreased rosette size. Thus, *tcp8,14,15*, more prominently than the *ces bee qM*, showed aspects of BR-deficient phenotypes. Plants of the *35S:TCP15* over-expression (*TCP15oe*) line were significantly larger than wild-type and formed more secondary rosette leaves, which were larger and more serrated (Figure 2A, B, D).

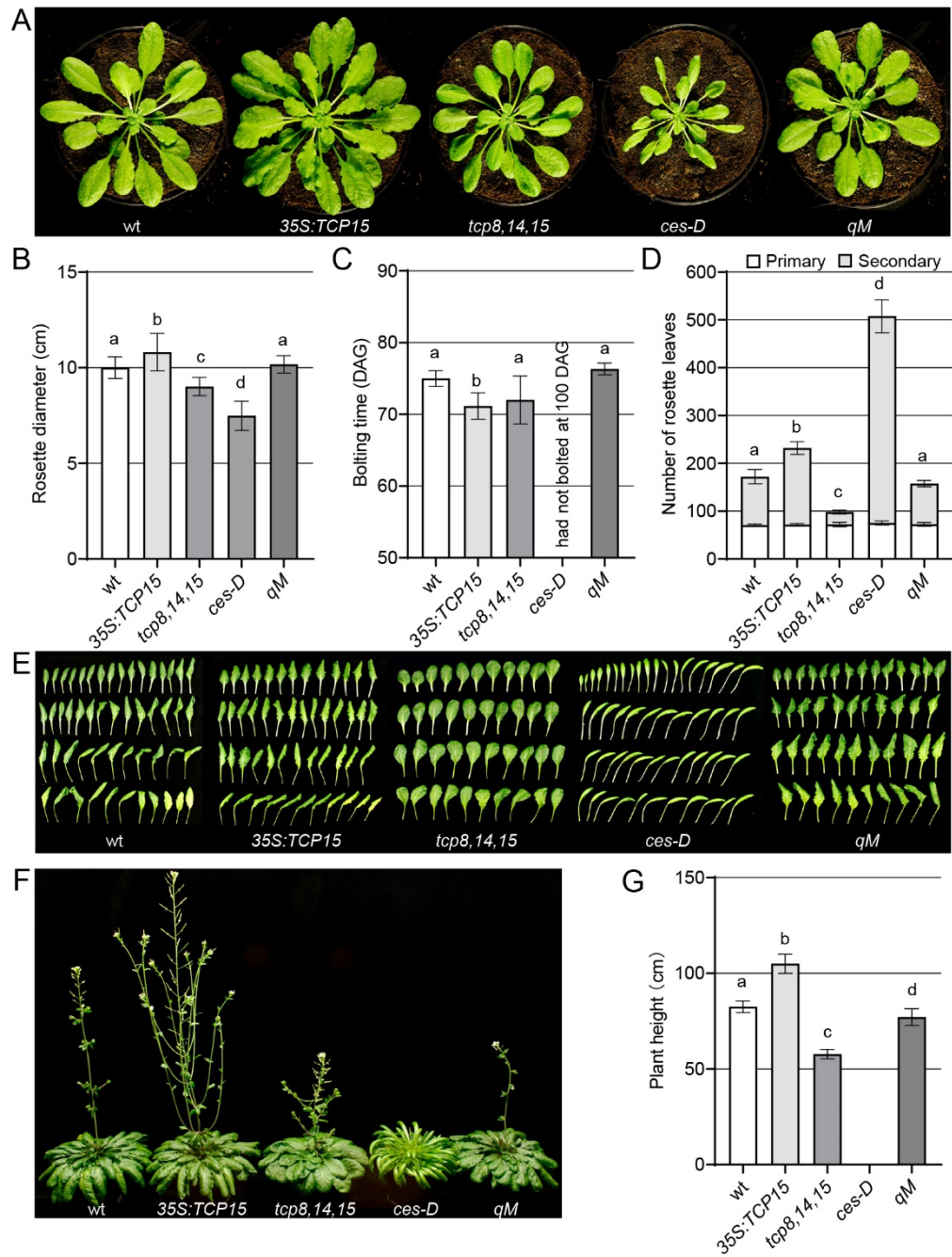


Figure 2. *tcp8,14,15* triple mutant plants show symptoms of BR deficiency

The indicated lines were grown in 8 hours light/ 16 hours dark cycles (short days) to document the morphology and quantify the rosette size, bolting time, total number of rosette leaves and plant height. (A-B) Plants at 7 weeks after germination, showing photos of representative plants from above (A) and the rosette diameter in cm (B). (C) Number of days after germination at bolting. (D-E, G) Plants at 15 weeks after germination, showing the total number of rosette leaves (D), photos of all primary rosette leaves of a representative plant (E) and plant height in cm (G). (F) Photos of representative plants at 13 weeks after germination. In the graphs: data show means \pm SD (n=12) and statistically significant difference at $P \leq 0.05$ is indicated with different letters and was determined with one-way ANOVA.

In summary, an over-expression of both *TCP15* and *CES* promotes secondary rosette leaf formation and alters leaf shape. A loss of TCP8, TCP14 and TCP15 function in *tcp8,14,15* repressed secondary rosette leaf development and produced aspects of BR-deficient phenotypes, such as more roundish leaves with shorter petioles in mutant plants.

2.1.3. *TCP15* over-expression promotes flowering

A process where both CES and TCPs have been shown to take part is the developmental phase transition from vegetative to reproductive development. Over-expression of both *TCP8* and *CES*, but also a loss of CES function, delayed flowering (Wang et al., 2019b; Albertos et al., 2022) and it was thus of interest to assess flowering time control in *TCP15oe* and *tcp8,14,15* plants. Consistent with previous results, *ces-D* did not flower in short-day growth conditions, whereas *TCP15oe* bolted significantly earlier than the wild-type, as evidenced by a bolting with fewer leaves than wild-type (Figure 2C). Flowering in the *tcp8,14,15* and *ces bee qM* was not changed.

A measurement of plant height at 15 weeks after germination showed that *TCP15oe* plants, in line with flowering early, were larger at this time point. The *tcp8,14,15* and *ces bee qM* had both developed shorter inflorescences than wild-type (Figure 2F, G).

2.1.4. *TCP15* over-expression decreases BR sensitivity in the light

Since TCP15 could interact with CES in yeast and some of the phenotypes of CES and TCP15 gain- and higher order loss-of-function mutants showed similarities, it was of interest to investigate if TCP15 and its homologues TCP8 and TCP14 may participate in CES modes of activity in BR-responsive growth. To do this, the response of *TCP15oe* and *tcp8,14,15* seedlings to the BR 24-epiBL (epiBL) was investigated and compared with *ces-D*. Wild-type, *ces-D*, *35S:TCP15*, *tcp8,14,15* and seeds were germinated on ½ MS medium with different concentrations of epiBL, stratified and incubated in low light conditions for 8 days before hypocotyl length was measured. Both absolute values and relative responses, as compared to the untreated control, were determined and are shown, together with pictures of representative plants, in Figure 3.

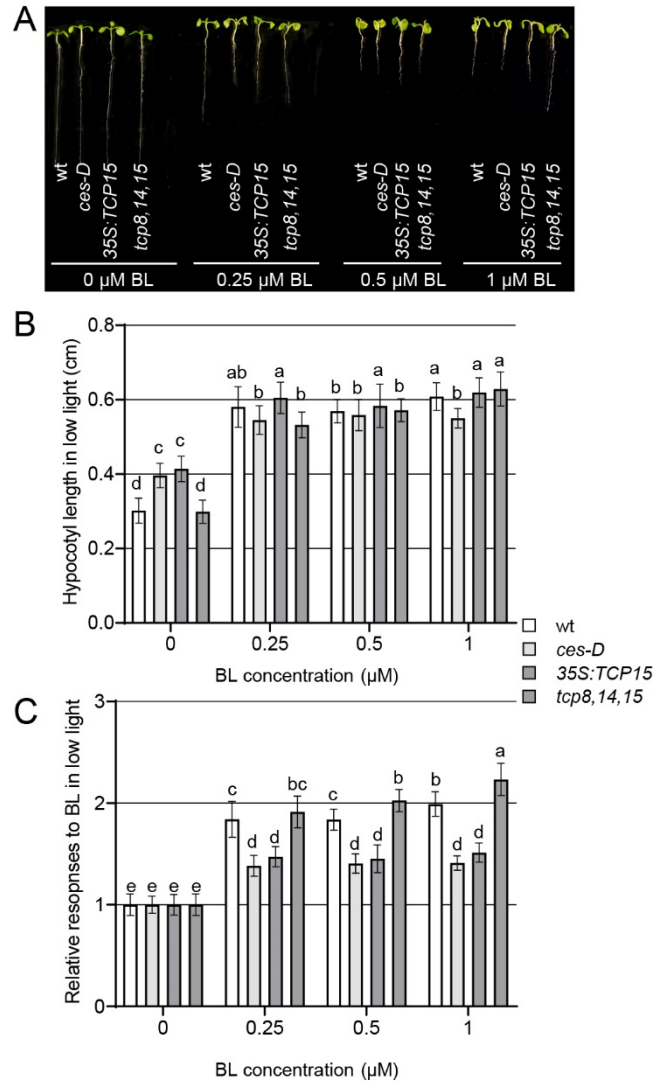


Figure 3. *TCP15* over-expression promotes hypocotyl elongation and reduces BR sensitivity in light-grown seedlings.

Seeds were plated on ½ MS medium containing the indicated concentrations of 24-epiBL or DMSO as a control (0) and incubated in long-days at low light levels of $30 \mu\text{mol} \cdot \text{m}^{-2} \cdot \text{s}^{-1}$ for 8 days, before hypocotyl length was measured. (A) Photos of representative seedlings. (B) Absolute hypocotyl length in cm. (C) Relative differences within the lines as compared to the untreated controls, data were calculated as the ratio of treated hypocotyl length to untreated hypocotyl length. Data show means \pm SD (n=12), with the letters indicating significant differences between genotypes and treatments ($P \leq 0.05$; two-way ANOVA).

In untreated conditions, *ces-D* had longer hypocotyls, which was consistent with previous findings (Poppenberger et al., 2011) and also the hypocotyls of *TCP15oe* were significantly longer (Figure 3A, B). *tcp8,14,15* mutant seedlings showed no difference in hypocotyl length in untreated conditions.

When epi-BL was applied to the medium, an elongation response was triggered in all lines (Figure 3B), with *ces-D* and *TCP15oe* seedlings responding significantly less to the hormone than wild-type

(Figure 3C). Moreover, importantly, the *tcp8,14,15* mutant was hypersensitive to epiBL, elongating more strongly, which was particularly evident at 0.5 μM and 1.0 μM epiBL (Figure 3C). Thus, in summary, TCP15, like CES, promotes hypocotyl elongation and is required for a proper BR-response in light-grown seedlings.

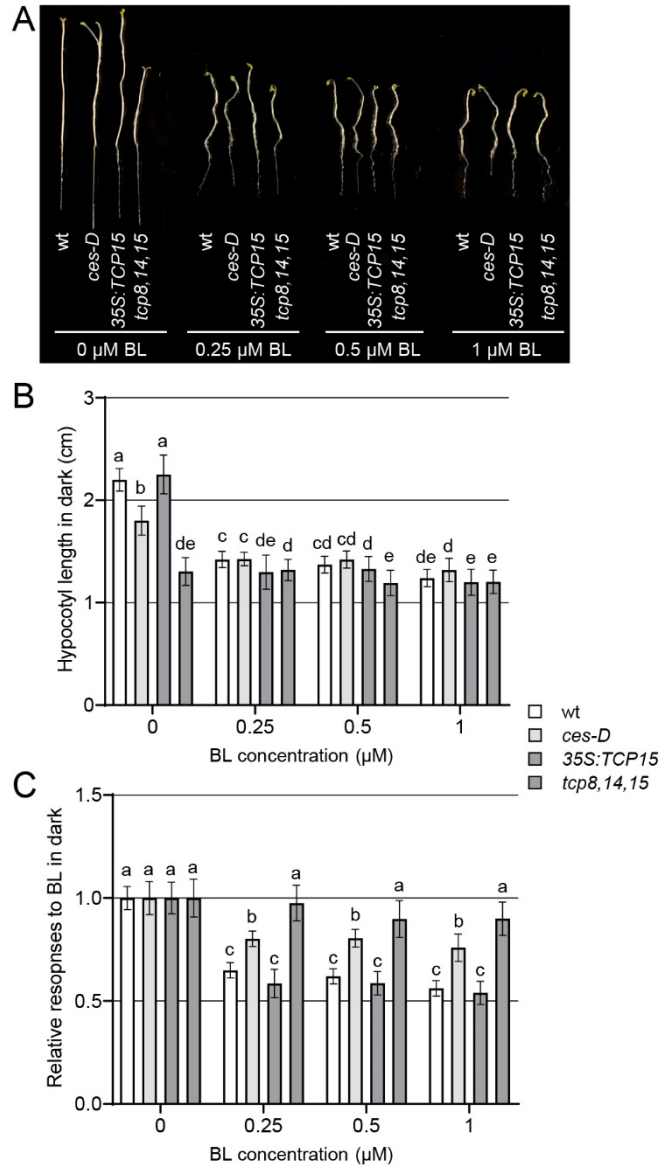


Figure 4. *tcp8,14,15* triple mutant plants are compromised in hypocotyl elongation and BR responses in the dark.

Seeds were plated on $\frac{1}{2}$ MS medium containing the indicated concentrations of 24-epiBL or DMSO as a control (0) and incubated in the dark for 8 days, before hypocotyl length was measured. (A) Photos of representative seedlings. (B) Absolute hypocotyl length in cm. (C) Relative differences within the lines as compared to the untreated controls, data were calculated as the ratio of treated hypocotyl length to untreated hypocotyl length. Data show means \pm SD (n=12), with the letters indicating significant differences between genotypes and treatments (P \leq 0.05; two-way ANOVA).

2.1.5. TCP15 and its homologues TCP8 and TCP14 are required for hypocotyl elongation in the dark

BRs play an essential role in hypocotyl elongation also in the dark, and the epiBL response of dark-grown seedlings was therefore also investigated. Seeds were plated on the same medium as before, stratified for 2 days, given a light impulse of 30 minutes and then incubated for 8 days in the dark. In the dark, *ces-D* showed aspects of de-etiolated growth, namely shorter hypocotyls and more open cotyledons with longer petioles, which could be rescued by epiBL treatment (Figure 4A).

While the *TCP15oe* line did not show a significant difference in hypocotyl length or BL responses to wild-type, the *tcp8,14,15* had much shorter hypocotyls in the dark, with a reduction of almost 50% as compared to wild-type (Figure 4A, B). Moreover, it was less responsive to the repressive effects of epiBL on hypocotyl elongation in the dark (Figure 4C). Thus, TCP15 and its homologues TCP8 and TCP14 are required for hypocotyl elongation and also for an adequate response to changes in BR homeostasis in the dark.

2.1.6. Over-expression of TCP15 alters BRZ sensitivity in the light and dark

To further analyze the role of TCP15 and its homologues TCP8 and TCP14 in responses to an altered BR homeostasis, treatments with the BR biosynthesis inhibitor BRZ were carried out, using the same experimental conditions both in the light and dark as described above, but with different concentrations of BRZ added to the medium. The results confirmed that *TCP15oe* seedlings had longer hypocotyls in the light, and showed that they are less sensitive to BRZ application, with the clearest difference at 0.25 μ M and 0.5 μ M BRZ (Figure 5A-C). Seedlings of the *tcp8,14,15* mutant did not show an altered BRZ response in the light.

In the dark, BRZ repressed hypocotyl elongation in all lines, but *ces-D* and *TCP15oe* seedlings were more resistant to the treatment, with significant differences at a concentration of 0.25 μ M BRZ (Figure 6A-C). *tcp8,14,15* mutant hypocotyls were significantly shorter on control plates, confirming the results from the epiBL experiment in the dark, and while still clearly responding to BRZ (Figure 6A-C), responded less in relative terms than wild-type.

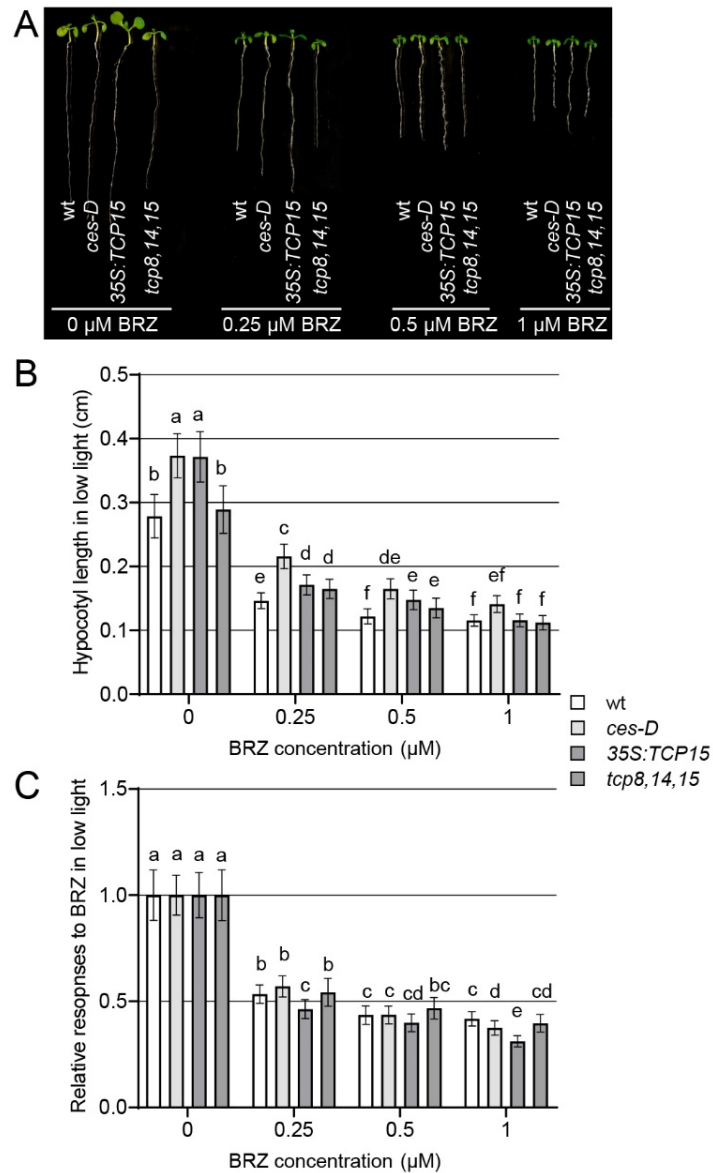


Figure 5. *TCP15* over-expression increases BRZ sensitivity of hypocotyls in light-grown seedlings.

Seeds were plated on $\frac{1}{2}$ MS medium containing the indicated concentrations of BRZ or DMSO as a control (0) and incubated in long-days at low light levels of $30 \mu\text{mol}\cdot\text{m}^{-2}\cdot\text{s}^{-1}$ for 8 days, before hypocotyl length was measured. (A) Photos of representative seedlings. (B) Absolute hypocotyl length in cm. (C) Relative differences within the lines as compared to the untreated controls, data were calculated as the ratio of treated hypocotyl length to untreated hypocotyl length. Data show means \pm SD (n=12), with the letters indicating significant differences between genotypes and treatments ($P \leq 0.05$; two-way ANOVA).

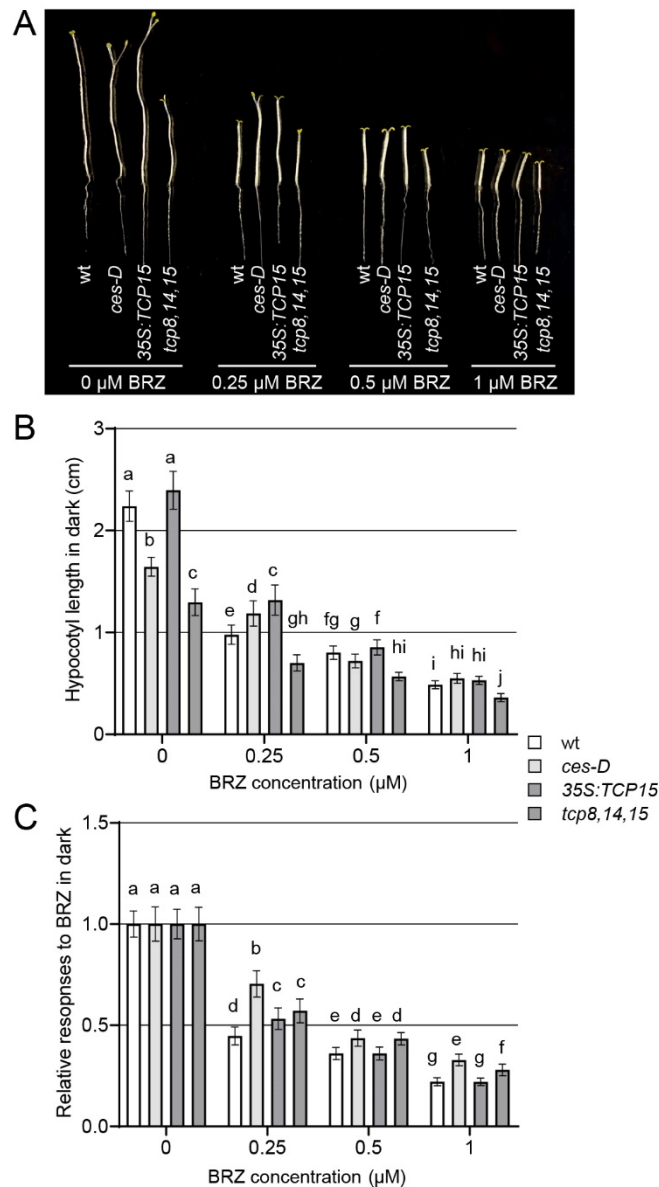


Figure 6. Seedlings of the *tcp8,14,15* triple mutant are less sensitive to BRZ in the dark.

Seeds were plated on ½ MS medium containing the indicated concentrations of BRZ or DMSO as a control (0) and incubated in the dark for 8 days, before hypocotyl length was measured. (A) Photos of representative seedlings. (B) Absolute hypocotyl length in cm. (C) Relative differences within the lines as compared to the untreated controls, data were calculated as the ratio of treated hypocotyl length to untreated hypocotyl length. Data show means ± SD (n=12), with the letters indicating significant differences between genotypes and treatments ($P \leq 0.05$; two-way ANOVA).

In summary, the hypocotyl elongation experiments showed that the *tcp8,14,15* mutant exhibited de-etiolated seedling growth in the dark, and an altered response to epiBL and BRZ treatments, a characteristic feature of BR deficient plants. In the light, while *tcp8,14,15* mutant plants looked clearly BR deficient, *tcp8,14,15* seedlings showed only a subtle BR phenotype, namely an increased

hypocotyl elongation response in presence of epiBL. *TCP15* over-expression promoted hypocotyl elongation in the light, decreased BR sensitivity and increased BRZ sensitivity particularly in the light.

2.1.7. Over-expression of *CES* in *tcp8,14,15* has pleiotropic effects

The phenotypic assessments suggested that *TCP15* and its homologues *TCP8* and *TCP14* may act synergistically with *CES* in the control of BR responses. Since *CES* can interact with these *TCPs* in yeast, it was aimed to investigate, if *CES* activity is promoted by them *in planta*. To do this, *ces-D* was introduced into *tcp8,14,15* by crossing and a *tcp8,14,15 x ces-D* quadruple mutant was isolated using genotyping (Figure 7A). This yielded not only a quadruple mutant, but also different mutant combinations, namely *tcp8 x ces-D* and *tcp14,15 x ces-D*, in which *CES* expression was determined by quantitative real-time PCR (qPCR). The result showed that *CES* expression decreased, with the increasing number of *tcp* T-DNA mutations introduced. The reduction was weakest in the *tcp8* single knock-out background and strongest in the *tcp8,14,15* triple mutant background, where *CES* mRNA levels were reduced by approximately two orders of magnitude, as compared to the parent line *ces-D* (Figure 7B). This is likely due to co-suppression of the 35S-enhancer elements in the activation-tag of *ces-D* (which drives *CES* expression; Poppenberger et al., 2011), by the 35S promoters contained in the *tcp* mutants, which are all SALK lines (Daxinger et al., 2008). The reduction in *CES* mRNA levels was correlated with a reduction of *ces-D* phenotypes, which was obvious in terms of flowering time and leaf shape (Figure 7B, D).

An expression analysis of *CES*, *TCP8*, *TCP14* and *TCP15* was also carried out in the *tcp8,14,15* parent line, which showed that *CES* expression was not changed significantly in this developmental stage. Moreover, while *TCP15* expression was reduced, *TCP8* and *TCP14* mRNA abundance was not significantly altered (Figure 7C). This is in line with previous reports. However, since in the *tcp8,14,15* triple mutant, the T-DNAs are integrated in the ORFs of all three genes, the line is considered a full knock-out (Kim et al., 2014).

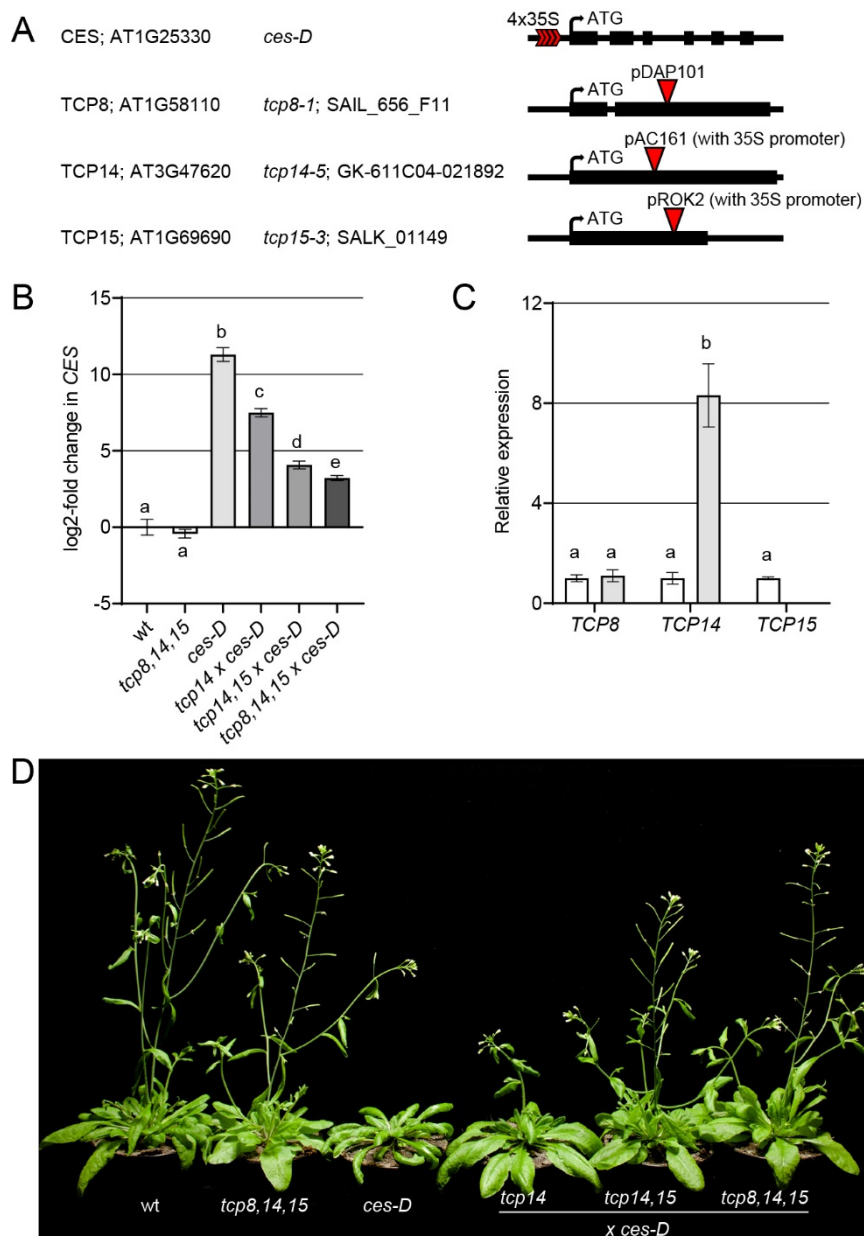


Figure 7. Isolation of *tcp ces-D* mutants.

(A) Single mutants that constitute *tcp ces-D* mutants and illustrations show the locus of T-DNA insertions. *ces-D* (Poppenberger *et al.*, 2011); *tcp* mutants (Kim *et al.*, 2014). (B-C) Relative expression changes of *CES* in indicated lines (B), and *TCP8*, *TCP14* and *TCP15* in *tcp8,14,15* (C) as compared to wild-type. Data was measured from 10-day-old seedlings that grown on ½ MS medium. Data shows the mean \pm SD. $n=4$ biological repeats, each measured in 3 technical replicates, normalized to *GAPC2*. Statistically significant difference at $P \leq 0.05$ is indicated with different letters and was determined with one-way ANOVA. (D) Photos of 40-day-old representative plants grown in 16 hours light/ 8 hours dark cycles (long days).

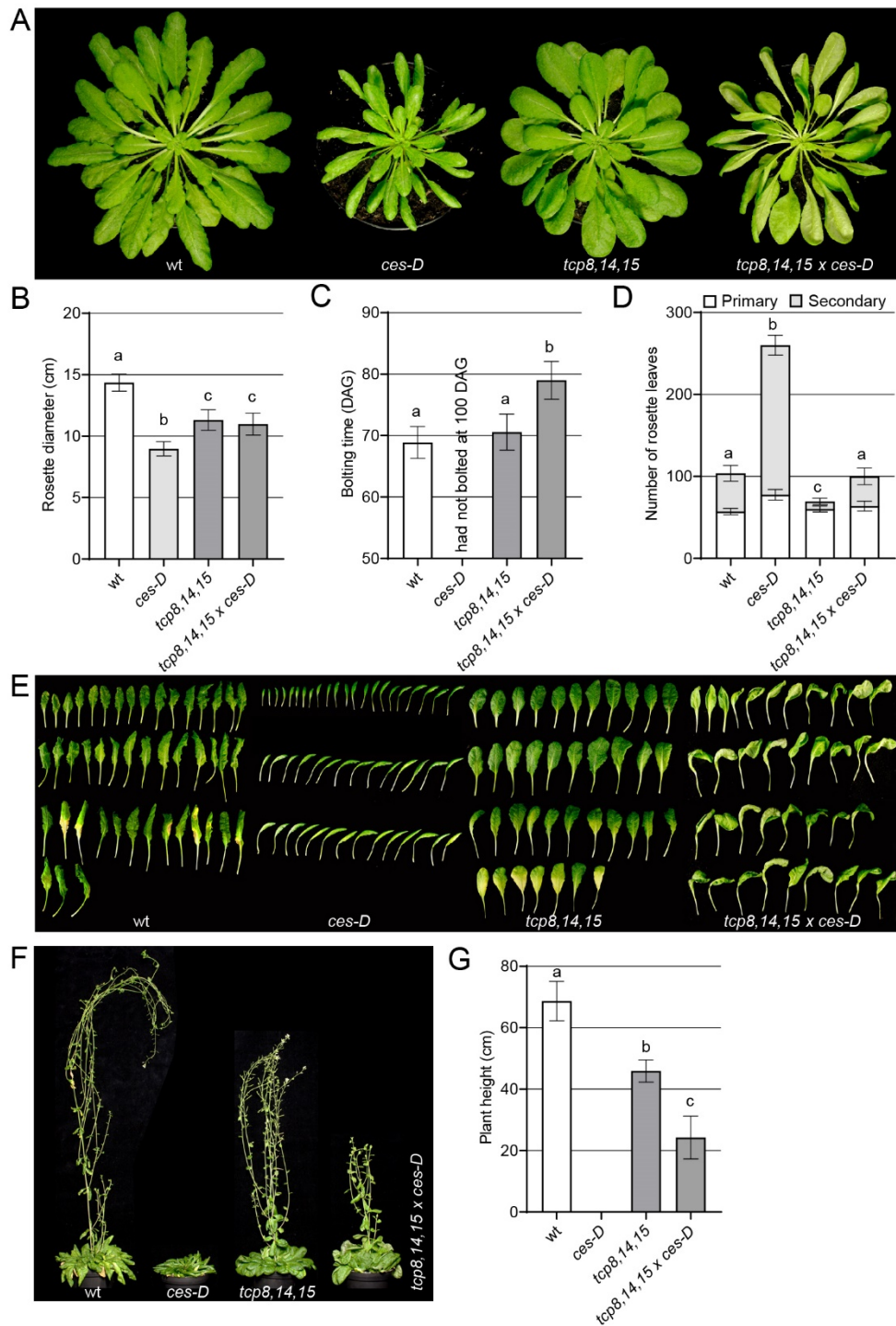


Figure 8. Over-expressing *CES* in *tcp8,14,15* triple mutant plants partly restores the symptoms of BR deficiency.

The indicated lines were grown in 8 hours light/ 16 hours dark cycles (short days) to document the morphology and quantify the rosette size, bolting time, total number of rosette leaves and plant height. (A-B) Plants at 7 weeks after germination, showing photos of representative plants from above (A) and the rosette diameter in cm (B). (C) Number of days after germination at bolting. (D-E, G) Plants at 15 weeks after germination, showing the total number of rosette leaves (D), photos of all primary rosette leaves of a representative plant (E) and plant height in cm (G). (F) Photos of representative plants at 13 weeks after germination. In the graphs: data show means \pm SD (n=12) and statistically significant difference at $P \leq 0.05$ is indicated with different letters and was determined with one-way ANOVA.

Since CES was co-suppressed in *tcp8,14,15 x ces-D*, the line was unsuitable to compare it with the *ces-D* parent, for assessing if the TCPs are required for CES activity. However, it was decided to still employ it, and investigate the effects of *CES* over-expression on the *tcp8,14,15* triple mutant phenotypes. For this purpose, the plants were grown in short days to the adult stage and rosette diameter, flowering time and the number of leaves at 8 weeks after germination were studied. This showed that, whereas the reduced rosette diameter of the *tcp8,14,15* triple mutant was not released by *CES* over-expression, the reduced leaf number was restored to wild-type (Figure 8B, D). Also, while the flowering time was not altered, the reduced height of 15-week-old *tcp8,14,15* triple mutant plants, was further reduced by *CES* over-expression in *tcp8,14,15 x ces-D* (Figure 8C, F, G).

In addition, the leaves lost their more roundish appearance and developed a very interesting morphology. The petioles grew strongly and twisted, resulting in the leaf blades being turned by 180° (and often more), with their abaxial surface mostly positioned upwards (Figure 8A). Moreover, the edges of the blades were bent in various directions, yielding sometimes a cup-shaped, at other times a partially epinastic appearance (Figure 8E).

2.1.8. Transcriptome analyses identify putative shared targets of CES and TCPs

Since there was evidence that TCP15 and its homologues TCP8 and TCP14 act in BR responses and interact with CES, it was of interest to investigate, if they may control over-lapping regulons of BR-target genes. To address this, available transcriptome data was used, specifically a data set which compared wild-type Col-0 with the *tcp8,14,15* triple mutant (Spears et al., 2022), a data set which compared wild-type Col-0 with *ces-D* (Poppenberger et al., 2011) and an unpublished data set from the Poppenberger group, which compared wild-type Col-0 with the *ces bee qM*. Differentially expressed genes (DEGs) were extracted and a comparison between the genotypes was performed, to identify co-regulated genes. Two types of comparison were made. On the one hand genes down-regulated in *ces-D* were compared with genes up-regulated in the *tcp8,14,15* triple and the *ces bee qM* quadruple mutant. This showed that a total of 648 genes was down-regulated in *ces-D*, while 1838 and 981 genes were up-regulated in the *tcp8,14,15* triple and the *ces bee qM* quadruple mutant, respectively. Among them, *tcp8,14,15* shared 67 and 140 DEGs with *ces-D* and *ces bee qM*, respectively, and 7 genes were differentially expressed in these three lines (Figure 9A).

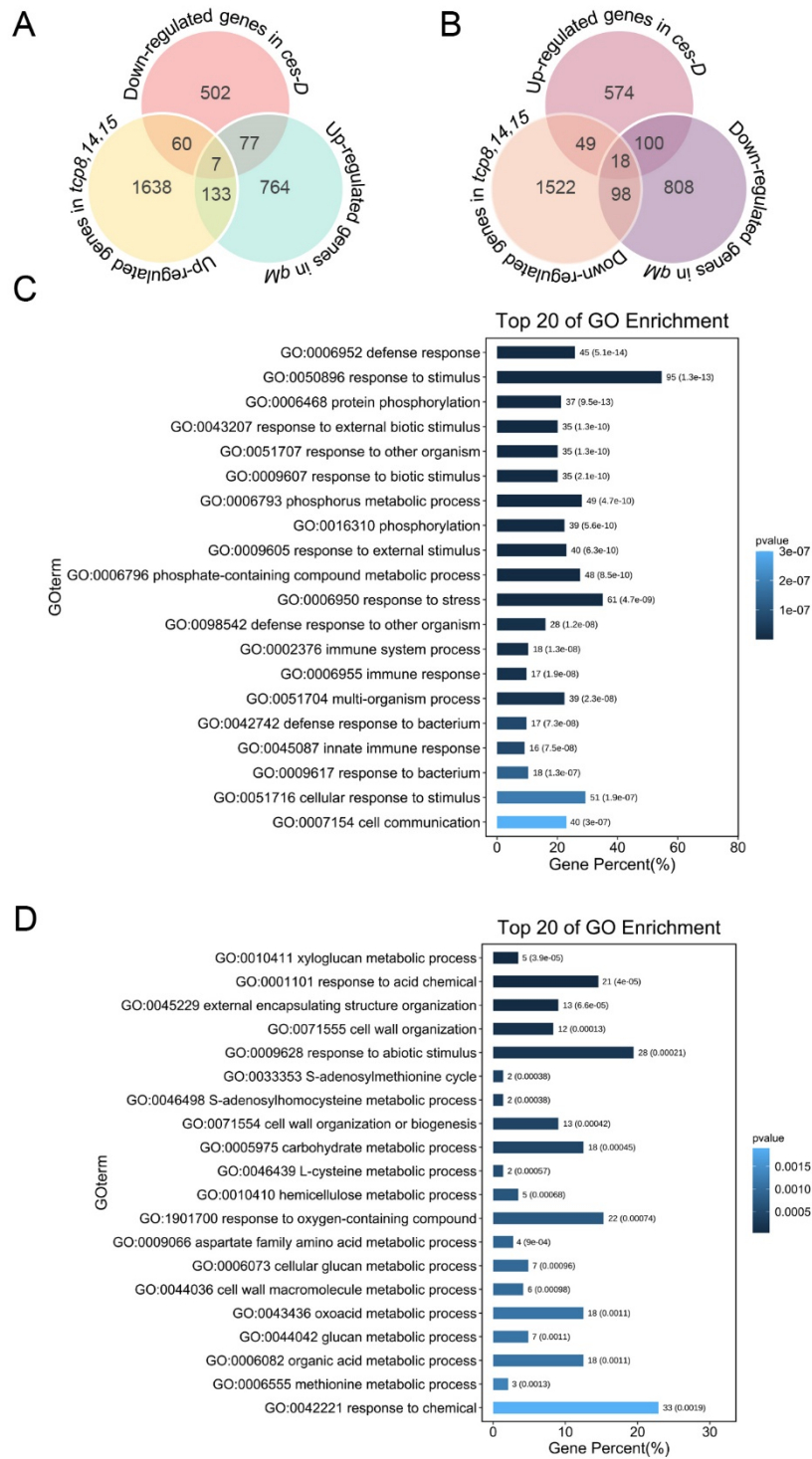


Figure 9. CES and TCPs share targets.

(A) Overlap of genes down-regulated in *ces-D* and genes up-regulated in *qM* and *tcp8,14,15*. (B) Overlap of genes up-regulated in *ces-D* and genes down-regulated in *qM* and *tcp8,14,15*. (C) Gene ontology term enrichment analysis of 200 genes upregulated in *tcp8,14,15* and differently expressed in *ces-D* and *qM*. (D) Gene ontology term enrichment analysis of 165 genes downregulated in *tcp8,14,15* and differently expressed in *ces-D* and *qM*.

A gene ontology (GO) analysis was performed with the 200 genes that were up-regulated in *tcp8,14,15*, and also up-regulated in *ces bee qM* or down-regulated in *ces-D* and the top 20 enriched GO terms were extracted. This showed that the 200 DEGs were mainly assigned to three functional categories: defense response to biotic stimulus, phosphorylation, and cell communication (Figure 9C), with the large majority of 15 GO groups falling into biotic stimuli or immune response categories. The seven genes that were found to be differentially expressed in all three lines are listed in Table 1 and include the TIR-NLR protein encoding locus *At4g14370* as well as CRK23 and PERK9, which are related to protein phosphorylation.

Table 1. Overlapping genes expressed identically in *tcp8,14,15* and *qM* but opposite in *ces-D*

Tair ID	Fold change(Log2)			Gene description
	<i>tcp8,14,15</i>	<i>ces-D</i>	<i>qM</i>	
AT2G26400	4.481	-2.165	3.320	ARD3; Acireductone dioxygenase 3
AT4G23310	2.714	-1.569	2.508	CRK23; Cysteine-rich RLK (RECEPTOR-like protein kinase) 23
AT2G18660	1.140	-1.761	3.007	PNP-A; Plant natriuretic peptide A
AT3G15356	0.732	-1.669	1.821	Legume lectin family protein
AT1G68690	0.715	-1.660	2.995	PERK9; Protein kinase superfamily protein
AT4G14370	0.657	-1.756	3.056	Disease resistance protein (TIR-NBS-LRR class) family
AT3G62150	0.643	-2.192	1.629	ABCB21; P-glycoprotein 21
AT3G28270	-1.709	2.649	-2.852	Transmembrane protein, putative (DUF677)
AT2G32100	-1.398	1.536	-2.867	OFF16; ovate family protein 16
AT5G22580	-1.161	2.737	-1.750	Stress responsive A/B Barrel Domain-containing protein
AT1G77690	-1.115	1.536	-2.260	LAX3; Like AUX1 3
AT3G11690	-0.912	1.541	-2.157	Hypothetical protein
AT1G69530	-0.701	1.728	-1.615	EXPA1; Expansin A1
AT1G74670	-0.699	2.015	-5.472	GASA6; Gibberellin-regulated family protein
AT3G28130	-0.608	1.611	-2.586	UMAMIT44; nodulin MtN21 /EamA-like transporter family protein
AT1G52190	-0.509	2.191	-2.400	Major facilitator superfamily protein
AT3G49940	-0.456	1.788	-1.767	LBD38; LOB domain-containing protein 38
AT4G37980	-0.447	1.530	-1.889	ELI3-1; Cinnamyl alcohol dehydrogenase 7
AT5G03760	-0.406	1.635	-1.394	ATCSLA09; Nucleotide-diphospho-sugar transferases superfamily protein
AT4G30020	-0.402	2.671	-2.975	PA-domain containing subtilase family protein
AT5G05690	-0.402	1.961	-1.578	CPD; Cytochrome P450 superfamily protein
AT5G01090	-0.292	1.637	-1.663	Concanavalin A-like lectin family protein
AT5G62350	-0.280	1.789	-1.515	Plant invertase/pectin methylesterase inhibitor superfamily protein
AT3G02570	-0.274	2.061	-1.119	MEE31; Mannose-6-phosphate isomerase, type I
AT4G37800	-0.254	3.028	-2.746	XTH7; xyloglucan endotransglucosylase/hydrolase 7

On the other hand, genes up-regulated in *ces-D* were compared with genes down-regulated in the *tcp8,14,15* triple and the *ces bee qM* quadruple mutant. This identified 741 *ces-D*-induced genes and 1687 and 1024 genes *tcp8,14,15* and *ces bee qM*, respectively, repressed genes. Among them,

tcp8,14,15 shared 67 and 116 DEGs with *ces-D* and *ces bee qM*, respectively. Among the 165 genes down-regulated in *tcp8,14,15* and altered in *ces-D* and the *ces bee qM* the GO analysis assigned genes to the categories abiotic stress response, response to oxygen-containing compounds or chemicals, metabolic processes and cell wall organization, among others (Figure 9B, D).

Eighteen genes were differentially expressed in all three lines (Figure 9B, Table 1) and included *CPD*, encoding a key enzyme in the BRs biosynthesis, and *XTH7* and *EXPA1*, which encode enzymes involved in cell wall organization (Liu et al., 2018; Ramakrishna et al., 2019). Moreover, also genes assigned to responses to other plant hormones were identified, such as *GASA6* and *LAX3* (Lee et al., 2015; Qu et al., 2016).

2.1.9. *TCP15* over-expression promotes *CPD* and *EXPA1* expression

CPD and *EXPA1* are both BR-regulated genes (Ohnishi et al., 2012; Graeff et al., 2021) and it was thus of interest to investigate, if their expression may be controlled by *TCP15*. To do so, additional *TCP15* over-expression lines were generated, by dipping *A. thaliana* Col-0 plants with a *35S::TCP15-YFP* construct and selecting multiple individuals that were homozygous for the transgene.

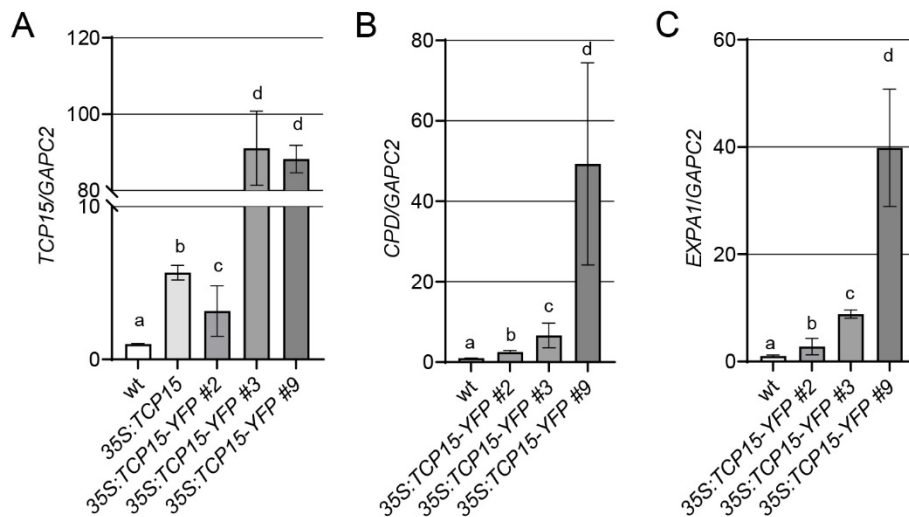


Figure 10. *TCP15* over-expression increases abundance of *CPD* and *EXPA1*.

Relative expression changes of *TCP15* (A), *CPD* (B) and *EXPA1* (C) in *TCP15*-overexpressed lines compared to wild-type (Col-0). Data was measured from 10-day-old seedlings that grown on ½ MS medium. Data shows the mean ±SD. n=4 biological repeats, each measured in 3 technical replicates, normalized to *GAPC2*. Statistically significant difference at P ≤ 0.05 is indicated with different letters and was determined with one-way ANOVA

An analysis of *TCP15* expression in these YFP-tagged lines showed that two lines had high *TCP15*-

BR-regulated transcription factors are often regulated by BIN2-mediated phosphorylation, and it was addressed if this may also be the case for the TCPs. For this purpose, the amino acid sequences of TCP8, TCP14 and TCP15 were aligned, and were screened for the presence of GSK3/shaggy-like kinase motifs, defined by the sequence S/TxxxS/T in multiple repeats (Cohen and Frame, 2001). This showed that in particular TCP14 and TCP15 contained multiple GSK3 recognition sites (Figure 11). To address, if TCP14 and/or TCP15 may be phosphorylated *in planta*, a publication was consulted in which the Arabidopsis proteome had been elucidated (Mergner et al., 2020), and data on TCP14 and TCP15 was extracted. This showed that in TCP14 the serines S58, S102, S193, S194 and S275 and in TCP15 the serines S128 and S129 were found to be phosphorylated. Since serines S128 and S129 of TCP15 and serines S193 and S194 are part of a conserved motif with a S/TxxxS/T signature (albeit only in single repeat), these sites are worth considering as BIN2 target sites.

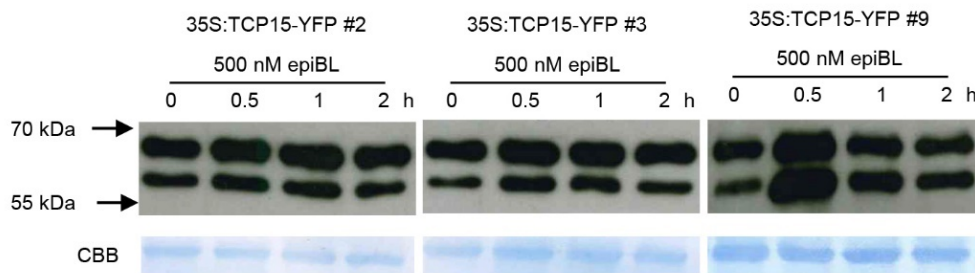


Figure 12. TCP15 abundance increases in response to BL treatment.

7-day-old seedlings grown on $\frac{1}{2}$ MS plates were transferred to $\frac{1}{2}$ MS liquid medium for 12 hours incubation and then treated with 500 nM 24-epiBL for indicated hours. TCP15-YFP was immunodetected with anti-GFP-HRP antibody. Membrane stained by Coomassie Brilliant Blue (CBB) was used as loading control.

Phosphorylation by BIN2 usually effects the protein abundance of BR-controlled transcription factors, and it was thus analyzed, if TCP15 protein levels may be altered by BR. For this purpose, 7-day-old seedlings of all three *35S:TCP15-YFP* over-expression lines were treated with epiBL for 0, 0.5, 1 and 2 hours, before TCP15-YFP was immunodetected with an anti-GFP-HRP antibody. This showed that after BL treatment TCP15 abundance increased significantly, between 0.5 and 1 hour, but returned to baseline levels at 2 hours (Figure 12). Also, very interestingly two bands were visible in all conditions: one with the predicted molecular weight of the TCP15-YFP fusion protein of approximately 61 kDa and a second band with a higher molecular mass, which may be a phosphorylated protein version.

In summary, TCP14 and TCP15 contain GSK3 recognition sites, some of which have been found to be phosphorylated *in planta*. TCP15-YFP was detectable in two different molecular weight versions, likely a phosphorylated and non-phosphorylated form, whose abundance increased in response to BL.

2.1.11. TCP14 and TCP15 directly bind to the promoter of *CES*

Class I TCPs regulate the expression of their downstream target genes by recognizing the conserved TCP I binding motif 5'-GGNCCCAC-3' in promoters and interestingly, such a motif was found to be present in the promoter of *CES*, -290 bases upstream from the transcriptional start (Figure 13A). To investigate if TCP15 and its homologues TCP8 and TCP14 can bind to this motif and regulate *CES* expression, a dual-luciferase reporter assay was carried out in *Arabidopsis* protoplast. Vector pGreenII-0800 was used (Hellens et al., 2005), which contains a Renilla-LUC driven by a 35S promoter and a Firefly-LUC driven by the target promoter fragment.

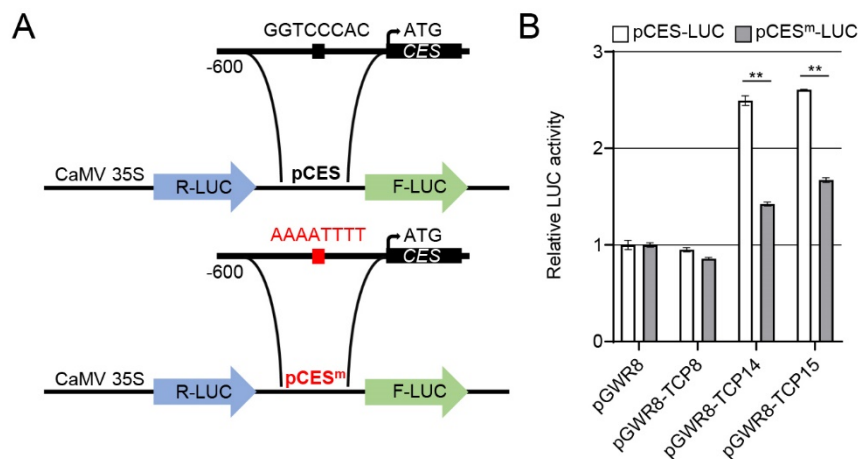


Figure 13. TCP14 and TCP15 can bind to the *CES* promoter *in planta*.

(A) Illustrations show a 600 bases promoter of *CES* contain a TCP I binding motif (pCES) or a variant motif (pCES^m) were used to generating the constructs. (B) Relative LUC activity was quantified by the ratio between the activities of Firefly LUC(F-LUC) with 35S promoter-driven Renilla LUC(R-LUC). Protoplast was isolated from rosette leaves of 4-week-old Col-0 plants. All data was normalized using the ratio obtained from empty pGWR8 vector which was set to 1. Data shows the mean \pm SD, n=6. Asterisks indicate significant differences (**P \leq 0.01, Student's t test).

600 bp of the wild-type *CES* promoter (pCES) as well as a version in which the TCP I binding motif was mutated (pCES^m), were cloned into the pGreen vector to drive Firefly-LUC expression, generating the constructs pCES-LUC and pCES^m-LUC. In addition, the coding sequences of the *TCP8*, *TCP14* and *TCP15* were cloned into vector pGWR8, which contains a 35S promoter (Rozhon

et al., 2010), for expression as effectors. Reporter and effector constructs were then co-transformed into protoplasts isolated from 4-week-old *Arabidopsis* rosette leaves and LUC activity was analyzed. Relative LUC activity was calculated as the ratio of Firefly-LUC to Renilla-LUC, and was equalized to the value obtained from protoplasts co-expressing empty pGWR8 with pCES-LUC, which served as a negative control and baseline.

The results showed that *CES* promoter activity was enhanced by more than two-fold when TCP14 and TCP15 were added as effectors, whereas TCP8 had almost no effect (Figure 13B). When the TCP I binding motif was mutated, the induction of *pCES-LUC* reporter expression by TCP14 and TCP15 was significantly attenuated, indicating that these TCPs regulate *CES* promoter activity by directly binding to the TCP motif.

2.2. SICES is a functional CES orthologue

2.2.1. SICES over-expression alters GA homeostasis

S. lycopersicum, the cultivated tomato, is the worlds' most important fruit crop. As a plant species that originates from subtropical climates, it has a high temperature requirement for optimal yield and lacks abilities to tolerate frost. Chilling injuries can occur already at a temperature of 12°C and temperatures below 19-20°C are suboptimal for its performance (Van Ploeg and Heuvelink. 2005). Therefore, an important aim of research is to identify factors that can increase the chilling tolerance of this crop and since *CES* can improve cold stress tolerance and fruit development in *A. thaliana*, it was aimed to test if these abilities are conserved in tomato.

Based on amino acid sequence similarity and the presence of a conserved BIN2-phosphorylation and a SUMOylation site, a tomato orthologue of *Arabidopsis* has been identified, which was encoded by locus *Solyc12g036470.1.1* and named *SICES*. To investigate if *SICES* functions in similar developmental processes like *CES* from *A. thaliana* two *35S:SICES-YFP* expressing lines, named *SICESoe-9* and *SICESoe-44*, that had previously been generated, were phenotyped. The work was initiated with an analysis of the hypocotyl length of soil-grown seedlings, which showed that hypocotyl elongation was significantly reduced (Figure 14A).

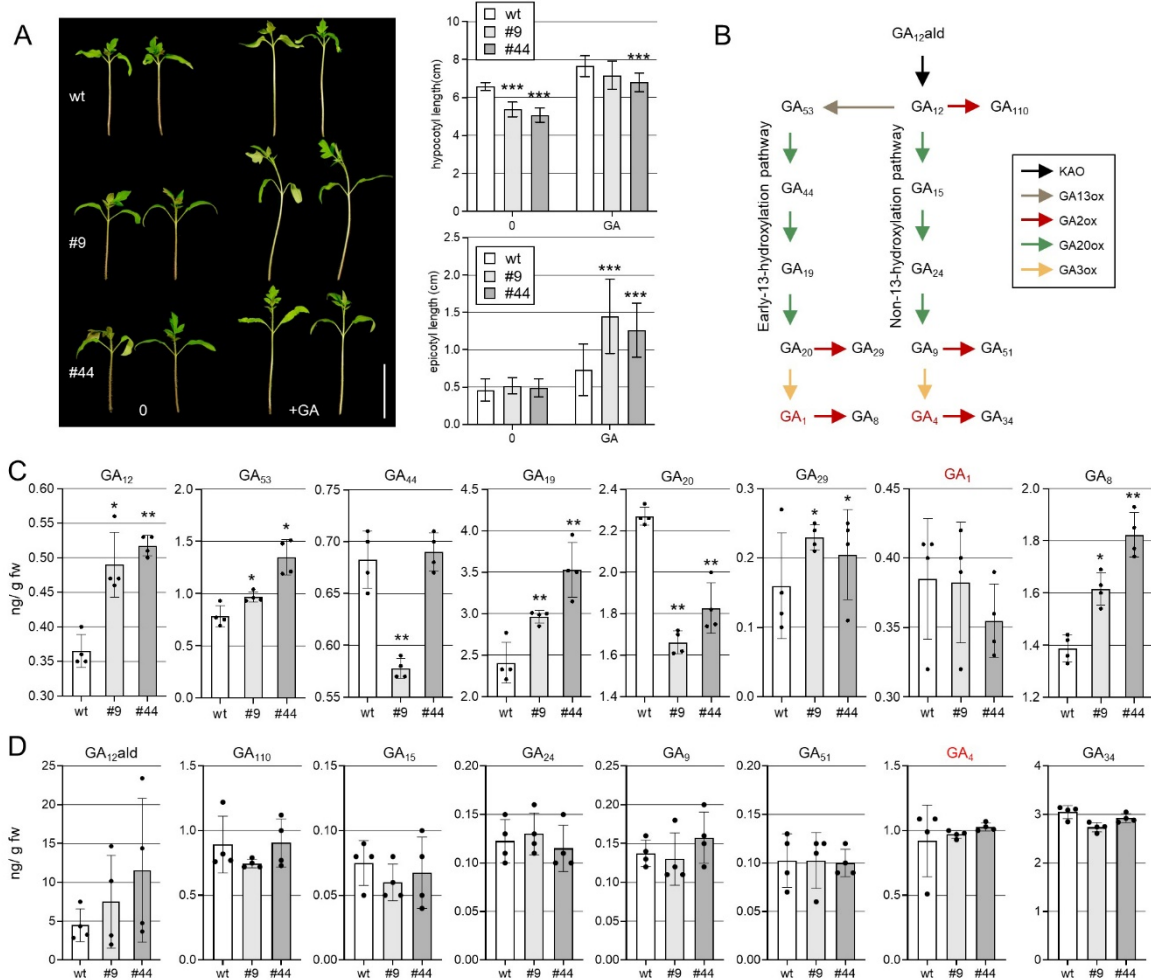


Figure 14. *SICES* over-expression alters GA homeostasis.

(A) Phenotype (left) and quantitative results (right) of 14-day-old soil-grown plants of *SICESoe* lines with or without GA treatment. 7-day-old soil-grown plants were treated with DMSO as a control (Mock), or with 50 μ M GA₄₊₇ (GA), once a day for a week. The results are shown as means \pm SD ($n > 12$). (B) Illustration of the GA biosynthetic pathway. Different enzyme classes are shown in different colors. (C-D) GC-MS measurements of early-13-hydroxylation pathway GAs (C) and non-13-hydroxylation pathway GAs (D) in aerial parts of 14-day-old plants. The values are given in ng/g fresh weight. The results of four biologically replicates and mean and standard deviations are shown. Asterisks indicate significant differences (* $P \leq 0.05$; ** $P \leq 0.01$; Student's *t* test).

Since AtCES can induce GA catabolism, it was tested, if this reduced hypocotyl elongation may relate to GA shortage. For this purpose, 7-day-old seedlings of the over-expression lines and wild-type were treated with GA, which showed that the hypocotyl elongation defects in both over-expression lines were alleviated through GA application. Moreover, the experiment showed that *SICESoe-9* and *SICESoe-44* seedlings were hyper-responsive to GA, since the epicotyls of both lines elongated significantly more strongly than wild-type in response to the GA treatment (Figure 14A).

To reveal, if the over-expression lines have defects in GA biosynthesis, the levels of different GA intermediates, both from the non and the early C13-hydroxylation pathway (Figure 14B; Hedden, 2020) were determined by GC-MS. Interestingly, in *SICESoe-9* and *SICESoe-44* plants, there were clear differences to wild-type in GA-levels of the early C13 hydroxylation pathway (leading to GA₁), while the non C13-hydroxylation pathway (leading to GA₄) was not significantly affected (Figure 14C, D). The precursor for both routes, GA₁₂, was significantly increased, and the level of GA₅₃, the first precursor of the early C13-hydroxylation pathway, which is derived directly from GA₁₂, was also significantly increased. However, GA₂₀, a direct product of GA₅₃ was significantly decreased in both over-expression lines, indicating a reduced activity of a GA20-oxidase (GA20ox) enzyme, which catalyzes this reaction.

While, somewhat surprisingly, levels of the bioactive GA GA₁, a direct product of GA₂₀, were not found to be significantly altered, levels of its catabolite GA₈ were significantly increased (Figure 14C), speaking for increased activity of a GA2-oxidase (GA2ox) that catalyzes conversion of GA₁ into GA₈. In line with increased GA2ox activity, also GA₂₉ levels were slightly increased, even though its substrate GA₂₀ was depleted in the *SICES* over-expression lines (Figure 14C), again indicates strong GA2ox activity. Thus, *SICES* over-expression has clear effects on the early C13 hydroxylation pathway of tomato.

2.2.2. *SICES* over-expression improves growth and fruit set at low ambient temperature

In *A. thaliana* CES can increase cold stress resistance when over-expressed (Eremina et al., 2016) and since tomato is a chilling-sensitive plant, it was of interest to test if *SICES* may also confer such abilities. To investigate this, wild-type and the *SICESoe-9* and *SICESoe-44* lines were first grown at normal ambient temperatures of 25°C +/- 3°C. This showed that *SICES* over-expression had a repressive effect on stem elongation in earlier stages of plant development (weeks 4-8), as evidenced by shorter epicotyls and shorter internodes. Interestingly, the plant height did show significant changes, but since the leaf number of *SICESoe-9* and *SICESoe-44* lines was increased as compared to wild-type, resulting in a slightly busier appearance (Figure 15).

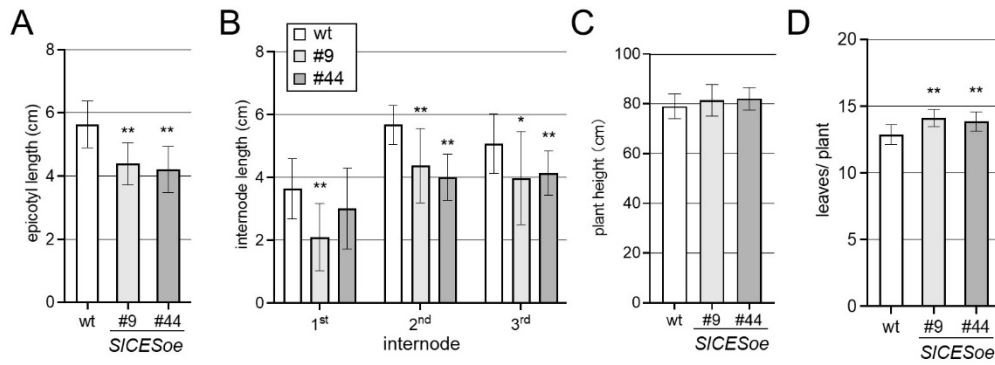


Figure 15. Over-expression of *SICES* represses shoot elongation, but promotes leaf formation in normal ambient temperatures.

SICES over-expressing plants and wild-type were grown in soil, in long-day conditions in the greenhouse at normal ambient temperatures of 25°C +/- 3°C. Different growth parameters were then assessed from 15 plants of each genotype, including epicotyl length after 5 weeks (A), and the length of the first three internodes (B), plant height (C) and the number of leaves (D) after 8 weeks. The results in all bar charts are shown as means ± SD (n=15). (*P<0.05; **P ≤ 0.01; Student's t test).

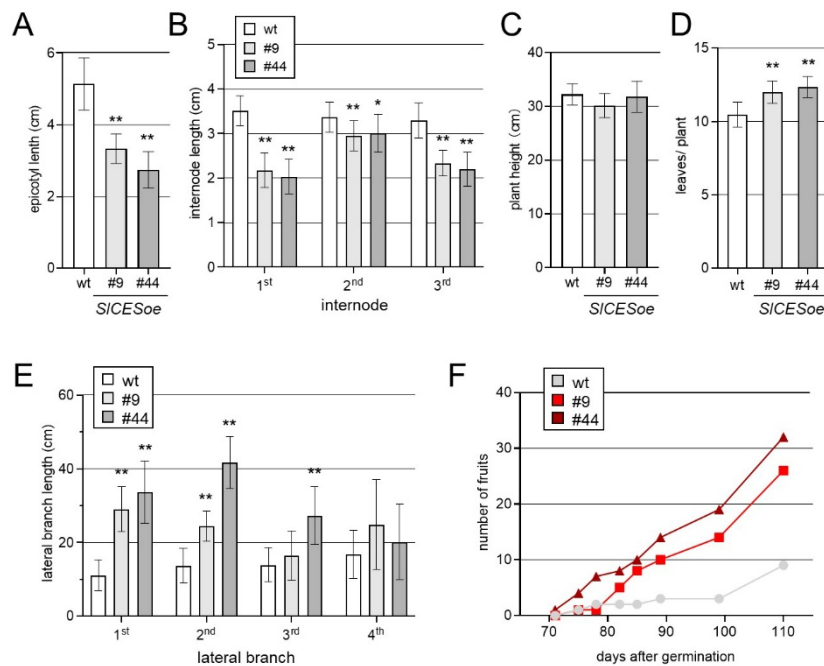


Figure 16. Over-expression of *SICES* represses internode elongation, but promotes lateral branch growth and fruit set in low ambient temperatures.

SICES over-expressing plants and wild-type were grown in low ambient temperatures of 18°C +/- 3°C, different growth parameters were then assessed from 15 plants of each genotype, including epicotyl length after 5 weeks (A), the length of the first three internodes (B), plant height (C), leaves per plant (D) and the length of the first 4 lateral branches (E) after 8 weeks. In addition, the number of fruits was counted at different stages of development (F). The results in all bar charts are shown as means ± SD (n=15). (*P ≤ 0.05; **P ≤ 0.01; Student's t test).

When the plants were grown at a low ambient temperature of 18°C +/- 3°C, the differences in leaf numbers and internode length to wild-type became more pronounced (Figure 16A-D). Furthermore, in the two over-expression lines the 1st and 2nd lateral branches developed significantly better (Figure 16E). Moreover, while in these growth conditions fruit development in wild-type was strongly suppressed, fruit set in plants of the *SICESoe-9* and *SICESoe-44* lines was much less affected, resulting in a significantly higher number of fruits at low temperatures (Figure 16F).

2.2.3. *SICES* over-expression impacts tomato fruit development

AtCES improves fertility by promoting extracellular matrix production and induced cell death in the reproductive tract, which is required for efficient pollen tube elongation. In addition, it also promotes growth of *A. thaliana* fruits, which are siliques with two fused carpels, leading to longer fruits with bent tips, when AtCES is ectopically expressed (Crawford and Yanofsky. 2011).



Figure 17. *SICES* over-expression alters the growth and shape of tomato fruits.

(A) Photos of representative fruits of *SICESoe* plants and wild-type at different developmental stages. For red fruits transverse and longitudinal sections are shown. (B) Average fruit weight of fully ripe fruits of *SICESoe* plants. 10-15 fully ripe fruits were harvested and weighed to obtain a total weight, which was then divided by the fruit number, to obtain a mean. Data shows the mean \pm SD of n=6 (***, $P < 0.001$; Student's t test). (C) Quantification of 100-seed weight. Seeds were collected from ripe fruits, air-dried and 100 seeds were weighted. Data shows the mean \pm SD of n=3 (***, $P \leq 0.001$; Student's t test).

To study if this function is conserved in fleshy fruit development, we assessed fruit growth in the two *SICES* over-expressing lines. This showed that *SICESoe-9* and *SICESoe-44* transgenic plants formed

longer fruits with more strongly pointed and slightly bent ends, a more cylindrical shape and an increased weight as compared to those of wild-type Heinz 1706 (Figure 17A, B). While seed set was increased, the seeds of *SICES* over-expressing plants were significantly smaller than those of wild-type (Figure 17C).

3. Discussion

BRs are plant hormones with versatile roles. They signal in a phosphorylation-dependent mode, to alter the phosphorylation state of transcription factors that control BR responsive genes in their expression. This is achieved through activities of GSK3/shaggy-like kinases such as BIN2, which target different types of transcriptional regulators, including the BES1/BZR1 protein family and bHLH proteins such as the BEEs and CES. In addition, there had been first evidence that also TCP proteins are components of BR signaling since TCP1, a class II TCP, was shown to induce expression of the BR biosynthetic gene *DWF4* and an over-expression of a dominant negative TCP1 version, resulted in dwarf phenotypes, similar to the BR-deficient mutant *det2-1* (Guo et al., 2010).

Here, evidence is provided that also the class I TCPs TCP14 and TCP15, take part in BR signal transduction, since they could interact with CES in yeast and since a loss of their function in the triple *tcp8,14,15* mutant produced aspects of phenotypes indicative of BR signaling deficiency. In the dark, *tcp8,14,15* mutant seedlings showed de-etiolated growth, most notably a much shorter hypocotyl, and had a reduced response to epiBL and enhanced response to BRZ treatment, characteristic features of BR signaling deficient mutants (Li and Chory. 1997; Li et al., 2002; Wang et al., 2002). In the light, *tcp8,14,15* seedlings, while not having shorter hypocotyls, had an increased hypocotyl elongation response to epiBL and plants showed characteristic features of BR/or GA deficiency, in particular rounder leaves, with shorter petioles and a reduced number of secondary rosettes.

Aspects of these light-grown phenotypes, in particular the rounder leaves with shorter petioles in mutant plants, had already been described for *tcp14,15* double mutants (Kieffer et al., 2011), and were explained with promotive effects of TCP14 and TCP15 on cell elongation. A *tcp14,15* double mutant in which *TCP8* and *TCP22* were additionally silenced, exhibited strong dwarfism and the plants were less responsive to GA, which was attributed to a role of these TCPs in controlling the expression of cell cycle genes, a function inhibited by the DELLAs (Davière et al., 2014). In terms of hypocotyl elongation, *tcp14,15* double knock-out plants did not show hypocotyl elongation defects in the light at normal ambient temperatures (Ferrero et al., 2019), which is in line with my results. However, at a higher ambient temperature of 29°C, *tcp14,15* plants exhibited defects in warmth-induced hypocotyl growth, a response in which BRs are also known to take part (Oh et al., 2012; Ferrero et al., 2019).

Thus, the results of this and previous work indicate that TCP15 and its homologues TCP8 and TCP14 play a role in BR and GA responsive growth and that this function is dependent on developmental stage, tissue type and environmental conditions such as temperature and light. This is supported, by gain-of-function data, since *TCP15* over-expression promoted hypocotyl elongation in the light and decreased BRZ sensitivity in the dark, seedling phenotypes that resemble those of *ces-D*. In the adult stage *TCP15oe* plants were similar to *ces-D* in terms of an increased secondary rosette formation, but not in other phenotypic features. The *35S:TCP15* line used for the phenotyping experiments, was not a strong over-expression line, as compared to *35S:TCP15-YFP* over-expressing lines, which were generated later during this work. Thus, it will be interesting to see, if a higher degree of TCP15 accumulation, may results in more noticeable phenotypes.

BR and GA modes of activity are strongly intertwined and one level of regulation is the BR control of GA biosynthetic genes. In *A. thaliana* *GA20ox1* and *GA3ox1* are BR-induced (Unterholzner et al., 2015; Albertos et al., 2022), a process in which BES1 takes part (Unterholzner et al., 2015). Moreover, CES/BEEs also contribute to the BR-induction of *GA3ox1* expression and it is interesting that TCP14 and TCP15 were found to induce *GA20ox1* and *GA3ox1* mRNA abundance. In light-grown seedlings of the double *tcp14,15* mutant, the expression of both genes was reduced and was less responsive to induction by warm temperatures (Ferrero et al., 2019). Thus, it was considered possible that TCP14 and/or TCP15 act synergistically with CES in the control of these and other target genes and to address this, a transcriptome analysis was carried out. This revealed that among the DEGs that were down-regulated in *tcp8/14/15* and the *ces bee qM* and up-regulated in *ces-D*, *CPD*, a key BR biosynthetic gene, which is CES-induced (Poppenberger et al., 2011) was present. Moreover, *EXPA1*, a BR-induced gene (Graeff et al., 2021), which promotes the initiation of lateral roots by promoting the division of pericycle cells (Ramakrishna et al., 2019), was also among these DEGs. Both genes were significantly over-expressed in *35S:TCP15-YFP* lines with high *TCP15* abundance, providing evidence that TCP15 can induce these genes. Since the transcriptome data, generated by RNA-Seq also showed that these genes are repressed in *tcp8,14,15* (Spears et al., 2022), it is likely that TCP15 and its homologues TCP8 and TCP14 induce expression of *CPD* and *EXPA1*, but this will require verification.

It is interesting that TCP15 can induce both *EXPA1*, which is BR-induced (Graeff et al., 2021) and

CPD, which is BR-repressed (Ohnishi et al., 2012). This function is similar to *CES*, *HBI1* and *PIF4*, which can all act as positive regulators of BR biosynthesis, but also of other BR responses (Poppenberger et al., 2011; Fan et al., 2014; Martínez et al., 2018). This ability differs to those of the *BZR1/BES1* proteins, which, while promoting BR responsive growth, repress BR biosynthesis, for a feedback adjustment of BR homeostasis (Wang et al., 2002). *HBI1* has been shown to be a TCP14- and TCP15-induced gene during warmth-induced growth and, when over-expressed, can rescue the compromised, warmth-induced hypocotyl elongation response of *tcp14,15* plants (Ferrero et al., 2019). *CES*, when over-expressed in the *tcp8,14,15* triple mutant, rescued other *tcp8,14,15* developmental defects, in particular a reduced secondary rosette formation and rounder leaf morphology. Rescue effects on the warmth-induced growth response of *tcp8,14,15* were not analyzed, here but since *CES* is a close homologue of *HBI1*, it will be interesting to see, if this is also effected in *tcp8,14,15 x ces-D* plants.

In analogy to *HBI1*, *CES* expression is TCP14- and TCP15-induced and here first evidence is provided that these TCPs can directly bind to a TCP I binding motif present in the *CES* promoter. In addition, there is evidence that *CES* can interact with TCP14 and TCP15 in yeast and it will be interesting to investigate, if this also occurs *in planta*. The cellular localization of these proteins comes in support of such a scenario, since *CES* as well as TCP8, TCP14 and TCP15 not only localize to the nucleus, but to distinct subnuclear compartments (Poppenberger et al., 2011; Kim et al., 2014).

CES is enriched in subnuclear compartments in a process that is activated by BR signaling and requires *CES* SUMOylation and there is *in vitro* evidence that also TCP8 and TCP15 can be SUMOylated (Mazur et al., 2017). Moreover, TCP8 nuclear body localization is thought to require BRs, and BRs repress TCP8 function in transcription (Spears et al., 2022). On the contrary, TCP14 DNA binding activity were shown to be enhanced through nuclear body enrichment, speaking for TCP- and/or promoter-specific effects (Yang et al., 2017). Thus, it will be interesting to test, if the protein abundance, nuclear localization and transcriptional activity of TCP15 and homologues is BR-controlled and here it was found that TCP15 protein levels increase in response to BL treatment.

Immuno-blotting using seedlings over-expressing a TCP15-YFP reporter, showed that protein level clearly increased following exposure to BL, but also revealed that TCP15 is detectable in two different

sizes, one with the predicted molecular weight of approximately 61 kDa and a larger protein with a size of 65 kDa, indicating posttranslational modification. Since TCP15, but also its homologues TCP8 and TCP14 contain multiple classical GSK3/shaggy like kinase motifs, it will be important to test, if these motifs may be phosphorylated by BIN2 or BR-controlled functional homologues *in planta*. First evidence supports this idea, since in a global phosphoproteome analysis of *A. thaliana*, TCP14 and TCP15 were found to be phosphorylated on serines (Mergner et al., 2020), which are part of a conserved GSK3/shaggy-like kinase recognition motifs.

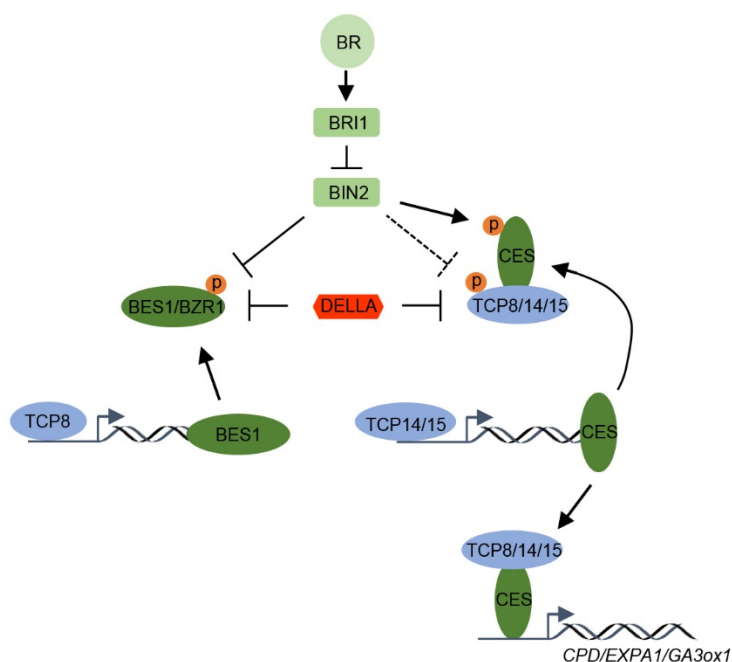


Figure 18. Model of TCP activity in BR signaling.

In the presence of BR, BR binds to BRI1, to activate inhibition of BIN2 kinase and thereby release the phosphorylation of the transcription factors BES1/BZR1, CES and maybe TCPs TCP8, TCP14 and TCP15. TCP14 and TCP15 increase the activity of *CES* promoter, and all these three TCPs can interact with CES. TCPs and CES complex jointly regulate the downstream genes including *CPD*, *EXPA1* and maybe *GA3ox1*. TCP8 promotes expression of and interact with BES1. Both BES1/BZR1 and TCPs interact with DELLA and are repressed by DELLA.

In summary, with the results of this and previous work, a working model for the contribution of TCP I transcription factors to BR signaling can be proposed, which is illustrated in Figure 18. In this model BRs increase the protein stability of TCP15 and potentially also TCP14, to enhance *CES* transcription and facilitate TCP15 interaction with CES and functional homologues. This allows for joined targets to be regulated such as *CPD* and *EXPA1*, but likely also others including *GA3ox1*, to contribute to

aspects of BR responses. Since TCP8 can promote expression of and interact with BES1, to contribute to the control of BES1/BZR1 gene regulons (Spears et al., 2022), it is possible that TCP8 also impacts CES activity. Similarly, TCP14 and TCP15 may affect BES1/BZR1 activities and this warrants further investigation. Since BES1/BZR1 and the TCPs have been shown to be controlled by the DELLAs (Bai et al., 2012b; Davière et al., 2014), the DELLAs may also be part of TCP-containing complexes, that impact BR responses via cooperation with CES and related bHLH proteins (Figure 18).

While we have come a long way in understanding BR activity in general and CES/BEE activity more specifically, in the model plant *A. thaliana*, we still have much to learn about their modes of activity in crops. Since CES gain of function increased cold stress tolerance and fruit development in *A. thaliana* (Crawford and Yanofsky, 2011; Poppenberger et al., 2011; Eremina et al., 2016), it was aimed to test if these abilities are conserved in the cultivated tomato *S. lycopersicum*, which is the world's most important fruit crop. As a plant species that originates from subtropical climates, *S. lycopersicum* has a high temperature requirement for optimal growth and yield and lacks abilities to tolerate frost. Chilling injuries can occur already at a temperature of 12°C and a temperature below 19-20°C is suboptimal for its performance (Van Ploeg and Heuvelink, 2005). Therefore, an important aim of research is to identify factors that can increase the chilling tolerance of this crop and here it was tested if CES has these abilities.

A CES orthologue, named SICES, was over-expressed in *S. lycopersicum* and repressed hypocotyl elongation in seedlings, a phenotype that could be rescued with external GA. Other phenotypes of *SICES* over-expressing plants, like reduced internode elongation and a GA hyper-responsiveness also indicated reduced levels of bioactive GA and, when GAs were measured, it was found that in aerial tissues of whole seedling, the levels of several intermediates of the early C13-hydroxylation pathway, which forms GA₁, were altered. GA₅₃ levels were increased, while GA₂₀ levels were significantly decreased; the intermediates GA₄₄ and GA₁₉ were not consistently changed in both *SICESoe* lines.

Given the GA-deficient phenotypes of the *SICESoe* lines, it was surprising that GA₁, a direct product of GA₂₀, was not altered, whereas its catabolite GA₈ was significantly increased. The increased GA₈ levels may indicate an increased activity of a GA 2-oxidase of class I or II, which directly convert C₁₉ GAs such as GA₂₀ and GA₁ to GA₂₉ and GA₈, respectively (Hedden, 2020; Lange and Pimenta Lange.

2020). In *A. thaliana* AtCES induces GA catabolism by increasing expression of the class III GA 2-oxidase GA2ox7, which converts GA₁₂ to GA₁₁₀ (Lange et al., 2020). However, since GA₁₁₀ levels were not altered in seedlings of the *SICESoe* lines, our data suggest that in the analyzed tissues *SICESoe* induces class I and/or II rather than class III GA 2-oxidases.

An increased activity of GA 2-oxidases that synthesize GA₈ should deplete GA₁, however GA₁ was not significantly decreased in the *SICESoe* lines, albeit a slight tendency to reduced levels was seen in line *SICESoe*-44. Thus, in this tissue and at this developmental stage, the increased conversion of GA₁ to GA₈ appears to be compensated for. This could occur via an induction of GA 3-oxidase activity, and the clear reduction of the GA 3-oxidase substrate GA₂₀ supports this idea. Since in *A. thaliana*, CES over-expression also induced GA 3-oxidase activity, there is clear evidence, that the complex roles of CES in the control of both GA biosynthesis and GA catabolism are conserved in tomato.

In *A. thaliana*, *CES* over-expression produced phenotypes indicative of GA deficiency during the vegetative growth phase of adult plants, however in hypocotyls of seedlings and also in fruits, growth was promoted, speaking for tissue and developmental stage specific outcomes (Crawford and Yanofsky. 2011; Albertos et al., 2022). In tomato, *SICES* over-expression suppressed hypocotyl elongation, a phenotype not seen in *A. thaliana*. However, in analogy with *AtCES* over-expression, *SICES* promoted fruit growth, yielding larger, more elongated fruits, with bent tips in the *SICESoe* lines. Such fruits formed more, but smaller seeds, a phenotype that was not reported in *A. thaliana* (Crawford and Yanofsky. 2011). When putting these results into context with other work, it is interesting that the expression of *SIGA3ox1* and *SIDWF4* in tomato fruits are inhibited by the TF JUNGBRUNNEN (JUB), which slows down growth in later stages of fruit development and increases amounts of glutamic acid, aspartic acid and GABA (Shahnejat-Bushehri et al., 2017). Since CES induces *GA3ox1* and *DWF4* expression in *A. thaliana*, a conserved function of *SICES* during tomato fruit development, would yield larger fruits, which is in line with my results.

Other BR signaling components, when over-expressed also impacted the development and metabolite composition of tomato fruits. *SIBRI1* over-expression promoted fruit ripening and caused an increase in carotenoids, ascorbic acid, soluble sugars and soluble solids (Nie et al., 2017). Over-expression of *SIBES1* promoted fruit softening and over-expression of a dominant version of *AtBZR1* enhanced

carotenoid accumulation (Liu et al., 2014; Liu et al., 2021). Over-expression of *SIBIM1a*, as well as its *A. thaliana* orthologue *AtBIM1*, however, repressed fruit growth and produced strongly dwarfed plants in *S. lycopersicum*, showing that BIM1 function in growth promotion in *A. thaliana* is not conserved in tomato, but that SIBIM1 rather acts as a negative regulator of pericarp development (Mori et al., 2021).

Since there was clear evidence that CES function in the control of GA homeostasis and growth is conserved, it was aimed to investigate if *SICES* over-expression can increase cold stress tolerance by assessing growth and fruit development at a low ambient temperature of 18°C. This showed that *SICESoe* plants were significantly less compromised than wild-type, both in vegetative growth and the ability of fruit set in these conditions.

S. lycopersicum has a low basal chilling tolerance, with a weak ability to cold acclimate and while it contains CBFs, they activate a much smaller CBF-regulon in response to cold than in *A. thaliana* (Zhang et al., 2004). *CBF* over-expression is not feasible for application, since it induces strong dwarfism in tomato and other plants (Zhang et al., 2004; Achard et al., 2008) and thus alternatives are in demand. An over-expression of the BR biosynthetic gene *SIDWF* had already been shown to improve the chilling tolerance of *S. lycopersicum* (Xia et al., 2018) and here evidence is provided that *SICES* is also a factor that is worth considering in breeding strategies, which aim to improve the yield stability of this crop at low temperatures. Since homologues of CES, in particular HBI1, repress immunity in *A. thaliana* (Malinovsky et al., 2014), potential trade-offs of this approach will have to be evaluated.

In conclusion, this work revealed that the class I TCP TCP15 and its homologues TCP8 and TCP14 contribute to BR signaling in *A. thaliana*. Evidence is provided that this involves an impact on the activity of CES and its homologues the BEEs and HBI1; but also additional BR-controlled transcriptional regulators including the BES1/BZR1 proteins take part. Moreover, in a translational research approach, using *S. lycopersicum* as a model, it was shown that CES modes of activity are conserved in other plant species and that CES over-expression bears potential to increase the cold stress tolerance of chilling sensitive crops, if potential trade-offs are addressed.

4. Materials and methods

4.1 Plant material

All the *Arabidopsis thaliana* mutants used in this study were in the background Columbia (Col-0). The 35S:*TCP15* line was obtained from Daniel H. Gonzalez, Universidad Nacional del Litoral (Viola et al., 2016). The *tcp8,14,15* was obtained from Walter Gassmann, University of Missouri (Kim et al., 2014). The *ces-D* and *ces bee qM* mutants were previously generated by the Poppenberger lab (Poppenberger et al., 2011; Eremina et al., 2016).

To generate *tcp8,14,15 x ces-D*, *tcp8,14,15* and *ces-D* were crossed and progeny homozygous for the mutant combinations *tcp8 x ces-D*, *tcp8,14 x ces-D* and *tcp8,14,15 x ces-D* were selected by genotyping using the primers: *tcp8* (TCP8-GT-F and TCP8-GT-R); *tcp14* (TCP14-GT-F and TCP14-GT-R); *tcp15* (TCP15-GT-F and TCP15-GT-R); *ces-D* (SOER2-ces-D-GT and SOEL2-ces-D-GT). For the sequences of all primers used in this work see supplementary table 1.

To generate 35S:*TCP15-YFP* lines, the coding region without STOP codon of *TCP15* (*At1g69690*) was PCR-amplified from Col-0 genomic DNA using the primers TCP15-Fw-NcoI and TCP15-Rev-NotI, and cloned into the vector pGWR8 (Rozhon et al., 2010), using the NcoI and NotI restriction sites. The YFP fragment was then isolated from pGWR8-CES-YFP using the NotI restriction site and ligated, in frame with TCP15 into pGWR8-TCP15. After confirming the pGWR8-TCP15-YFP construct by sequencing, it was transformed into *A. thaliana* Col-0 and progeny homozygous for the transgene was selected using the Kanamycin resistance marker and genotyping.

In case of *Solanum lycopersicum*, the sequenced cultivar Heinz 1706 (Tomato Genome Consortium, 2012) was used as the wild-type. The 35S:*SICES-YFP* line #9 had previously been isolated in the Poppenberger lab. To obtain a second independent *SICES*-overexpression line, #44 had been selected and seeds of the T2 generation were available at the start of this thesis. From those a homozygous T3 line was selected using the glufosinate resistance of the line and genotyping.

4.2. Phenotyping in the seedling stage

For phenotyping of *Arabidopsis* early seedling development, surface sterilized seeds were sown in lines on square plates (9x9 cm), containing ½ MS medium (Murashige and Skoog, 1962) with 1%

sucrose and 0.7% agar, set to pH 6.0, and stratified at 4 °C in the dark for two days. Then the plates were incubated vertically in a growth incubator (Bright Boy; CLF Plant Climatics, Germany), set to 16 hours white light/ 8 hours dark with a light intensity of 80 $\mu\text{mol}\cdot\text{m}^{-2}\cdot\text{s}^{-1}$, a relative humidity 50-60% and a temperature of 21°C +/- 2°C. For evaluation of seedling development in the dark, the imbibed and stratified seeds were exposed to 30 minutes of light, before the plates were wrapped up in multiple layers of aluminum foil and incubated in the same conditions, as for the light phenotyping. For epiBL and BRZ seedling response assays, seeds were sown on plates containing certain concentration of epiBL or BRZ. DMSO was added as control. Plates were transferred to incubator with low light conditions (30 $\mu\text{mol}\cdot\text{m}^{-2}\cdot\text{s}^{-1}$ light intensity without any other setting changes) after stratification. 8-day-old seedlings were stretched and taken pictures by the camera. The hypocotyl length was then measured from these pictures using ImageJ (<https://imagej.nih.gov/ij/>). To calculate the relative responses to epiBL or BRZ, the treated hypocotyl length was divided by the untreated length and the value in the untreated conditions was set to 1.

For tomato seedling phenotyping, surface sterilized seeds were sown directly into soil in pots and kept at 4°C for two days. Then the pots were transferred to the incubator with the growth condition set to the standard conditions as for Arabidopsis. GA treatments were performed by spraying the seedlings with water containing 50 μmM GA₄₊₇ (Duchefa, Haarlem, NL) until dripping wet. The GA treatments were started at 7 days post germination and were done daily for 7 days, before hypocotyl and epicotyl elongation was measured. For hypocotyl and epicotyl length measurement, seedlings were cut off roots and taken pictures by the camera, ImageJ was used for the measurement.

4.3. Phenotyping of adult plants

For phenotyping of growth parameters in the adult stage of Arabidopsis, 2-week-old plate-grown seedlings were transferred to soil and grown in short-day conditions (8 hours white light/ 16 hours dark without any other setting changes). Rosette diameter was measured with ImageJ after being photographed. Bolting time was counted as days from seeds germination to the first day that inflorescence grown. Number of rosette leaves were counted after cutting them off the plants and the primary rosette leaves were photographed.

For phenotyping of growth parameters in the adult stage of tomato, 2-week-old seedlings were

transferred to the greenhouse and grown without artificial lightning at a temperature of 25°C +/- 3°C for standard growth conditions or 18°C +/- 3°C for low temperature phenotyping. The experiments were conducted between August and October in Freising (Germany; 48° 24' N, 11° 45' O). All lengths were measured with a ruler and only fully expanded true leaves were counted as leaves number. Seeds were extracted once fruits ripe and were air-dried at a room temperature.

4.4. Quantitative real-time PCRs (qPCRs)

For qPCRs total RNA was isolated from plant materials using the E.Z.N.A. Plant RNA Kit (Omega Bio-tec, USA) according to the manufacturer's instructions. A total 1 µg RNA was treated with DNase I (Thermo Scientific, USA) to remove the DNA residues. cDNA synthesis was performed with the Revert Aid First Strand cDNA Synthesis Kit (Thermo Scientific, USA). The generated cDNA was diluted 1:10 in nuclease-free water and stored at -20°C for PCR or qPCR analysis.

qPCR analysis was performed with a Mastercycler Realplex (Eppendorf, Germany). The total reaction volume was 20 µL and included 10 µL 2 x qPCRBIO SyGreen qPCR master mix (Bioline, UK), 0.8 µL 5 µM primers mix and 2 µL cDNA sample. For quantification eight standards (cloned cDNAs) in the range of 3×10^2 to 1×10^6 copies/µL were run under the same conditions. The amplification program started with an initial denaturation at 95°C for 2 min. Next, 40 cycles were run with a denaturation phase at 95°C for 10 s and an annealing and extension phase at 60°C for 20 s. A melting curve was recorded by increasing the temperature linearly from 60°C to 95°C within 20 min. Expression levels were normalized to the internal standard *GAPC2* and measured in three to four technical replicates.

4.5. Immunoblotting for detection of TCP15-YFP

7-day-old seedlings, grown vertically on plates, were transferred to liquid ½ MS medium and incubated, with gentle shaking, for 12 hours in the same conditions as before. Then 500 nM epiBL was added to the liquid medium and seedlings were collected after the certain treatment time. DMSO treatments were also performed as control.

Samples were frozen in liquid nitrogen and ground to a fine powder. The same volume of protein extraction buffer (150 mM NaCl, 100 mM Tris-HCl pH=7.5, 0.25% Nonidet p-40, 1mM PMSF, 1% Protease inhibitor) was added and mixed by vortex. The supernatant was collected after centrifugation

at 13000 rpm at 4°C for 15 min. Protein concentration was then measured and the samples were mixed with 2x loading buffer (100 mM Tris-HCl pH=6.8, 200 mM DTT, 4% SDS, 20% glycerol, 0.025% bromophenol blue) and heated at 95°C for 10 min. Samples were stored at -20°C for further analysis. Approximately 12 µg of samples were separated by 10% SDS-PAGE gel and transferred to a PVDF membrane (Merck Millipore, USA). The membrane was blocked in blocking buffer (150 mM NaCl, 0.05% Tween 20, 10mM Tris-HCl pH=8.0, 5% milk) for 2 hours, and then incubated in a 1:5000 dilution of anti-GFP-HRP (Miltenyi Biotec, Germany) in blocking buffer with gentle shaking at 4°C overnight. HRP substrate was provided through incubation with the Amersham ECL Prime Western Blotting Detection Reagent (GE Healthcare, USA) following the manufacturer's instructions. The TCP15-YFP abundance was detected by exposing 1 min to Amersham Hyperfilm ECL film (GE Healthcare, USA) under dark conditions. Afterwards the membrane was stained with Coomassie brilliant blue R250 staining solution to verify the protein loading amounts.

4.6. Dual-luciferase reporter assay in Arabidopsis protoplasts

For the LUC reporter assays, TCP8, (encoded by At1g58100), TCP14 (encoded by At3g47620) and TCP15 (encoded by At1g69690) were cloned to serve as effectors. For this purpose, their coding regions were amplified by PCR from Col-0 cDNA. The amplicons were digested and ligated into pGWR8, using the NcoI and NotI restriction sites. To clone the pCES:LUC reporter construct, a 600 bp fragment of the CES promoter, which includes the TCP I motif, was PCR-amplified from Col-0 genomic DNA and cloned into pGreenII-0800 by using the HindIII and PstI restriction sites. To generate the CES promoter containing a TCP I variant motif, overlap extension PCR was performed. Two fragments of CES promoter were first PCR-amplified with the primer combinations pCES-600-Fw-HindIII/pCES-OEPCR-Rev and pCES-OEPCR-Fw/ pCES-Rev-PstI respectively. 200 ng each PCR products were then used as templates to perform PCR to ligate them with the primers pCES-600-Fw-HindIII and pCES-Rev-PstI. All the vectors were sequenced before use.

Protoplast isolation from Arabidopsis leave mesophyll cells was performed from rosette leaves of 4-week-old Col-0 plants, grown in the incubator run at the standard conditions described above, using a standard protocol (Yoo et al., 2007). Protoplast were transformed with 1 pmol reporter and effector vectors respectively and incubated over-night at a room temperature in the dark. After incubation, the

protoplasts were collected by centrifugation at 100g for 2 min and frozen in liquid nitrogen.

The luciferase reaction was initiated with the Dual-Luciferase Reporter Assay kit (Promega, USA) and LUC activity detected with a Lumat LB9501 luminometer (Berthold, Germany). Briefly, 100 μ L protoplast lysis buffer was added to the frozen protoplast and mixed by vortex. The measurements were conducted with 50 μ L of Luciferase Assay Reagent II solution, which was added to luminometer tubes; the baseline activity was recorded and set to 0. Then 10 μ L of the transformed protoplasts were added and the firefly luciferase activity was recorded. 50 μ L of the Stop&Glo Reagent was added and mixed by pipetting, and the Renilla luciferase activity was recorded. Relative LUC activity was quantified by the ratio between the activities of firefly luciferase with Renilla luciferase. All data was normalized using the ratio obtained from effector pGWR8 which was set to 1.

4.7. Yeast two-hybrid assays

The coding regions of *TCP8*, *TCP14*, *TCP15* and *CES* were PCR-amplified from Col-0 cDNA. The *TCP8* and *TCP14* amplicons were ligated into pGADT7 and pGBKT7, using the EcoRI and BamHI restriction sites. The amplicon of *TCP15* was ligated into pGADT7 and pGBKT7 using the NdeI and EcoRI restriction sites. The amplicon of *CES* was ligated into pGADT7 and pGBKT7 using the NdeI and BamHI restriction sites. All the vectors were sequenced before use.

For the Y2H assays, competent cell of yeast strain AH109 was transformed, using a PEG-mediated transformation protocol (Gietz and Schiestl. 2007), with the corresponding plasmids. SD medium (1x drop out amino acid mix, 2% sucrose, 6.7% yeast nitrogen base, 2% agar) was used for the selection. Transformed cells were first grown on SD-TL medium (SD medium without tryptophan and leucine) at 28°C for 72 hours. A single colony grown on SD-TL medium was picked and diluted in ddH₂O to have a OD₆₀₀ of 0.05, the solution was then diluted 10-fold and 100-fold respectively. 2 μ L each solution was potted on SD-TLH medium (SD medium without tryptophan, leucine and histidine) and 10 mM 3-AT was added as auto-activation inhibitor. Yeast cells were grown at 28°C for 5 days until pictures taken.

4.8. Transcriptome analysis

For transcriptome analysis, the differentially expressed genes come from different sources but all was

measured in seedling stage and in Col-0 background, *ces-D* (Eremina et al., 2016), *ces bee qM* (unpublished data in Poppenberger lab) and *tcp8,14,15* (Spears et al., 2022). Genes up-regulated in *ces-D* were grouped with genes down-regulated in *ces bee qM* or *tcp8,14,15*, on the contrary, genes down-regulated in *ces-D* were grouped with genes up-regulated in *ces bee qM* and *tcp8,14,15*. Pairwise comparisons were performed first and the overlap genes were then compared again to find the genes that mis-regulated in all these three lines, all these comparisons were performed within the group. Microsoft Excel was used as tool for the comparisons and the DEGs were then performed GO enrichment analysis with the online GO analysis tool (www.omicsshare.com). All the DEGs were listed in supplementary table 2 and 3.

4.9. GA measurement

Quantitative analysis of endogenous GAs was performed from aerial parts of 2-week-old plants, grown in soil, in the incubator run at the standard conditions described above. The concentrations of GAs were measured in the samples using gas-chromatography-mass spectrometry (GC-MS) by Prof. Theo Lange from the University of Braunschweig as described previously (Lange et al., 2005).

4.10. Statistical analyses

All graphed data was analyzed with GraphPad Prism 8 (www.graphpad.com) and the statistical analyses were performed using the tools in this software.

References

- Achard P., Gong F., Cheminant S., Alioua M., Hedden P. and Genschik P.** (2008). The cold-inducible CBF1 factor-dependent signaling pathway modulates the accumulation of the growth-repressing DELLA proteins via its effect on gibberellin metabolism. *PLANT CELL* 20(8): 2117-2129.
- Ackerman-Lavert M. and Savaldi-Goldstein S.** (2020). Growth models from a brassinosteroid perspective. *CURR OPIN PLANT BIOL* 53: 90-97.
- Albertos P., Wlk T., Griffiths J., Pimenta Lange M. J., Unterholzner S. J., Rozhon W., Lange T., Jones A. M. and Poppenberger B.** (2022). Brassinosteroid-regulated bHLH transcription factor CESTA induces the gibberellin 2-oxidase GA2ox7. *PLANT PHYSIOL* 00: 1-14.
- Asami T., Mizutani M., Fujioka S., Goda H., Min Y. K., Shimada Y., Nakano T., Takatsuto S., Matsuyama T. and Nagata N.** (2001). Selective interaction of triazole derivatives with DWF4, a cytochrome P450 monooxygenase of the brassinosteroid biosynthetic pathway, correlates with brassinosteroid deficiency in planta. *J BIOL CHEM* 276(28): 25687-25691.
- Bai M., Fan M., Oh E. and Wang Z.** (2012a). A triple helix-loop-helix/basic helix-loop-helix cascade controls cell elongation downstream of multiple hormonal and environmental signaling pathways in Arabidopsis. *PLANT CELL* 24(12): 4917-4929.
- Bai M., Shang J., Oh E., Fan M., Bai Y., Zentella R., Sun T. and Wang Z.** (2012b). Brassinosteroid, gibberellin and phytochrome impinge on a common transcription module in Arabidopsis. *NAT CELL BIOL* 14(8): 810-817.
- Bajguz A., Chmur M. and Gruszka D.** (2020). Comprehensive overview of the brassinosteroid biosynthesis pathways: substrates, products, inhibitors, and connections. *FRONT PLANT SCI* 11: 1034.
- Bancosí S., Nomura T., Sato T., Molnár G., Bishop G. J., Koncz C., Yokota T., Nagy F. and Szekeres M.** (2002). Regulation of transcript levels of the Arabidopsis cytochrome P450 genes involved in brassinosteroid biosynthesis. *PLANT PHYSIOL* 130(1): 504-513.
- Bishop G. J.** (2007). Refining the plant steroid hormone biosynthesis pathway. *TRENDS PLANT SCI* 12(9): 377-380.
- Bishop G. J., Nomura T., Yokota T., Harrison K., Noguchi T., Fujioka S., Takatsuto S., Jones J. D. and Kamiya Y.** (1999). The tomato DWARF enzyme catalyses C-6 oxidation in brassinosteroid biosynthesis. *P NATL ACAD SCI USA* 96(4): 1761-1766.
- Caño-Delgado A., Yin Y., Yu C., Vafeados D., Mora-García S., Cheng J. C., Nam K. H., Li J. and Chory J.** (2004). BRL1 and BRL3 are novel brassinosteroid receptors that function in vascular differentiation in Arabidopsis. *DEVELOPMENT* 131(21): 5341-5351.
- Chen W., Lv M., Wang Y., Wang P. A., Cui Y., Li M., Wang R., Gou X. and Li J.** (2019). BES1 is activated by EMS1-TPD1-SERK1/2-mediated signaling to control tapetum development in Arabidopsis thaliana. *NAT COMMUN* 10(1): 1-12.
- Chi C., Li X., Fang P., Xia X., Shi K., Zhou Y., Zhou J. and Yu J.** (2020). Brassinosteroids act as a positive regulator of NBR1-dependent selective autophagy in response to chilling stress in tomato. *J EXP BOT* 71(3): 1092-1106.

- Choe S.** (2006). Brassinosteroid biosynthesis and inactivation. *PHYSIOL PLANTARUM* 126(4): 539-548.
- Choe S., Dilkes B. P., Fujioka S., Takatsuto S., Sakurai A. and Feldmann K. A.** (1998). The DWF4 gene of *Arabidopsis* encodes a cytochrome P450 that mediates multiple 22 α -hydroxylation steps in brassinosteroid biosynthesis. *PLANT CELL* 10(2): 231-243.
- Clouse S. D.** (2011). Brassinosteroids. *ARABIDOPSIS BOOK* 9: e0151.
- Clouse S. D., Langford M. and McMorris T. C.** (1996). A brassinosteroid-insensitive mutant in *Arabidopsis thaliana* exhibits multiple defects in growth and development. *PLANT PHYSIOL* 111(3): 671-678.
- Cohen P. and Frame S.** (2001). The renaissance of GSK3. *NAT REV MOL CELL BIO* 2(10): 769-776.
- Costa M. M. R., Fox S., Hanna A. I., Baxter C. and Coen E.** (2005). Evolution of regulatory interactions controlling floral asymmetry. *DEVELOPMENT* 132(22): 5093-5101.
- Crawford B. C. and Yanofsky M. F.** (2011). HALF FILLED promotes reproductive tract development and fertilization efficiency in *Arabidopsis thaliana*. *DEVELOPMENT* 138(14): 2999-3009.
- Cubas P., Lauter N., Doebley J. and Coen E.** (1999). The TCP domain: a motif found in proteins regulating plant growth and development. *PLANT J* 18(2): 215-222.
- Danisman S., van Dijk A. D., Bimbo A., van der Wal F., Hennig L., de Folter S., Angenent G. C. and Immink R. G.** (2013). Analysis of functional redundancies within the *Arabidopsis* TCP transcription factor family. *J EXP BOT* 64(18): 5673-5685.
- Davière J. M., Wild M., Regnault T., Baumberger N., Eisler H., Genschik P. and Achard P.** (2014). Class I TCP-DELLA interactions in inflorescence shoot apex determine plant height. *CURR BIOL* 24(16): 1923-1928.
- Daxinger L., Hunter B., Sheikh M., Jauvion V., Gascioli V., Vaucheret H., Matzke M. and Furner I.** (2008). Unexpected silencing effects from T-DNA tags in *Arabidopsis*. *TRENDS PLANT SCI* 13(1): 4-6.
- Eremina M., Unterholzner S. J., Rathnayake A. I., Castellanos M., Khan M., Kugler K. G., May S. T., Mayer K. F., Rozhon W. and Poppenberger B.** (2016). Brassinosteroids participate in the control of basal and acquired freezing tolerance of plants. *P NATL ACAD SCI USA* 113(40): E5982-E5991.
- Fan M., Bai M., Kim J., Wang T., Oh E., Chen L., Park C. H., Son S., Kim S., Mudgett M. B. and Wang Z.** (2014). The bHLH transcription factor HBI1 mediates the trade-off between growth and pathogen-associated molecular pattern-triggered immunity in *Arabidopsis*. *PLANT CELL* 26(2): 828-841.
- Fang P., Wang Y., Wang M., Wang F., Chi C., Zhou Y., Zhou J., Shi K., Xia X., Foyer C. H. and Yu J.** (2021). Crosstalk between Brassinosteroid and Redox Signaling Contributes to the Activation of CBF Expression during Cold Responses in Tomato. *ANTIOXID* 10(4): 509.
- Ferrero L. V., Viola I. L., Ariel F. D. and Gonzalez D. H.** (2019). Class I TCP transcription factors target the gibberellin biosynthesis gene GA20ox1 and the growth promoting genes HBI1 and PRE6 during thermomorphogenic growth in *Arabidopsis*. *PLANT CELL PHYSIOL* 60(8): 1633-1645.
- Friedrichsen D. M., Nemhauser J., Muramitsu T., Maloof J. N., Alonso J., Ecker J. R., Furuya M. and Chory J.** (2002). Three redundant brassinosteroid early response genes encode putative bHLH transcription factors required for normal growth. *GENETICS* 162(3): 1445-1456.
- Fujioka S. and Sakurai A.** (1997a). Biosynthesis and metabolism of brassinosteroids. *PHYSIOL*

PLANTARUM 100(3): 710-715.

Fujioka S. and Sakurai A. (1997b). Brassinosteroids. NAT PROD REP 14(1): 1-10.

Fujioka S. and Yokota T. (2003). Biosynthesis and metabolism of brassinosteroids. ANNU REV PLANT BIOL 54(1): 137-164.

Fujita S., Ohnishi T., Watanabe B., Yokota T., Takatsuto S., Fujioka S., Yoshida S., Sakata K. and Mizutani M. (2006). Arabidopsis CYP90B1 catalyses the early C-22 hydroxylation of C27, C28 and C29 sterols. PLANT J 45(5): 765-774.

Gallego-Bartolomé J., Minguet E. G., Grau-Enguix F., Abbas M., Locascio A., Thomas S. G., Alabadí D. and Blázquez M. A. (2012). Molecular mechanism for the interaction between gibberellin and brassinosteroid signaling pathways in Arabidopsis. P NATL ACAD SCI USA 109(33): 13446-13451.

Gietz R. D. and Schiestl R. H. (2007). High-efficiency yeast transformation using the LiAc/SS carrier DNA/PEG method. NAT PROTOC 2(1): 31-34.

Graeff M., Rana S., Wendrich J. R., Dorier J., Eekhout T., Fandino A. C. A., Guex N., Bassel G. W., De Rybel B. and Hardtke C. S. (2021). A single-cell morpho-transcriptomic map of brassinosteroid action in the Arabidopsis root. MOL PLANT 14(12): 1985-1999.

Guo Z., Fujioka S., Blancaflor E. B., Miao S., Gou X. and Li J. (2010). TCP1 modulates brassinosteroid biosynthesis by regulating the expression of the key biosynthetic gene DWARF4 in Arabidopsis thaliana. PLANT CELL 22(4): 1161-1173.

He J., Gendron J. M., Sun Y., Gampala S. S., Gendron N., Sun C. Q. and Wang Z. (2005). BZR1 is a transcriptional repressor with dual roles in brassinosteroid homeostasis and growth responses. SCIENCE 307(5715): 1634-1638.

He J., Gendron J. M., Yang Y., Li J. and Wang Z. (2002). The GSK3-like kinase BIN2 phosphorylates and destabilizes BZR1, a positive regulator of the brassinosteroid signaling pathway in Arabidopsis. P NATL ACAD SCI USA 99(15): 10185-10190.

Hedden P. (2020). The Current Status of Research on Gibberellin Biosynthesis. PLANT CELL PHYSIOL 61(11): 1832-1849.

Hellens R. P., Allan A. C., Friel E. N., Bolitho K., Grafton K., Templeton M. D., Karunairetnam S., Gleave A. P. and Laing W. A. (2005). Transient expression vectors for functional genomics, quantification of promoter activity and RNA silencing in plants. PLANT METHODS 1(1): 1-14.

Holtton N., Caño-Delgado A., Harrison K., Montoya T., Chory J. and Bishop G. J. (2007). Tomato BRASSINOSTEROID INSENSITIVE1 is required for systemin-induced root elongation in Solanum pimpinellifolium but is not essential for wound signaling. PLANT CELL 19(5): 1709-1717.

Hothorn M., Belkhadir Y., Dreux M., Dabi T., Noel J., Wilson I. A. and Chory J. (2011). Structural basis of steroid hormone perception by the receptor kinase BRI1. NATURE 474(7352): 467-471.

Hu S., Liu L., Li S., Shao Z., Meng F., Liu H., Duan W., Liang D., Zhu C. and Xu T. (2020). Regulation of fruit ripening by the brassinosteroid biosynthetic gene SICYP90B3 via an ethylene-dependent pathway in tomato. HORTICULTURE RES 7: 163.

Jang J. C., Fujioka S., Tasaka M., Seto H., Takatsuto S., Ishii A., Aida M., Yoshida S. and Sheen J. (2000).

A critical role of sterols in embryonic patterning and meristem programming revealed by the fackel mutants of *Arabidopsis thaliana*. *GENE DEV* 14(12): 1485-1497.

Joung J. K., Ramm E. I. and Pabo C. O. (2000). A bacterial two-hybrid selection system for studying protein–DNA and protein–protein interactions. *P NATL ACAD SCI USA* 97(13): 7382-7387.

Khan M., Rozhon W., Unterholzner S. J., Chen T., Eremina M., Wurzinger B., Bachmair A., Teige M., Sieberer T. and Isono E. (2014). Interplay between phosphorylation and SUMOylation events determines CESTA protein fate in brassinosteroid signalling. *NAT COMMUN* 5: 4687.

Kieffer M., Master V., Waites R. and Davies B. (2011). TCP14 and TCP15 affect internode length and leaf shape in *Arabidopsis*. *PLANT J* 68(1): 147-158.

Kim S. H., Son G. H., Bhattacharjee S., Kim H. J., Nam J. C., Nguyen P. D. T., Hong J. C. and Gassmann W. (2014). The *Arabidopsis* immune adaptor SRFR 1 interacts with TCP transcription factors that redundantly contribute to effector-triggered immunity. *PLANT J* 78(6): 978-989.

Kim T., Guan S., Sun Y., Deng Z., Tang W., Shang J., Sun Y., Burlingame A. L. and Wang Z. (2009). Brassinosteroid signal transduction from cell-surface receptor kinases to nuclear transcription factors. *NAT CELL BIOL* 11(10): 1254-1260.

Kim T. W., Hwang J. Y., Kim Y. S., Joo S. H., Chang S. C., Lee J. S., Takatsuto S. and Kim S. K. (2005). *Arabidopsis* CYP85A2, a cytochrome P450, mediates the Baeyer-Villiger oxidation of castasterone to brassinolide in brassinosteroid biosynthesis. *PLANT CELL* 17(8): 2397-2412.

Kim Y., Song J., Park S., Jeong Y. and Kim S. (2017). Brassinosteroid-induced transcriptional repression and dephosphorylation-dependent protein degradation negatively regulate BIN2-interacting AIF2 (a BR signaling-negative regulator) bHLH transcription factor. *PLANT CELL PHYSIOL* 58(2): 227-239.

Kosugi S. and Ohashi Y. (1997). PCF1 and PCF2 specifically bind to cis elements in the rice proliferating cell nuclear antigen gene. *PLANT CELL* 9(9): 1607-1619.

Kosugi S. and Ohashi Y. (2002). DNA binding and dimerization specificity and potential targets for the TCP protein family. *PLANT J* 30(3): 337-348.

Kushiro M., Nakano T., Sato K., Yamagishi K., Asami T., Nakano A., Takatsuto S., Fujioka S., Ebizuka Y. and Yoshida S. (2001). Obtusifoliol 14 α -demethylase (CYP51) antisense *Arabidopsis* shows slow growth and long life. *BIOCHEM BIOPH RES CO* 285(1): 98-104.

Lange T., Kappler J., Fischer A., Frisse A., Padeffke T., Schmidtke S. and Lange M. J. P. (2005). Gibberellin biosynthesis in developing pumpkin seedlings. *PLANT PHYSIOL* 139(1): 213-223.

Lange T., Kramer C. and Pimenta Lange M. J. (2020). The Class III Gibberellin 2-Oxidases AtGA2ox9 and AtGA2ox10 Contribute to Cold Stress Tolerance and Fertility. *PLANT PHYSIOL* 184(1): 478-486.

Lange T. and Pimenta Lange M. J. (2020). The Multifunctional Dioxygenases of Gibberellin Synthesis. *Plant CELL PHYSIOL* 61(11): 1869-1879.

Lee H. W., Cho C. and Kim J. (2015). Lateral organ boundaries domain16 and 18 act downstream of the AUXIN1 and LIKE-AUXIN3 auxin influx carriers to control lateral root development in *Arabidopsis*. *PLANT PHYSIOL* 168(4): 1792-1806.

Li C., Potuschak T., Colón-Carmona A., Gutiérrez R. A. and Doerner P. (2005). *Arabidopsis* TCP20 links

regulation of growth and cell division control pathways. *P NATL ACAD SCI USA* 102(36): 12978-12983.

Li J. and Chory J. (1997). A putative leucine-rich repeat receptor kinase involved in brassinosteroid signal transduction. *CELL* 90(5): 929-938.

Li J., Nagpal P., Vitart V., McMorris T. C. and Chory J. (1996). A role for brassinosteroids in light-dependent development of *Arabidopsis*. *SCIENCE* 272(5260): 398-401.

Li J., Wen J., Lease K. A., Doke J. T., Tax F. E. and Walker J. C. (2002). BAK1, an *Arabidopsis* LRR receptor-like protein kinase, interacts with BRI1 and modulates brassinosteroid signaling. *CELL* 110(2): 213-222.

Li Q., Xu F., Chen Z., Teng Z., Sun K., Li X., Yu J., Zhang G., Liang Y. and Huang X. (2021). Synergistic interplay of ABA and BR signal in regulating plant growth and adaptation. *NAT PLANTS* 7(8): 1108-1118.

Li X., Chen X., Guo X., Yin L., Ahammed G. J., Xu C., Chen K., Liu C., Xia X. and Shi K. (2016). DWARF overexpression induces alteration in phytohormone homeostasis, development, architecture and carotenoid accumulation in tomato. *PLANT BIOTECHNOL J* 14(3): 1021-1033.

Liu H., Liu L., Liang D., Zhang M., Jia C., Qi M., Liu Y., Shao Z., Meng F., Hu S., Yin Y., Li C. and Wang Q. (2021). SIBES1 promotes tomato fruit softening through transcriptional inhibition of PME1. *ISCIENCE* 24(8): 102926.

Liu K., Li Y., Chen X., Li L., Liu K., Zhao H., Wang Y. and Han S. (2018). ERF72 interacts with ARF6 and BZR1 to regulate hypocotyl elongation in *Arabidopsis*. *J EXP BOT* 69(16): 3933-3947.

Liu L., Jia C., Zhang M., Chen D., Chen S., Guo R., Guo D. and Wang Q. (2014). Ectopic expression of a BZR1-1D transcription factor in brassinosteroid signalling enhances carotenoid accumulation and fruit quality attributes in tomato. *PLANT BIOTECHNOL J* 12(1): 105-115.

Louvet O., Doignon F. and Crouzet M. (1997). Stable DNA-binding yeast vector allowing high-bait expression for use in the two-hybrid system. *BIOTECHNIQUES* 23(5): 816-820.

Malinovsky F. G., Batoux M., Schwessinger B., Youn J. H., Stransfeld L., Win J., Kim S. K. and Zipfel C. (2014). Antagonistic regulation of growth and immunity by the *Arabidopsis* basic helix-loop-helix transcription factor homolog of brassinosteroid enhanced expression2 interacting with increased leaf inclination1 binding bHLH1. *PLANT PHYSIOL* 164(3): 1443-1455.

Martín-Trillo M. and Cubas P. (2010). TCP genes: a family snapshot ten years later. *TRENDS PLANT SCI* 15(1): 31-39.

Martínez C., Espinosa-Ruíz A., de Lucas M., Bernardo-García S., Franco-Zorrilla J. M. and Prat S. (2018). PIF 4-induced BR synthesis is critical to diurnal and thermomorphogenic growth. *EMBO J* 37(23): e99552.

Mazur M. J., Spears B. J., Djajasaputra A., Van Der Gragt M., Vlachakis G., Beerens B., Gassmann W. and Van den Burg H. A. (2017). *Arabidopsis* TCP transcription factors interact with the SUMO conjugating machinery in nuclear foci. *FRONT PLANT SCI* 8: 2043.

Mergner J., Frejno M., List M., Papacek M., Chen X., Chaudhary A., Samaras P., Richter S., Shikata H. and Messerer M. (2020). Mass-spectrometry-based draft of the *Arabidopsis* proteome. *NATURE* 579(7799): 409-414.

- Miura K., Jin J. B., Lee J., Yoo C. Y., Stirn V., Miura T., Ashworth E. N., Bressan R. A., Yun D. J. and Hasegawa P. M.** (2007). SIZ1-mediated sumoylation of ICE1 controls CBF3/DREB1A expression and freezing tolerance in Arabidopsis. *PLANT CELL* 19(4): 1403-1414.
- Mora-García S., Vert G., Yin Y., Caño-Delgado A., Cheong H. and Chory J.** (2004). Nuclear protein phosphatases with Kelch-repeat domains modulate the response to brassinosteroids in Arabidopsis. *GENE DEV* 18(4): 448-460.
- Mori K., Lemaire-Chamley M., Jorly J., Carrari F., Conte M., Asamizu E., Mizoguchi T., Ezura H. and Rothan C.** (2021). The conserved brassinosteroid-related transcription factor BIM1a negatively regulates fruit growth in tomato. *J EXP BOT* 72(4): 1181-1197.
- Murashige T. and Skoog F.** (1962). A revised medium for rapid growth and bio assays with tobacco tissue cultures. *PHYSIOL PLANTARUM* 15(3): 473-497.
- Nicolas M. and Cubas P.** (2016). TCP factors: new kids on the signaling block. *CURR OPIN PLANT BIOL* 33: 33-41.
- Nie S., Huang S., Wang S., Cheng D., Liu J., Lv S., Li Q. and Wang X.** (2017). Enhancing brassinosteroid signaling via overexpression of tomato (*Solanum lycopersicum*) SIBRI1 improves major agronomic traits. *FRONT PLANT SCI* 8: 1386.
- Nolan T. M., Vukašinović N., Liu D., Russinova E. and Yin Y.** (2020). Brassinosteroids: multidimensional regulators of plant growth, development, and stress responses. *PLANT CELL* 32(2): 295-318.
- Oh E., Zhu J. and Wang Z.** (2012). Interaction between BZR1 and PIF4 integrates brassinosteroid and environmental responses. *NAT CELL BIOL* 14(8): 802-809.
- Ohnishi T.** (2018). Recent advances in brassinosteroid biosynthetic pathway: insight into novel brassinosteroid shortcut pathway. *J PESTIC SCI*: D18-040.
- Ohnishi T., Godza B., Watanabe B., Fujioka S., Hategan L., Ide K., Shibata K., Yokota T., Szekeres M. and Mizutani M.** (2012). CYP90A1/CPD, a brassinosteroid biosynthetic cytochrome P450 of Arabidopsis, catalyzes C-3 oxidation. *J BIOL CHEM* 287(37): 31551-31560.
- Ohnishi T., Szatmari A., Watanabe B., Fujita S., Bancos S., Koncz C., Lafos M., Shibata K., Yokota T. and Sakata K.** (2006). C-23 hydroxylation by Arabidopsis CYP90C1 and CYP90D1 reveals a novel shortcut in brassinosteroid biosynthesis. *PLANT CELL* 18(11): 3275-3288.
- Poppenberger B., Rozhon W., Khan M., Husar S., Adam G., Luschnig C., Fujioka S. and Sieberer T.** (2011). CESTA, a positive regulator of brassinosteroid biosynthesis. *EMBO J* 30(6): 1149-1161.
- Qu J., Kang S. G., Hah C. and Jang J.** (2016). Molecular and cellular characterization of GA-Stimulated Transcripts GASA4 and GASA6 in Arabidopsis thaliana. *PLANT SCI* 246: 1-10.
- Ramakrishna P., Duarte P. R., Rance G. A., Schubert M., Vordermaier V., Dai Vu L., Murphy E., Barro A. V., Swarup K. and Moirangthem K.** (2019). EXPANSIN A1-mediated radial swelling of pericycle cells positions anticlinal cell divisions during lateral root initiation. *P NATL ACAD SCI USA* 116(17): 8597-8602.
- Ramirez V. E. and Poppenberger B.** (2020). Modes of brassinosteroid activity in cold stress tolerance. *FRONT PLANT SCI*: 1685.
- Resentini F., Felipo-Benavent A., Colombo L., Blázquez M. A., Alabadí D. and Masiero S.** (2015). TCP14

and TCP15 mediate the promotion of seed germination by gibberellins in *Arabidopsis thaliana*. *MOL PLANT* 8(3): 482-485.

Rozhon W., Akter S., Fernandez A. and Poppenberger B. (2019). Inhibitors of brassinosteroid biosynthesis and signal transduction. *MOLECULES* 24(23): 4372.

Rozhon W., Mayerhofer J., Petutschnig E., Fujioka S. and Jonak C. (2010). ASK θ , a group-III *Arabidopsis* GSK3, functions in the brassinosteroid signalling pathway. *PLANT J* 62(2): 215-223.

Shahnejat-Bushehri S., Allu A. D., Mehterov N., Thirumalaikumar V. P., Alseekh S., Fernie A. R., Mueller-Roeber B. and Balazadeh S. (2017). *Arabidopsis* NAC Transcription Factor JUNGBRUNNEN1 Exerts Conserved Control Over Gibberellin and Brassinosteroid Metabolism and Signaling Genes in Tomato. *FRONT PLANT SCI* 8: 214.

She J., Han Z., Kim T. W., Wang J., Cheng W., Chang J., Shi S., Wang J., Yang M. and Wang Z. Y. (2011). Structural insight into brassinosteroid perception by BRI1. *NATURE* 474(7352): 472-476.

Shimada Y., Fujioka S., Miyauchi N., Kushihiro M., Takatsuto S., Nomura T., Yokota T., Kamiya Y., Bishop G. J. and Yoshida S. (2001). Brassinosteroid-6-oxidases from *Arabidopsis* and tomato catalyze multiple C-6 oxidations in brassinosteroid biosynthesis. *PLANT PHYSIOL* 126(2): 770-779.

Spears, B. J., McInturf, S. A., Collins, C., Chlebowski, M., Cseke, L. J., Su, J., Mendoza-Cózatl, D. G. and Gassmann, W. (2022). Class I TCP transcription factor AtTCP8 modulates key brassinosteroid-responsive genes. *PLANT PHYSIOL* 190(2), 1457–1473.

Srivastava M., Srivastava A. K., Orosa-Puente B., Campanaro A., Zhang C. and Sadanandom A. (2020). SUMO conjugation to BZR1 enables brassinosteroid signaling to integrate environmental cues to shape plant growth. *CURR BIOL* 30(8): 1410-1423. e1413.

Sun Y., Han Z., Tang J., Hu Z., Chai C., Zhou B. and Chai J. (2013). Structure reveals that BAK1 as a co-receptor recognizes the BRI1-bound brassinolide. *CELL RES* 23(11): 1326-1329.

Szekerés M., Németh K., Koncz-Kálmán Z., Mathur J., Kauschmann A., Altmann T., Rédei G. P., Nagy E., Schell J. and Koncz C. (1996). Brassinosteroids rescue the deficiency of CYP90, a cytochrome P450, controlling cell elongation and de-etiolation in *Arabidopsis*. *CELL* 85(2): 171-182.

Takeda T., Amano K., Ohto M., Nakamura K., Sato S., Kato T., Tabata S. and Ueguchi C. (2006). RNA interference of the *Arabidopsis* putative transcription factor TCP16 gene results in abortion of early pollen development. *PLANT MOL BIOL* 61(1): 165-177.

Tatematsu K., Nakabayashi K., Kamiya Y. and Nambara E. (2008). Transcription factor AtTCP14 regulates embryonic growth potential during seed germination in *Arabidopsis thaliana*. *PLANT J* 53(1): 42-52.

Tomato Genome Consortium T. (2012). The tomato genome sequence provides insights into fleshy fruit evolution. *NATURE* 485(7400): 635.

Tong H., Xiao Y., Liu D., Gao S., Liu L., Yin Y., Jin Y., Qian Q. and Chu C. (2014). Brassinosteroid regulates cell elongation by modulating gibberellin metabolism in rice. *PLANT CELL* 26(11): 4376-4393.

Trémousaygue D., Garnier L., Bardet C., Dabos P., Hervé C. and Lescure B. (2003). Internal telomeric repeats and 'TCP domain' protein-binding sites co-operate to regulate gene expression in *Arabidopsis thaliana* cycling cells. *PLANT J* 33(6): 957-966.

- Tsuge T., Tsukaya H. and Uchimiya H.** (1996). Two independent and polarized processes of cell elongation regulate leaf blade expansion in *Arabidopsis thaliana* (L.) Heynh. *DEVELOPMENT* 122(5): 1589-1600.
- Unterholzner S. J., Rozhon W., Papacek M., Ciomas J., Lange T., Kugler K. G., Mayer K. F., Sieberer T. and Poppenberger B.** (2015). Brassinosteroids are master regulators of gibberellin biosynthesis in *Arabidopsis*. *PLANT CELL* 27(8): 2261-2272.
- Van Ploeg D. and Heuvelink E.** (2005). Influence of sub-optimal temperature on tomato growth and yield: a review. *J HORTIC SCI BIOTECHNOL* 80(6): 652-659.
- Vert G. and Chory J.** (2006). Downstream nuclear events in brassinosteroid signalling. *NATURE* 441(7089): 96-100.
- Viola I. L., Camoirano A. and Gonzalez D. H.** (2016). Redox-dependent modulation of anthocyanin biosynthesis by the TCP transcription factor TCP15 during exposure to high light intensity conditions in *Arabidopsis*. *PLANT PHYSIOL* 170(1): 74-85.
- Wang L., Einig E., Almeida-Trapp M., Albert M., Fliegmann J., Mithöfer A., Kalbacher H. and Felix G.** (2018). The systemin receptor SYR1 enhances resistance of tomato against herbivorous insects. *NAT PLANTS* 4(3): 152-156.
- Wang S., Hu T., Tian A., Luo B., Du C., Zhang S., Huang S., Zhang F. and Wang X.** (2020). Modification of Serine 1040 of SIBRI1 Increases Fruit Yield by Enhancing Tolerance to Heat Stress in Tomato. *INT J MOL SCI* 21(20): 7681.
- Wang S., Liu J., Zhao T., Du C., Nie S., Zhang Y., Lv S., Huang S. and Wang X.** (2019a). Modification of Threonine-1050 of SIBRI1 regulates BR Signalling and increases fruit yield of tomato. *BMC PLANT BIOL* 19(1): 1-13.
- Wang S., Lv S., Zhao T., Jiang M., Liu D., Fu S., Hu M., Huang S., Pei Y. and Wang X.** (2021). Modification of Threonine-825 of SIBRI1 Enlarges Cell Size to Enhance Fruit Yield by Regulating the Cooperation of BR-GA Signaling in Tomato. *INT J MOL SCI* 22(14): 7673.
- Wang X. and Chory J.** (2006). Brassinosteroids regulate dissociation of BKI1, a negative regulator of BRI1 signaling, from the plasma membrane. *SCIENCE* 313(5790): 1118-1122.
- Wang X., Kota U., He K., Blackburn K., Li J., Goshe M. B., Huber S. C. and Clouse S. D.** (2008). Sequential transphosphorylation of the BRI1/BAK1 receptor kinase complex impacts early events in brassinosteroid signaling. *DEV CELL* 15(2): 220-235.
- Wang X., Xu X., Mo X., Zhong L., Zhang J., Mo B. and Kuai B.** (2019b). Overexpression of TCP8 delays *Arabidopsis* flowering through a FLOWERING LOCUS C-dependent pathway. *BMC PLANT BIOL* 19(1): 1-10.
- Wang Z., Nakano T., Gendron J., He J., Chen M., Vafeados D., Yang Y., Fujioka S., Yoshida S. and Asami T.** (2002). Nuclear-localized BZR1 mediates brassinosteroid-induced growth and feedback suppression of brassinosteroid biosynthesis. *DEV CELL* 2(4): 505-513.
- Wang Z., Seto H., Fujioka S., Yoshida S. and Chory J.** (2001). BRI1 is a critical component of a plasma-membrane receptor for plant steroids. *NATURE* 410(6826): 380-383.
- Xia X. J., Fang P. P., Guo X., Qian X. J., Zhou J., Shi K., Zhou Y. H. and Yu J. Q.** (2018). Brassinosteroid-

mediated apoplastic H₂O₂-glutaredoxin 12/14 cascade regulates antioxidant capacity in response to chilling in tomato. *PLANT CELL ENVIRON* 41(5): 1052-1064.

Yan M., Xie D., Cao J., Xia X., Shi K., Zhou Y., Zhou J., Foyer C. H. and Yu J. (2020). Brassinosteroid-mediated reactive oxygen species are essential for tapetum degradation and pollen fertility in tomato. *PLANT J* 102(5): 931-947.

Yanai O., Shani E., Russ D. and Ori N. (2011). Gibberellin partly mediates LANCEOLATE activity in tomato. *PLANT J* 68(4): 571-582.

Yang L., Teixeira P. J. P. L., Biswas S., Finkel O. M., He Y., Salas-Gonzalez I., English M. E., Epple P., Mieczkowski P. and Dangl J. L. (2017). *Pseudomonas syringae* type III effector HopBB1 promotes host transcriptional repressor degradation to regulate phytohormone responses and virulence. *CELL HOST MICROBE* 21(2): 156-168.

Yang Z., Yan B., Dong H., He G., Zhou Y. and Sun J. (2021). BIC 1 acts as a transcriptional coactivator to promote brassinosteroid signaling and plant growth. *EMBO J* 40(1): e104615.

Ye H., Li L., Guo H. and Yin Y. (2012). MYBL2 is a substrate of GSK3-like kinase BIN2 and acts as a corepressor of BES1 in brassinosteroid signaling pathway in *Arabidopsis*. *P NATL ACAD SCI USA* 109(49): 20142-20147.

Yin Y., Vafeados D., Tao Y., Yoshida S., Asami T. and Chory J. (2005). A new class of transcription factors mediates brassinosteroid-regulated gene expression in *Arabidopsis*. *CELL* 120(2): 249-259.

Yin Y., Wang Z., Mora-Garcia S., Li J., Yoshida S., Asami T. and Chory J. (2002). BES1 accumulates in the nucleus in response to brassinosteroids to regulate gene expression and promote stem elongation. *CELL* 109(2): 181-191.

Yoo S., Cho Y. and Sheen J. (2007). *Arabidopsis* mesophyll protoplasts: a versatile cell system for transient gene expression analysis. *NAT PROTOC* 2(7): 1565-1572.

Zhang D., Ye H., Guo H., Johnson A., Zhang M., Lin H. and Yin Y. (2014). Transcription factor HAT 1 is phosphorylated by BIN 2 kinase and mediates brassinosteroid repressed gene expression in *Arabidopsis*. *PLANT J* 77(1): 59-70.

Zhang L., Han Q., Xiong J., Zheng T., Han J., Zhou H., Lin H., Yin Y. and Zhang D. (2019). Sumoylation of BRI1-EMS-SUPPRESSOR 1 (BES1) by the SUMO E3 ligase SIZ1 negatively regulates brassinosteroid signaling in *Arabidopsis thaliana*. *PLANT CELL PHYSIOL* 60(10): 2282-2292.

Zhang X., Fowler S. G., Cheng H., Lou Y., Rhee S. Y., Stockinger E. J. and Thomashow M. F. (2004). Freezing-sensitive tomato has a functional CBF cold response pathway, but a CBF regulon that differs from that of freezing-tolerant *Arabidopsis*. *PLANT J* 39(6): 905-919.

Zhao B. and Li J. (2012). Regulation of brassinosteroid biosynthesis and inactivation. *J INTEGR PLANT BIOL* 54(10): 746-759.

Zhao J., Peng P., Schmitz R. J., Decker A. D., Tax F. E. and Li J. (2002). Two putative BIN2 substrates are nuclear components of brassinosteroid signaling. *PLANT PHYSIOL* 130(3): 1221-1229.

Supplementary Information

Supplementary Tables

Supplementary Table 1. Primers used in this study.

Name	Sequence (5'-3')	Purpose
pCES-600-Fw-HindIII	CCCAAGCTTGATTAAAGTTTACCAAAAACACAAATG	LUC assays
pCES-OEPCR-Fw	ACATTGAACATGAAAATTTAAATCTACTGCACAGTGATAAA	LUC assays
pCES-OEPCR-Rev	GCAGTAGATTTTAAAAATTTTCATGTTCAATGTTAGATATATCTAACTTG	LUC assays
pCES-Rev-PstI	CCAATGCATTGGTTCTGCAGTAGAGACACTACAAATTAATCAAAATATG	LUC assays
TCP8-Fw-NcoI	CATGCCATGGCTATGGATCTCTCCGACATCCGAAAC	LUC assays
TCP8-Rev-NotI	ATAGTTTAGCGGCCGCTCACTCAGAGCTATTTGAGTTCTCCTCTC	LUC assays
TCP14-Fw-NcoI	CATGCCATGGCTATGAAAAGCCAACATCAAGT	LUC assays
TCP14-Rev-NotI	ATAGTTTAGCGGCCGCTAATCTTGCTGATCCTCCTCA	LUC assays
TCP15-Fw-NcoI	CATGCCATGGCTATGGATCCGGATCCGGATCA	LUC assays
TCP15-Rev-NotI	ATAGTTTAGCGGCCGCTAGGAATGATGACTGGTGCT	LUC assays
SOER2-cesD-GT	GCAGGCATGCAAGCTTATCGATATCTAGA	<i>ces-D</i> genotyping
SOEL2-cesD-GT	TGATGTGATATCTAGATCCGAAACTATCA	<i>ces-D</i> genotyping
TCP8-GT-F	TGTGAAAAGTTATTTTCTCCCC	<i>tcp8,14,15</i> genotyping
TCP8-GT-R	GGCGACGTATGAGCAGCAA	<i>tcp8,14,15</i> genotyping
TCP14-GT-F	GATTGAGCAGAAATTAACGTTG	<i>tcp8,14,15</i> genotyping
TCP14-GT-R	CACCACCGCAGATTCCTCT	<i>tcp8,14,15</i> genotyping
TCP15-GT-F	TCTGAATCGCTGAAATTTTCG	<i>tcp8,14,15</i> genotyping
TCP15-GT-R	GCAGGACTCTGACTCGTAGG	<i>tcp8,14,15</i> genotyping
CES-Fw-NdeI	GGAATTCCATATGATGGCACGTTTGAGC	Y2H
CES-Rev-BamHI	CGGGATCCTCAAAAGGGTAATGTTGAACGT	Y2H
TCP8-Fw-EcoRI	GGAATTCATGGATCTCTCCGACATCCGAAAC	Y2H
TCP8-Rev-BamHI	CGGGATCCTCACTCAGAGCTATTTGAGTTCTCCTCTC	Y2H
TCP14-Fw-EcoRI	GGAATTCATGAAAAGCCAACATCAAGT	Y2H
TCP14-Rev-BamHI	CGGGATCCCTAATCTTGCTGATCCTCCTCA	Y2H
TCP15-Fw-NdeI	GGAATTCCATATGATGGATCCGGATCCGGATCA	Y2H
TCP15-Rev-EcoRI	GGAATTCCTAGGAATGATGACTGGTGCT	Y2H
TCP15-Fw-NcoI	CATGCCATGGCTATGGATCCGGATCCGGATCA	<i>TCP15</i> -overexpression lines
TCP15-Rev-NotI	ATAGTTTAGCGGCCGCTGGAATGATGACTGGTGCTTCCATC	<i>TCP15</i> -overexpression lines
TCP8-qPCR-Fw	AGCTATTGTTGCTGCTACAGGT	Quantitative PCR
TCP8-qPCR-Rev	GAGTCAATCCAAGAGCACCGT	Quantitative PCR
TCP14-qPCR-Fw	CAAGAGGAATCTGCGGTGGT	Quantitative PCR
TCP14-qPCR-Rev	AACGCCGGCATCCTTATTCT	Quantitative PCR
TCP15-qPCR-Fw	ACAGCCTTTGGCTTCTGGTT	Quantitative PCR
TCP15-qPCR-Rev	GTTATGGTTCCCGTCTCCG	Quantitative PCR
CPD-qPCR-Fw	CTTGCTCAACTCAAGGAAGAG	Quantitative PCR
CPD-qPCR-Rev	CTCGTAGCGTCTCATTAACCAC	Quantitative PCR
EXPA1-qPCR-Fw	GATGTCAAGAACTGGGGACA	Quantitative PCR
EXPA1-qPCR-Rev	GAAAGACCAGCTGCGTTAG	Quantitative PCR
GAPC2-qPCR-Fw	TTGGTGACAACAGGTCAAGCA	Quantitative PCR
GAPC2-qPCR-Rev	AAACTTGTCGCTCAATGCAATC	Quantitative PCR

Supplementary Table 2. Overlap DEGs in *tcp8,14,15* and *ces-D*.

Tair ID	Fold change in <i>tcp8,14,15</i>	Fold change in <i>ces-D</i>	Description
AT2G26400	4.4810	-2.1653	ARD3; Encodes a protein predicted to belong to the acireductone dioxygenase (ARD/ARD#Aeo) family
AT1G47890	4.2883	-3.8921	RLP7; Receptor like protein 7
AT1G53480	3.1902	-6.9767	MRD1; Down-regulated in <i>mto1-1</i> mutant that over-accumulates soluble methionine.
AT3G45130	2.8038	-1.6528	LAS1; Lanosterol synthase 1
AT4G23310	2.7145	-1.5686	CRK23; Encodes a cysteine-rich receptor-like protein kinase
AT5G62920	2.6867	-1.5848	ARR6; Encodes a Type-A response regulator that is responsive to cytokinin treatment
AT1G19050	2.0603	-1.7563	ARR7; Involved in response to cytokinin and meristem stem cell maintenance.
AT2G15042	1.9931	-1.6696	Leucine-rich repeat (LRR) family protein
AT1G53340	1.7351	-1.8535	Cysteine/Histidine-rich C1 domain family protein
AT5G59680	1.6533	-1.5802	Leucine-rich repeat protein kinase family protein
AT3G46370	1.6203	-1.7510	Leucine-rich repeat protein kinase family protein
AT5G65600	1.5952	-1.5353	Concanavalin A-like lectin protein kinase family protein
AT5G25910	1.5540	-1.7545	RLP52; Putative disease resistance protein induced by chitin oligomers
AT1G53490	1.3738	-2.5934	HEI10; Encodes HEI10, a RING finger-containing protein required for class I crossover formation.
AT2G15880	1.2194	-2.6769	Leucine-rich repeat (LRR) family protein
AT4G01740	1.1821	-3.8397	Cysteine/Histidine-rich C1 domain family protein
AT3G27940	1.1675	-1.7318	LBD26; LOB domain-containing protein 26
AT2G18660	1.1403	-1.7611	PNP-A; it is stress responsive and can enhance its own expression
AT4G25070	1.1106	-1.6836	caldesmon-like protein
AT2G31141	1.0958	-3.0273	Hypothetical protein
AT4G13572	1.0913	-1.6585	Hypothetical protein
AT4G11521	1.0515	-2.0432	Receptor-like protein kinase-related family protein
AT1G44800	0.9897	-1.9168	SIAR2, nodulin MtN21 /EamA-like transporter family protein
AT4G13810	0.9495	-8.6668	RLP47; Receptor like protein 47
AT4G36850	0.9107	-1.6518	PQ-loop repeat family protein / transmembrane family protein
AT1G51800	0.8981	-1.7432	IOS1; Leucine-rich repeat protein kinase family protein
AT5G14940	0.8712	-1.6625	Major facilitator superfamily protein
AT2G37980	0.8000	-1.6414	O-fucosyltransferase family protein
AT2G39510	0.7824	-1.6762	UMAMIT14; nodulin MtN21 /EamA-like transporter family protein
AT1G13650	0.7712	-1.5576	Hypothetical protein
AT5G64000	0.7615	-1.9515	SAL2; Inositol monophosphatase family protein
AT3G15400	0.7462	-2.5960	ATA20; Encodes a protein with novel repeat sequences and a glycine-rich domain
AT4G01720	0.7362	-1.7675	WRKY47; Member of WRKY Transcription Factor; Group II-b
AT3G15356	0.7316	-1.6695	Legume lectin family protein
AT1G73890	0.7257	-3.0283	Bifunctional inhibitor/lipid-transfer protein/seed storage 2S albumin superfamily protein
AT1G68690	0.7153	-1.6597	PERK9; Encodes a member of the proline-rich extensin-like receptor kinase (PERK) family
AT5G54710	0.7129	-1.5333	Ankyrin repeat family protein
AT1G56510	0.7048	-8.4845	WRR4; Disease resistance protein (TIR-NBS-LRR class)
AT1G78090	0.6813	-1.9429	TPPB; trehalose-6-phosphate phosphatase
AT2G27402	0.6593	-6.1161	Plastid transcriptionally active protein
AT4G14370	0.6566	-1.7557	Disease resistance protein (TIR-NBS-LRR class) family
AT3G62150	0.6429	-2.1922	ACBC21; Encodes a facultative transporter controlling auxin concentrations in plant cells
AT4G16960	0.6285	-2.0574	Disease resistance protein (TIR-NBS-LRR class)
AT4G19090	0.6180	-2.1110	Transmembrane protein, putative (DUF594)
AT4G12120	0.5913	-1.6188	SEC1B; Sec1/munc18-like (SM) proteins superfamily
AT1G15960	0.5841	-1.6245	NRAMP6; NRAMP metal ion transporter 6
AT1G58190	0.5796	-1.5495	RLP9; Receptor like protein 9
AT1G27045	0.5583	-1.5648	ATHB54; Encodes ATHB54, a member of the homeodomain leucine zipper (HD-Zip) family protein

AT4G01430	0.5565	-2.0170	UMAMIT29; nodulin MtN21 /EamA-like transporter family protein
AT1G71890	0.5441	-1.6189	SUC5; Encodes a sucrose transporter that is expressed in the endosperm
AT2G37460	0.5279	-1.9687	UMAMIT12; nodulin MtN21 /EamA-like transporter family protein
AT4G11830	0.5224	-2.2430	PLDGAMMA2; Encodes one of three phospholipase D enzymes of the gamma class
AT4G16860	0.5097	-25.9257	RPP4; Disease resistance protein (TIR-NBS-LRR class) family
AT5G11650	0.4817	-1.5733	alpha/beta-Hydrolases superfamily protein
AT4G16900	0.4657	-3.6004	Disease resistance protein (TIR-NBS-LRR class) family
AT1G58602	0.4588	-15.6427	LRR and NB-ARC domains-containing disease resistance protein
AT2G32340	0.4542	-1.5468	TraB family protein
AT2G26710	0.4410	-1.9533	BAS1; A control point between multiple photoreceptor systems and brassinosteroid signal transduction
AT3G16420	0.4180	-1.6744	PBP1; PYK10-binding protein 1
AT2G32560	0.3779	-1.8041	F-box family protein
AT4G00980	0.3732	-2.8656	zinc knuckle (CCHC-type) family protein
AT1G56520	0.3691	-3.2745	Disease resistance protein (TIR-NBS-LRR class) family
AT1G59560	0.3624	-2.8389	ZCF61; E3 Ubiquitin ligase family protein
AT1G55730	0.3575	-1.6180	CAX5; Member of Low affinity calcium antiporter CAX2 family
AT1G22590	0.3189	-1.5184	AGL87; AGAMOUS-like 87
AT2G31150	0.2546	-5.3952	ATP binding / ATPase
AT4G13160	0.2495	-1.8146	zein-binding protein (Protein of unknown function, DUF593)
AT4G19430	-2.6542	4.8886	Hypothetical protein
AT5G38120	-2.1765	1.9041	4CL8; AMP-dependent synthetase and ligase family protein
AT2G19960	-2.0180	1.6835	hAT family dimerization domain-containing protein
AT4G08040	-1.9007	1.6763	ACS11; 1-aminocyclopropane-1-carboxylate synthase 11
AT3G46490	-1.7744	2.3177	2-oxoglutarate (2OG) and Fe(II)-dependent oxygenase superfamily protein
AT3G28270	-1.7085	2.6492	Transmembrane protein, putative (DUF677)
AT5G03230	-1.5404	2.7897	Senescence regulator (Protein of unknown function, DUF584)
AT1G31710	-1.4614	1.7578	Copper amine oxidase family protein
AT4G36430	-1.4025	1.5468	Peroxidase superfamily protein
AT1G23060	-1.4024	5.1879	MDP40; hypothetical protein
AT2G32100	-1.3981	1.5356	OFP16; ovate family protein 16
AT1G75590	-1.3772	1.9454	SAUR52; SAUR-like auxin-responsive protein family
AT1G62520	-1.3645	1.6768	Sulfated surface-like glycoprotein
AT2G02850	-1.2753	3.0549	ARPN; Encodes plantacyanin one of blue copper proteins
AT3G61810	-1.1936	2.5787	Glycosyl hydrolase family 17 protein
AT3G17130	-1.1753	2.1189	Plant invertase/pectin methylesterase inhibitor superfamily protein
AT5G22580	-1.1609	2.7374	Stress responsive A/B Barrel Domain-containing protein
AT1G77690	-1.1147	1.5363	LAX3; Encodes an auxin influx carrier LAX3 (Like Aux1) that promotes lateral root emergence
AT2G16990	-1.0158	2.1872	Major facilitator superfamily protein
AT4G37295	-0.9461	1.5027	Hypothetical protein
AT1G67050	-0.9449	1.6979	Membrane-associated kinase regulator
AT2G38530	-0.9405	2.7098	LTP2; Involved in lipid transfer between membranes
AT1G52565	-0.9267	1.6462	Cytochrome P450 family protein
AT3G11690	-0.9119	1.5407	Hypothetical protein
AT5G22460	-0.8581	2.4958	alpha/beta-Hydrolases superfamily protein
AT2G17880	-0.8352	1.6088	Chaperone DnaJ-domain superfamily protein
AT1G01420	-0.8029	1.6674	UGT72B3; UDP-glucosyl transferase 72B3
AT2G47180	-0.7833	2.4406	GolS1; GolS1 is a galactinol synthase
AT4G30650	-0.7560	1.6024	Low temperature and salt responsive protein family
AT5G50335	-0.7531	1.9290	Hypothetical protein
AT4G19810	-0.7364	3.1455	ChiC; ChiC encodes a Class V chitinase
AT3G44990	-0.7050	1.5635	XTH31; Encodes a xyloglucan endotransglycosylase/hydrolase

AT3G49970	-0.7020	1.5540	Phototropic-responsive NPH3 family protein
AT1G69530	-0.7015	1.7281	EXPA1; Involved in the formation of nematode-induced syncytia in roots of <i>Arabidopsis thaliana</i>
AT1G74670	-0.6990	2.0145	GASA6; Gibberellin-regulated family protein
AT2G42900	-0.6842	2.7823	Plant basic secretory protein (BSP) family protein
AT1G51170	-0.6681	1.7968	UCN; Protein kinase superfamily protein
AT4G39950	-0.6522	1.5128	CYP79B2; Belongs to cytochrome P450 and is involved in tryptophan metabolism
AT1G61795	-0.6331	1.6561	PAK-box/P21-Rho-binding family protein
AT4G33490	-0.6271	3.7563	Eukaryotic aspartyl protease family protein
AT5G62360	-0.6269	5.1575	Plant invertase/pectin methylesterase inhibitor superfamily protein
AT1G13080	-0.6126	1.8803	CYP71B2; Cytochrome P450 monooxygenase
AT3G28130	-0.6079	1.6113	UMAMIT44; nodulin MtN21 /EamA-like transporter family protein
AT4G16515	-0.6033	4.2363	RGF6; Encodes a root meristem growth factor (RGF)
AT2G31560	-0.5908	1.5260	Signal transducer/transcription protein, putative (DUF1685)
AT5G16340	-0.5550	1.9164	AMP-dependent synthetase and ligase family protein
AT1G52190	-0.5086	2.1914	Encodes a low affinity nitrate transporter that is expressed in the plasma membrane
AT1G32170	-0.4892	1.5675	XTH30; xyloglucan endotransglycosylase-related protein (XTR4)
AT3G22790	-0.4621	1.5103	NET1A; Kinase interacting (KIP1-like) family protein
AT3G49940	-0.4561	1.7880	LBD38; LOB domain-containing protein 38
AT4G37980	-0.4468	1.5301	ELI3-1; Cinnamyl alcohol dehydrogenase 7
AT4G18750	-0.4447	1.5144	DOT4; Encodes a pentatricopeptide (PPR) protein involved in leaf and root development
AT3G01490	-0.4316	2.6899	Protein kinase superfamily protein
AT5G12950	-0.4273	1.7593	proline-tRNA ligase (DUF1680)
AT2G21590	-0.4187	3.0922	APL4; Encodes the large subunit of ADP-glucose pyrophosphorylase
AT5G58550	-0.4151	1.6546	EOL2; Encodes a paralog of ETO1, which is a negative regulator of ACS5
AT5G03760	-0.4056	1.6355	ATCSLA09; Nucleotide-diphospho-sugar transferases superfamily protein
AT4G30020	-0.4020	2.6707	PA-domain containing subtilase family protein
AT5G05690	-0.4020	1.9611	CPD; Cytochrome P450 superfamily protein
AT4G25260	-0.3813	1.9520	Plant invertase/pectin methylesterase inhibitor superfamily protein
AT3G05810	-0.3555	1.5489	IGR motif protein
AT1G51070	-0.3253	1.5231	bHLH115; basic helix-loop-helix (bHLH) DNA-binding superfamily protein
AT2G30230	-0.3107	1.6273	6,7-dimethyl-8-ribityllumazine synthase
AT5G01090	-0.2918	1.6366	Concanavalin A-like lectin family protein
AT5G62350	-0.2799	1.7894	Plant invertase/pectin methylesterase inhibitor superfamily protein
AT3G02570	-0.2736	2.0607	MEE31; Encodes a protein with phosphomannose isomerase activity
AT4G37800	-0.2540	3.0278	XTH7; xyloglucan endotransglucosylase/hydrolase 7

Supplementary Table 3. Overlap DEGs in *tcp8,14,15* and *ces bee qM*.

Tair ID	Fold change in <i>t8t14t15</i>	Fold change in <i>qM</i>	Gene description
AT3G28510	4.9196	3.0437	P-loop containing nucleoside triphosphate hydrolases superfamily protein
AT5G52730	4.6435	4.2347	Copper transport protein family
AT2G26400	4.4810	3.3196	ARD3; Encodes a protein predicted to belong to the acireductone dioxygenase (ARD/ARD#Aeo) family
AT2G39030	3.4967	4.6816	NATA1; Encodes a protein that acts as an ornithine N-delta-acetyltransferase
AT5G02780	3.1426	2.7203	GSTL1; Encodes a member of the lambda family of glutathione transferases
AT4G23310	2.7145	2.5080	CRK23; Encodes a cysteine-rich receptor-like protein kinase
AT3G57260	2.5433	2.4785	BGL2; beta-1,3-glucanase 2
AT3G55970	1.8256	6.0659	JRG21; Jasmonate-regulated gene 21
AT3G24900	1.6891	3.7681	RLP39; Receptor like protein 39
AT4G40020	1.4829	3.0444	Myosin heavy chain-related protein
AT3G25010	1.4406	2.2970	RLP41; Receptor like protein 41
AT1G79680	1.4227	2.3488	WAKL10; Encodes a twin-domain, kinase-GC signaling molecule that may function in biotic stress responses
AT5G61010	1.2884	0.7953	EXO70E2; Exocyst subunit exo70 family protein E2
AT4G23160	1.2281	2.3505	CRK8; Encodes a cysteine-rich receptor-like protein kinase
AT2G26560	1.1900	2.5550	PLA2A; Encodes a lipid acyl hydrolase that accumulates upon infection by fungal and bacterial pathogens
AT1G18390	1.1749	2.6196	Serine/Threonine kinase family catalytic domain protein
AT1G61560	1.1740	3.3417	MLO6; Seven transmembrane MLO family protein
AT4G09420	1.1593	2.2653	Disease resistance protein (TIR-NBS class)
AT2G18660	1.1403	3.0072	PNP-A; Encodes PNP-A (Plant Natriuretic Peptide A), it is stress responsive and can enhance its own expression
AT3G47540	1.1087	2.3845	Chitinase family protein
AT2G17290	1.0204	1.4052	CPK6; Encodes calcium dependent protein kinase 6 (CPK6), a member of the Arabidopsis CDPK gene family.
AT1G21250	1.0085	0.9117	WAK1; Cell wall-associated kinase, may function as a signaling receptor of extracellular matrix component
AT4G21850	0.9649	2.0109	MSRB9; Methionine sulfoxide reductase B9
AT1G05000	0.9558	2.9809	PFA-DSP1; Encodes an atypical dual-specificity phosphatase
AT5G10760	0.9482	1.8447	Eukaryotic aspartyl protease family protein
AT1G21240	0.9136	1.9334	WAK3; Encodes a wall-associated kinase
AT4G08850	0.9011	0.9950	Leucine-rich repeat receptor-like protein kinase family protein
AT1G66500	0.8995	1.7176	Pre-mRNA cleavage complex II
AT5G25250	0.8785	1.6087	FLOT1; SPFH/Band 7/PHB domain-containing membrane-associated protein family
AT5G46350	0.8699	2.1282	WRKY8; WRKY DNA-binding protein 8
AT5G25930	0.8552	1.7605	Kinase family with leucine-rich repeat domain-containing protein
AT4G01910	0.8431	2.7637	Cysteine/Histidine-rich C1 domain family protein
AT5G25440	0.8366	1.2292	Protein kinase superfamily protein
AT2G41380	0.8035	2.9110	S-adenosyl-L-methionine-dependent methyltransferases superfamily protein
AT4G28490	0.7347	2.2454	HAE; Member of Receptor kinase-like protein family; Controls the separation step of floral organ abscission
AT3G15356	0.7316	1.8206	Legume lectin family protein
AT2G17500	0.7265	2.7057	Auxin efflux carrier family protein
AT1G68690	0.7153	2.9946	PERK9; Encodes a member of the proline-rich extensin-like receptor kinase (PERK) family
AT4G18210	0.7130	2.0364	PUP10; Member of a family of proteins related to PUP1, a purine transporter
AT4G23190	0.7099	1.5126	CRK11; Encodes receptor-like protein kinase that is induced by <i>Ralstonia solanacearum</i>
AT4G21400	0.7053	1.8234	CRK28; Encodes a cysteine-rich receptor-like protein kinase
AT1G74360	0.7014	2.6748	Leucine-rich repeat protein kinase family protein
AT5G52800	0.6765	1.2000	DNA primase
AT4G35110	0.6743	1.8905	Phospholipase-like protein (PEARLI 4) family protein
AT3G27210	0.6739	2.1277	Hypothetical protein
AT2G46270	0.6652	2.7292	GBF3; Encodes a bZIP G-box binding protein whose expression is induced by ABA
AT1G07000	0.6582	1.3335	EXO70B2; Exocyst subunit exo70 family protein B2
AT2G13790	0.6568	1.1440	SERK4; Somatic embryogenesis receptor-like kinase 4

AT4G14370	0.6566	3.0562	Disease resistance protein (TIR-NBS-LRR class) family
AT3G14050	0.6475	2.3596	RSH2; RELA/SPOT homolog 2
AT3G62150	0.6429	1.6292	ACBC21; Encodes a facultative transporter controlling auxin concentrations in plant cells
AT5G47590	0.6407	1.5161	Heat shock protein HSP20/alpha crystallin family
AT5G33290	0.6301	1.2523	XGD1; Acts as a xylogalacturonan xylosyltransferase within the XGA biosynthesis pathway
AT4G08470	0.6273	1.0339	MEKK3; Encodes a member of the A1 subgroup of the MEKK (MAPK/ERK kinase kinase) family
AT1G23840	0.6216	1.5338	Transmembrane protein
AT1G66920	0.6216	1.8814	Protein kinase superfamily protein
AT1G19180	0.6207	1.4733	JAZ1; JAZ1 is a nuclear-localized protein involved in jasmonate signaling
AT5G49520	0.6027	2.3352	WRKY48; Encodes WRKY48, a member of the WRKY Transcription Factor
AT2G13800	0.5909	1.1865	SERK5; Somatic embryogenesis receptor-like kinase 5
AT1G12290	0.5887	3.0175	Disease resistance protein (CC-NBS-LRR class) family
AT2G15480	0.5819	2.0090	UGT73B5; UDP-glucosyl transferase 73B5
AT2G02220	0.5762	1.1029	PSKR1; Encodes a protein interacting with phytoalkaline, a five amino acid sulfated peptide (YIYTQ)
AT1G28190	0.5702	2.9016	Hypothetical protein
AT1G03370	0.5692	1.4257	C2 calcium/lipid-binding and GRAM domain containing protein
AT4G23550	0.5563	3.7260	WRKY29; Encodes WRKY DNA-binding protein 29 (WRKY29)
AT1G72280	0.5493	2.1460	ERO1; Endoplasmic reticulum oxidoreductins 1
AT2G35290	0.5430	3.5551	Hypothetical protein
AT5G37740	0.5394	1.8156	Calcium-dependent lipid-binding (CaLB domain) family protein
AT2G04430	0.5384	1.6743	NUDT5; Nudix hydrolase homolog 5
AT1G10050	0.5357	2.0832	glycosyl hydrolase family 10 protein / carbohydrate-binding domain-containing protein
AT1G67800	0.5350	1.4297	Copine (Calcium-dependent phospholipid-binding protein) family
AT1G30620	0.5133	2.2145	MUR4; NAD(P)-binding Rossmann-fold superfamily protein
AT3G13380	0.5103	2.9453	BRL3; Similar to BRI, brassinosteroid receptor protein
AT1G24150	0.5060	1.4113	FH4; Encodes a group I formin; Localized to cell junctions; Polymerizes actin. Binds profilin
AT1G22280	0.4995	0.9528	PAPP2C; phytochrome-associated protein phosphatase type 2C
AT5G40170	0.4962	1.1851	RLP54; Receptor like protein 54
AT1G08930	0.4886	1.2322	ERD6; Encodes a putative sucrose transporter whose gene expression is induced by dehydration and cold
AT1G17990	0.4827	1.4753	FMN-linked oxidoreductases superfamily protein
AT1G28380	0.4808	1.0044	NSL1; Involved in negatively regulating salicylic acid-related defense responses and cell death programs
AT2G31090	0.4786	1.0091	Transmembrane protein
AT4G22780	0.4669	1.9206	ACR7; Member of a family of ACT domain containing proteins; ACT domains are involved in amino acid binding
AT2G37710	0.4654	1.1158	RLK; Receptor lectin kinase; Induced in response to Salicylic acid
AT2G19710	0.4614	1.6240	Regulator of Vps4 activity in the MVB pathway protein
AT3G55430	0.4526	1.8716	O-Glycosyl hydrolases family 17 protein
AT5G20400	0.4492	1.7971	2-oxoglutarate (2OG) and Fe(II)-dependent oxygenase superfamily protein
AT1G09970	0.4429	1.1533	LRR XI-23; Leucine-rich receptor-like protein kinase family protein
AT3G54950	0.4393	2.9718	pPLAIIIbeta; Encodes pPLAIIIbeta, a member of the Group 3 patatin-related phospholipases
AT1G05805	0.4377	1.7407	Basic helix-loop-helix (bHLH) DNA-binding superfamily protein
AT2G05940	0.4305	1.6744	RIPK; Encodes a receptor-like cytoplasmic kinase leading to the activation of a plant innate immune receptor RPM1
AT2G28890	0.4304	1.0794	PLL4; Encodes a protein phosphatase 2C like gene, similar to POL; Involved in leaf development
AT1G20100	0.4146	0.7548	DNA ligase-like protein
AT5G43060	0.4134	2.0709	RD21B; Granulin repeat cysteine protease family protein
AT1G32940	0.4109	2.5630	SBT3.5; Subtilase family protein
AT5G53370	0.3972	0.9085	PMEPCRF; Pectin methyltransferase PCR fragment F
AT3G60640	0.3893	1.8877	ATG8G; Ubiquitin-like superfamily protein
AT2G23450	0.3882	1.1471	Protein kinase superfamily protein
AT4G23270	0.3823	2.3608	CRK19; Encodes a cysteine-rich receptor-like protein kinase
AT1G61360	0.3767	2.1001	S-locus lectin protein kinase family protein
AT5G61210	0.3735	1.0691	SNAP33; Membrane localized, probably involved in cytokinesis and cell plate formation
AT3G53780	0.3678	1.3421	RBL4; RHOMBOID-like protein 4

AT4G25900	0.3661	1.4974	Galactose mutarotase-like superfamily protein
AT4G33430	0.3629	1.6062	BAK1; BRI1-associated receptor kinase; Leu-rich receptor Serine/threonine protein kinase
AT5G63370	0.3625	1.2917	Protein kinase superfamily protein
AT4G37640	0.3624	1.4300	ACA2; Calcium ATPase 2
AT3G57330	0.3613	0.9327	ACA11; Autoinhibited Ca ²⁺ -ATPase 11
AT5G61530	0.3424	1.1440	Small G protein family protein / RhoGAP family protein
AT4G22920	0.3401	2.0303	NYE1; Similar to the tomato senescence-inducible chloroplast stay-green protein 1
AT3G28450	0.3388	1.2785	BIR2; BAK1-interacting receptor-like kinase 2
AT1G18890	0.3244	1.6200	CDPK1; Encodes a calcium-dependent protein kinase whose expression is induced by dehydration and high salt
AT1G77370	0.3139	0.7508	Glutaredoxin family protein
AT3G07780	0.3134	0.9062	OBE1; Plays an important role in the maintenance and/or establishment of the root and shoot apical meristems
AT1G76520	0.3124	1.0478	Auxin efflux carrier family protein
AT2G46620	0.3027	2.4562	P-loop containing nucleoside triphosphate hydrolases superfamily protein
AT1G65520	0.3013	1.6587	ECI1; Encodes a peroxisomal delta3, delta2-enoyl CoA isomerase, involved in unsaturated fatty acid degradation
AT4G19140	0.3011	1.1868	Exopolysaccharide production negative regulator
AT1G54130	0.2985	1.2986	RSH3; RELA/SPOT homolog 3
AT5G62740	0.2964	1.9899	HIR1; SPFH/Band 7/PHB domain-containing membrane-associated protein family
AT3G54810	0.2879	1.7082	BME3; Plant-specific GATA-type zinc finger transcription factor family protein
AT1G03290	0.2827	1.2072	ELKS/Rab6-interacting/CAST family protein
AT5G13190	0.2809	1.0694	GILP; Acts as a negative regulation of hypersensitive cell death
AT3G43230	0.2765	1.1984	RING/FYVE/PHD-type zinc finger family protein
AT4G23850	0.2639	0.8355	LACS4; AMP-dependent synthetase and ligase family protein
AT4G02370	0.2621	1.3704	Pectinesterase (Protein of unknown function, DUF538)
AT5G53310	0.2581	0.9491	Myosin heavy chain-like protein
AT5G50630	0.2550	1.0141	Major facilitator superfamily protein
AT2G40880	0.2503	0.4735	CYSA; Encodes a protein with cysteine proteinase inhibitor activity
AT3G18370	0.2500	1.1971	ATSYTF; C2 domain-containing protein
AT4G21560	0.2477	1.0668	Vacuolar protein sorting-associated protein-like protein
AT5G35460	0.2435	0.7429	Membrane protein
AT5G50430	0.2380	1.2465	UBC33; Ubiquitin-conjugating enzyme 33
AT3G18820	0.2361	0.6489	RAB7B; RAB GTPase homolog G3F
AT1G68000	0.2338	1.1480	PIS1; Phosphatidylinositol synthase 1
AT5G35200	0.2305	0.9176	ENTH/ANTH/VHS superfamily protein
AT2G44180	0.2295	1.1466	MAP2A; Encodes a MAP2 like methionine aminopeptidase
AT2G17130	0.2195	1.1571	IDH2; Encodes a regulatory subunit of the mitochondrially-localized NAD ⁺ - dependent isocitrate dehydrogenase
AT3G19240	0.2154	1.8115	Vacuolar import/degradation, Vid27-related protein
AT3G15810	0.2130	1.1590	LURP-one-like protein (DUF567)
AT5G19000	0.1992	1.4039	BPM1; Encodes a member of the MATH-BTB domain proteins (BPMs)
AT1G12760	0.1880	0.9329	Zinc finger, C3HC4 type (RING finger) family protein
AT4G00355	0.1729	1.0402	ATi2; Mesoderm induction early response protein
AT3G21460	-2.4025	-1.6484	Glutaredoxin family protein
AT2G20670	-2.0910	-2.0866	Sugar phosphate exchanger, putative (DUF506)
AT3G28270	-1.7085	-2.8516	Transmembrane protein, putative (DUF677)
AT2G32100	-1.3981	-2.8673	OFP16; ovate family protein 16
AT5G22580	-1.1609	-1.7505	Stress responsive A/B Barrel Domain-containing protein
AT1G18000	-1.1398	-1.4394	Major facilitator superfamily protein
AT1G77690	-1.1147	-2.2604	LAX3; Encodes an auxin influx carrier LAX3 (Like Aux1) that promotes lateral root emergence
AT5G06790	-1.0365	-2.9279	MPH15.15; Cotton fiber protein
AT5G25190	-0.9918	-2.5527	ESE3; Encodes a member of the ERF subfamily B-6 of ERF/AP2 transcription factor family
AT5G65390	-0.9899	-4.2143	AGP7; Arabinogalactan protein 7
AT3G29670	-0.9777	-2.4808	PMAT2; Encodes a malonyltransferase that may play a role in phenolic xenobiotic detoxification
AT4G24780	-0.9544	-2.4490	Pectin lyase-like superfamily protein

AT3G11690	-0.9119	-2.1571	Hypothetical protein
AT4G29905	-0.8965	-1.9856	Hypothetical protein
AT5G59080	-0.8508	-0.9952	Hypothetical protein
AT4G26530	-0.8430	-2.5709	FBA5; Aldolase superfamily protein
AT2G25200	-0.8426	-1.8245	Hypothetical protein (DUF868)
AT2G03750	-0.8289	-1.8579	P-loop containing nucleoside triphosphate hydrolases superfamily protein
AT2G36870	-0.8173	-1.1126	XTH32; Encodes a xyloglucan endotransglycosylase/hydrolase
AT1G15260	-0.8013	-1.2801	LOW protein: ATP-dependent RNA helicase-like protein
AT4G26850	-0.7774	-1.1593	VTC2; Encodes a novel protein involved in ascorbate biosynthesis
AT3G23810	-0.7609	-2.0263	SAHH2; S-adenosyl-l-homocysteine (SAH) hydrolase 2
AT5G25980	-0.7479	-1.6778	TGG2; Myrosinase (thioglucoside glucohydrolase) gene involved in glucosinolate metabolism
AT1G13930	-0.7433	-1.3748	Involved in response to salt stress; Knockout mutants are hypersensitive to salt stress
AT5G19190	-0.7078	-1.1455	Hypothetical protein
AT1G69530	-0.7015	-1.6151	EXPA1; Involved in the formation of nematode-induced syncytia in roots of Arabidopsis thaliana
AT1G74670	-0.6990	-5.4723	GASA6; Gibberellin-regulated family protein
AT3G17640	-0.6974	-3.2561	Leucine-rich repeat (LRR) family protein
AT3G20820	-0.6941	-2.1283	Leucine-rich repeat (LRR) family protein
AT4G23820	-0.6871	-2.0518	Pectin lyase-like superfamily protein
AT2G23690	-0.6849	-2.6719	HTH-type transcriptional regulator
AT3G01440	-0.6768	-1.7451	PnsL3; Encodes a subunit of the NAD(P)H complex located in the chloroplast thylakoid lumen
AT3G05936	-0.6733	-3.8874	Hypothetical protein
AT5G65730	-0.6539	-3.1034	XTH6; xyloglucan endotransglucosylase/hydrolase 6
AT3G54400	-0.6417	-2.8713	Eukaryotic aspartyl protease family protein
AT1G68520	-0.6390	-1.6595	BBX14; B-box type zinc finger protein with CCT domain-containing protein
AT2G33735	-0.6324	-3.4936	Chaperone DnaJ-domain superfamily protein
AT5G67280	-0.6288	-2.1764	RLK; receptor-like kinase
AT4G17090	-0.6272	-1.0733	BAM3; BMY8; Encodes a beta-amylase targeted to the chloroplast
AT1G09750	-0.6187	-2.7438	Eukaryotic aspartyl protease family protein
AT3G12120	-0.6146	-0.9665	FAD2; Major enzyme responsible for the synthesis of 18:2 fatty acids in the endoplasmic reticulum
AT3G28130	-0.6079	-2.5856	UMAMIT44; nodulin MtN21 /EamA-like transporter family protein
AT4G36540	-0.6069	-2.0354	BEE2; Encodes the brassinosteroid signaling component BEE2 (BR-ENHANCED EXPRESSION 2)
AT4G13840	-0.5877	-1.2508	HXXXD-type acyl-transferase family protein
AT3G14210	-0.5809	-2.1398	ESM1; GDSSL-like lipase/acylhydrolase superfamily protein
AT2G45470	-0.5726	-2.1618	FLA8; FASCICLIN-like arabinogalactan protein 8
AT5G40380	-0.5665	-2.0512	CRK42; cysteine-rich RLK (RECEPTOR-like protein kinase) 42
AT5G52780	-0.5604	-0.8156	Transmembrane protein, putative (DUF3464)
AT4G26960	-0.5471	-4.4198	Hypothetical protein
AT5G25460	-0.5372	-2.3206	DGR2; Transmembrane protein, putative (Protein of unknown function, DUF642)
AT4G12390	-0.5350	-1.2117	PME1; Pectin methylesterase inhibitor 1
AT4G27440	-0.5276	-2.2920	PORB; Light-dependent NADPH:protochlorophyllide oxidoreductase B
AT2G45960	-0.5160	-1.1994	PIP1B; A member of the plasma membrane intrinsic protein subfamily PIP1
AT1G49500	-0.5137	-1.2372	Transcription initiation factor TFIIID subunit 1b-like protein
AT2G28900	-0.5131	-1.5795	OEP16-1; Encodes AtOEP16 involved in plastid import of protochlorophyllide oxidoreductase A
AT3G08030	-0.5118	-1.4548	DNA-directed RNA polymerase subunit beta (Protein of unknown function, DUF642)
AT1G52190	-0.5086	-2.3999	Encodes a low affinity nitrate transporter that is expressed in the plasma membrane
AT1G01430	-0.4835	-1.5989	TBL25; Encodes a member of the TBL gene family containing a plant-specific DUF231 domain.
AT4G39980	-0.4778	-1.2587	DHS1; Encodes a 2-deoxy-D-arabino-heptulosonate 7-phosphate (DAHP) synthase
AT3G53750	-0.4722	-1.8592	ACT3; Member of the Actin gene family; Expressed in mature pollen
AT5G62670	-0.4689	-2.0696	HA11; H[+]-ATPase 11
AT4G33660	-0.4654	-1.9095	Cysteine-rich TM module stress tolerance protein
AT5G14410	-0.4584	-1.9707	Hypothetical protein
AT3G49940	-0.4561	-1.7673	LBD38; LOB domain-containing protein 38

AT3G56070	-0.4482	-1.1343	ROC2; Rotamase cyclophilin 2 exhibiting peptidyl-prolyl cis-trans isomerase activity involved in signal transduction.
AT4G37980	-0.4468	-1.8891	ELI3-1; Cinnamyl alcohol dehydrogenase 7
AT3G51950	-0.4445	-1.6947	Zinc finger (CCCH-type) family protein / RNA recognition motif (RRM)-containing protein
AT3G12610	-0.4391	-1.6818	DRT100; Leucine-rich repeat (LRR) family protein; Plays role in DNA-damage repair/toleration
AT5G10150	-0.4261	-1.4095	UPSTREAM OF FLC protein (DUF966)
AT3G06145	-0.4232	-1.9570	RING zinc finger protein
AT5G28300	-0.4091	-2.0106	GT2L; Encodes a Ca(2+)-dependent CaM-binding protein
AT5G17170	-0.4086	-1.1686	Rubredoxin family protein
AT5G15230	-0.4058	-1.5996	GASA4; Encodes gibberellin-regulated protein GASA4; Promotes GA responses and exhibits redox activity
AT5G03760	-0.4056	-1.3940	ATCSLA09; Nucleotide-diphospho-sugar transferases superfamily protein
AT4G30020	-0.4020	-2.9746	PA-domain containing subtilase family protein
AT5G05690	-0.4020	-1.5779	CPD; Cytochrome P450 superfamily protein
AT5G67070	-0.4016	-3.1003	RALFL34; Shows sequence similarity to tobacco Rapid Alkalinization Factor (RALF)
AT2G43340	-0.3938	-2.3099	Hypothetical protein (DUF1685)
AT3G06590	-0.3916	-1.6564	Basic helix-loop-helix (bHLH) DNA-binding superfamily protein
AT3G57150	-0.3752	-1.2064	NAP57; Encodes a putative pseudouridine synthase (NAP57)
AT2G38210	-0.3750	-3.8988	PDX1L4; Putative PDX1-like protein 4
AT1G78820	-0.3728	-2.0557	D-mannose binding lectin protein with Apple-like carbohydrate-binding domain-containing protein
AT1G55360	-0.3695	-1.0787	tRNA-splicing ligase (DUF239)
AT2G35960	-0.3646	-1.7849	NHL12; Sequence is similar to tobacco HIN1 and Arabidopsis non-race specific disease resistance gene (NDR1).
AT4G13940	-0.3594	-0.6308	HOG1; Encodes a S-adenosyl-L-homocysteine hydrolase required for DNA methylation-dependent gene silencing
AT3G18490	-0.3547	-0.7924	ASPG1; Functions in drought avoidance through abscisic acid (ABA) signalling in guard cells
AT2G40540	-0.3469	-1.5185	KT2; Putative potassium transporter AtKT2p (AtKT2) mRNA
AT3G53460	-0.3455	-1.7676	CP29; Encodes a nuclear gene with a consensus RNA-binding domain that is localized to the chloroplast
AT1G17100	-0.3389	-1.2255	HBP1; SOUL heme-binding family protein
AT5G65010	-0.3338	-1.2069	ASN2; Encodes asparagine synthetase (ASN2)
AT4G13930	-0.3262	-1.1058	SHM4; Encodes a serine hydroxymethyltransferase maximally expressed in root
AT5G11790	-0.3231	-1.3569	NDL2; N-MYC downregulated-like 2
AT2G46710	-0.3216	-2.4389	ROPGAP3; Rho GTPase activating protein with PAK-box/P21-Rho-binding domain-containing protein
AT1G14345	-0.3183	-1.7460	NAD(P)-linked oxidoreductase superfamily protein
AT5G53880	-0.3176	-1.8804	Hypothetical protein
AT2G26110	-0.3123	-1.9533	Bromodomain protein (DUF761)
AT3G46550	-0.3047	-1.0629	SOS5; Salt overly sensitive 5
AT1G64720	-0.2964	-0.9132	CP5; Polyketide cyclase/dehydrase and lipid transport superfamily protein
AT5G38420	-0.2948	-1.4478	RBCS2B; Encodes a member of the Rubisco small subunit (RBCS) multigene family
AT5G01090	-0.2918	-1.6630	Concanavalin A-like lectin family protein
AT1G25440	-0.2901	-1.4204	BBX15; B-box type zinc finger protein with CCT domain-containing protein
AT4G23740	-0.2864	-1.5981	Leucine-rich repeat protein kinase family protein
AT2G04030	-0.2859	-1.0591	CR88; A chloroplast-targeted 90-kDa heat shock protein involved in red-light mediated deetiolation response
AT5G57120	-0.2823	-0.7923	Nucleolar/coiled-body phosphoprotein
AT5G62350	-0.2799	-1.5148	Plant invertase/pectin methylesterase inhibitor superfamily protein
AT3G02570	-0.2736	-1.1187	MEE31; Encodes a protein with phosphomannose isomerase activity
AT1G74070	-0.2727	-1.9668	Cyclophilin-like peptidyl-prolyl cis-trans isomerase family protein
AT1G48920	-0.2629	-0.7930	NUC-L1; This protein is involved in rRNA processing, ribosome biosynthesis, and vascular pattern formation
AT2G26900	-0.2544	-1.0858	BASS2; Sodium Bile acid symporter family
AT4G37800	-0.2540	-2.7456	XTH7; xyloglucan endotransglucosylase/hydrolase 7
AT5G17920	-0.2526	-0.7629	ATMS1; Encodes a cytosolic cobalamin-independent methionine synthase, involved in methionine regeneration
AT1G77030	-0.2447	-1.6368	Putative DEAD-box ATP-dependent RNA helicase 29
AT3G06980	-0.2342	-1.7067	DEA(D/H)-box RNA helicase family protein
AT2G45590	-0.2201	-1.3833	Protein kinase superfamily protein
AT5G23070	-0.2173	-4.0573	TK1b; Encodes a thymidine kinase that salvages DNA precursors
AT1G45230	-0.1793	-1.7256	DCL protein (DUF3223)

Acknowledgements

I would like to express my sincere gratitude to my supervisor Prof. Dr. Brigitte Poppenberger for giving me the opportunity to conduct my research in her group. The sudden epidemic made studying abroad more difficult, but her concern for my research and life gave me confidence. After each of our discussions, her advice and fruitful critiques helped me grow in scientific research and put me on the right path. Forever grateful and will follow her example.

I am grateful to all former and present colleagues from the Institute Biotechnology of horticultural crops and Plant growth regulation group, for the supporting in the experiments and scientific discussion, for the great and scientific working atmosphere during my PhD study.

Many thanks to Irene Ziegler and other technical staff in our lab and greenhouse for providing technical support.

Many thanks to Christina Duffner, the secretary of our lab, for her assistance in my working.

I am greatly obliged to Prof. Dr. Caroline Gutjahr for chairing the examination committee and Prof. Dr. Gerd Patrick Bienert for being the examiner in my examination committee.

Special thanks to the China Scholarship Council (CSC) for providing me the opportunity to study abroad and the financial support.

Finally, I would like to express my thanks to my family for their support and understanding through the process.